Imperial College
London

Modelling and Sustainability Assessment of Industrial Ionic Liquid Production and Applications using Life Cycle Thinking

by Husain A. Baaqel

Centre for Process Systems Engineering
Department of Chemical Engineering
Imperial College London

Submitted in partial fulfilment of the requirements for the degree of Doctor of Philosophy from the Imperial College London and the Diploma of the Imperial College London

London, October 2022

I hereby declare that this thesis and the work reported herein was composed by and originated entirely from me. Information derived from the published and unpublished work of others has been acknowledged in the text and references are given in the list of sources.

Husain Ahmad Baaqel

Abstract

The main goal of this dissertation is to build on the current state-of-the-art research regarding ionic liquid (IL) sustainability assessment to help answer the research question, "how sustainable are ILs as alternatives to conventional technologies?" This is accomplished by developing a systematic computer-aided framework that integrates life cycle assessment (LCA) and life cycle costing (LCC) with process modelling and simulation for the consistent and complete economic and environmental assessment of ILs. The work further explores the use of monetization and an advanced framework that couples uncertainty analysis and global sensitivity analysis to enhance decision-making. The main novelties of the thesis are the methodological components and the case studies, in which the production of different ILs are evaluated in the context of relevant applications including their use.

This thesis has contributed to the existing body of research by developing the following aspects. First, an integrated framework that combines LCA, LCC with process modelling and simulation was applied to evaluate the production of 1-butyl-3-methylimidazolium tetrafluoroborate using two synthesis routes and compare them with two conventional solvents in terms of their application in fuel desulfurization. Second, the developed framework was enhanced by incorporating factors of monetization, and this was applied to a case study involving hydrogen sulfate-based ILs to quantify their externalities and compare the true cost of these ILs with that of conventional solvents in biomass pretreatment applications. Finally, LCA uncertainty and global sensitivity analysis (GSA) was included in the framework to improve uncertainty analysis by accounting for process model uncertainties and identifying key parameters in non-linear systems, which was demonstrated in a case study involving the production of dialkylimidazolium ILs.

The results show that the use of data from detailed process models, as highlighted in the holistic framework, makes a big difference compared to the use of simplified methods. Unlike short-cut methods, the framework accounts for process efficiency, emissions, and waste and covers a wide range of environmental impact categories for a more consistent and complete assessment. Additionally, coupling monetization with LCA can improve the assessment by turning a multi-objective problem into a single-objective problem, and hence, facilitating decision-making. The environmental externalities quantified through monetization reveal hidden costs that are usually overlooked when conducting a conventional economic assessment. Moreover, the importance of including foreground uncertainties in the uncertainty analysis was demonstrated by the results

obtained from applying uncertainty-GSA analysis. In particular, foreground uncertainties can significantly overlap with the background uncertainties because of the multiplicative effect, which impacts decision-making. Furthermore, using GSA can help correctly identify uncertain parameters by accounting for collaborative effects in non-linear systems.

Finally, case studies were used to test the efficiency of the developed framework and its methodological components. The contributions of this thesis build on the state-of-the-art economic assessment and LCA for ILs and support research on evaluating the sustainability of ILs and similar novel chemicals. This in turn will help us better understand the potential of such chemicals in terms of their sustainability performance as decision-making in most industries today is driven by policies pursuing sustainable development.

Acknowledgements

I would like to express my deepest appreciation and gratitude to my supervisors, Professors Jason Hallett, Benoît Chachuat, and Gonzalo Guillén-Gosálbez, for their unlimited support, patience, and guidance throughout my PhD journey. They have continuously challenged me while also providing me with the necessary tools and feedback I needed to sharpen my research and technical skills, which shaped the researcher I am today. Special thanks to Jason for his kindness and for all the research opportunities he gave me, including my stay at ETH and Monash University, which taught me a lot and provided me with all the resources I needed since my first day. Many thanks to Dr. Coby Clarke for the opportunity to collaborate. I would also like to extend my gratitude to Prof. Nilay Shah for his mentorship and positivity, and Dr. Agi Brandt-Talbot for her kind support and insightful suggestions that gave me the push I needed during the early stages of my PhD. Thank you, Prof. Claire Adjiman and Dr. Miao Guo, for the teaching opportunity and support, and for the constructive feedback. Many thanks to Prof. Douglas MacFarlane for hosting me at Monash University and the opportunity to collaborate with his brilliant team on one of his exciting research projects. I am also extremely thankful to the government of Saudi Arabia for the generous PhD scholarship.

My experience as a PhD student at Imperial College London has been invaluable and rewarding. I am very thankful to the Department of Chemical Engineering and the Centre for Process Systems Engineering and all the staff for meeting our needs and for their continuous administrative and technical support. I am truly grateful to have shared my time with many wonderful people. Many thanks to Aida, Amir, Andrea, Ariel, Diego, Elysia, Francisco, Hunnan, Lucian, and Pedro. I appreciate the valuable contribution that Dr. Ismael Díaz and Dr. Víctor Tulus made to my first paper. Special thanks to Raúl, who has been an incredible friend and colleague since the first day, and for his willingness to consistently help me with everything I needed at Imperial and ETH, and Amjad for her amazing friendship and the joy she always brought to our group, including her endless support during and after her PhD. Thank you, Andrés and Daniel, for the kind help and support and for answering all of my questions. I'd like to extend my gratitude to everyone I've met at ETH and Monash University. Thank you, Sebastiano, for taking care of my IT needs at ETH and for the recommendations during my stay. Thank you, Dr. Karolina and Saliha, for the warm welcome and support and for providing me with everything I needed to conduct my work at Monash University.

I would like to acknowledge and extend my gratitude to Dr. Esam Hamad, Mr. Hassan

Babiker, and Dr. Christos Kalamaras from Saudi Aramco for their continuous support. Special thanks to Esam for his outstanding mentorship at Saudi Aramco RDC. I truly admire his extensive knowledge, professionalism, and influential leadership. Thank you, Hassan, for always addressing my concerns and for the positive attitude and emotional support.

Finally, I would like to thank my parents for their unconditional love and support. Many thanks to my wife Huda for her patience, understanding, and continuous support since I started my undergraduate studies. I am truly grateful for everything you've done for me and extremely indebted to your commitment and for always being there through the ups and downs. I am also very proud of what you've accomplished in your education and career and wish you more growth and success. Finally, many thanks to my beautiful children, Ahmed and Marline, for all the happiness and joy they have brought to our home. They have been a source of inspiration and motivation. I feel truly blessed to have them in my life and to watch them learn and grow. They have always asked when I will finish my studies and I can tell you now that the time has come to celebrate, and soon, I'll pass the baton for a bright future.

Publications

Husain Baaqel, Ismael Díaz, Víctor Tulus, Benoit Chachuat, Gonzalo Guillén-Gosálbez and Jason Hallett. Role of life-cycle externalities in the valuation of protic ionic liquids–a case study in biomass pretreatment solvents. *Green Chemistry*, 2020. DOI: 10.1039/D0GC00058B

Husain Baaqel, Víctor Tulus, Benoit Chachuat, Gonzalo Guillén-Gosálbez and Jason Hallett. Uncovering the True Cost of Ionic Liquids using Monetization. *Computer Aided Chemical Engineering*, 2020. DOI: 10.1016/B978-0-12-823377-1.50305-0

Husain Baaqel, Jason P Hallett, Gonzalo Guillén-Gosálbez and Benoît Chachuat. Uncertainty analysis in life-cycle assessment of early-stage processes and products: a case study in dialkyl-imidazolium ionic liquids. *Computer Aided Chemical Engineering*, 2021. DOI: 10.1016/B978-0-323-88506-5.50123-6

Husain Baaqel, Jason Hallett, Gonzalo Guillén-Gosálbez and Benoît Chachuat. Sustainability Assessment of Alternative Synthesis Routes to Aprotic Ionic Liquids: The Case of 1-Butyl-3-Methylimidazolium Tetrafluoroborate for Fuel Desulfurization. *Sustainable Chemistry and Engineering*, 2021. DOI: 10.1021/acssuschemeng.1c06188

Coby Clarke, Husain Baaqel, Richard Matthews, Yiyan Chen, Kevin Lovelock, Jason Hallett, and Peter Licence. Halometallate ionic liquids: thermal properties, decomposition pathways, and life-cycle considerations. *Green Chemistry*, 2022. DOI: 10.1039/D2GC01983C

Conferences

Husain A Baaqel, Ismael Díaz, Jason P Hallett, Benoit Chachuat, Gonzalo Guillén-Gosálbez and Ángel Galán Martín "Estimating True Cost of Ionic Liquids Using Monetization", *AIChE*, 2019

Contributions to the Thesis

Two published papers and one working manuscript form the basis of this thesis. External collaborators contributed to one published paper. Therefore, the contributions of the external collaborators are acknowledged here:

- Chapter 4 is based on the following published paper: Husain Baaqel, Jason Hallett, Gonzalo Guillén-Gosálbez and Benoît Chachuat. Sustainability Assessment of Alternative Synthesis Routes to Aprotic Ionic Liquids: The Case of 1-Butyl-3-Methylimidazolium Tetrafluoroborate for Fuel Desulfurization. *Sustainable Chemistry and Engineering*, 2021. DOI: 10.1021/acssuschemeng.1c06188.

  No external collaborators were involved.

- Chapter 5 is based on the following published paper: Husain Baaqel, Ismael Diaz, Victor Tulus, Benoit Chachuat, Gonzalo Guillén-Gosálbez and Jason Hallett. Role of life-cycle externalities in the valuation of protic ionic liquids–a case study in biomass pretreatment solvents. *Green Chemistry*, 2020. DOI: 10.1039/D0GC00058B.

  Dr. Ismael Diaz and Dr. Victor Tulus provided tips and feedback to improve the quality of the paper.

- Chapter 6 is based on a working manuscript.

  No external collaborators were involved.

Contents

List of Tables

List of Figures

Nomenclature

Acronyms

A^-	Conjugate base
AH	Bronsted acid
AIL	Aprotic ionic liquid
B	Bronsted base
CED	Cumulative energy demand
CEPCI	Chemical Engineering Plant Cost Index
DALY	Disability-adjusted life-years
ECO	Ecosphere
GSA	Global sensitivity analysis
GWP	Global warming potential
HB^+	Conjugate acid
HDMR	High-dimensional model representation
IL	Ionic liquid
LCA	Life-cycle assessment
LCC	Life-cycle costing
LCIA	Life-cycle impact assessment
LCI	Life-cycle inventory
LCSA	Life-cycle sustainability assessment
OTSA	One-at-a-time sensitivity analysis
PCES	Property constant estimation system
PIL	Protic ionic liquid
QMC	Quasi-Monte Carlo

RS-HDMR	Random-sampling high-dimensional model representation
S-LCA	Social life-cycle assessment
SDGs	Sustainable Development Goals
SWOT	Strengths, Weaknesses, Opportunities and Threats analysis
TAC	Total annualised cost
TEC	Technosphere
TRL	Technology-readiness level
UN	United Nations
VOC	Volatile organic chemical

Chemicals

$AlCl_3$	Aluminium chloride
[BBIM][BF_4]	1,3-Di-N-butylimidazolium tetrafluoroborate
[BF_4]$^-$	Tetrafluoroborate
[BMIM]$^+$	1-Butyl-3-methylimidazolium
[BMIM][BF_4]	1-Butyl-3-methylimidazolium tetrafluoroborate
[BMIM]Br	1-Butyl-3-methylimidazolium bromide
[BMIM]Cl	1-Butyl-3-methylimidazolium chloride
[BMIM][OAc]	1-Butyl-3-methylimidazolium acetate
[BMIM][PF_6]	1-Butyl-3-methylimidazolium hexafluorophosphate
$C_2H_2O_2$	Glyoxal
$C_4H_{11}N$	N-butylamine
CFC 142b	1-Chloro-1,1-difluoroethane
CH_2O	Formaldehyde
CO_2	Carbon dioxide
DMF	Dimethylformamide
[EMIM]$^+$	1-Ethyl-3-methylimidazolium
[EMIM]Cl	1-Ethyl-3-methylimidazolium chloride
[EMIM][OAc]	1-Ethyl-3-methylimidazolium acetate
[EMIM][PF_6]	1-Ethyl-3-methylimidazolium hexafluorophosphate

H_2O	Water
HCl	Hydrochloric acid
[HMIM][HSO_4]	1-Methylimidazolium hydrogen sulphate
HPF_6	Hexafluorophosphoric acid
$LiPF_6$	Lithium hexafluorophosphate
[mebupy][BF_4]	4-Methyl-N-butylpyridinium tetrafluoroborate
[mebupy][CH_3SO_4]	4-Methyl-N-butylpyridinium methyl sulphate
[MMIM][BF_4]	1,2,3-trimethylimidazolium tetrafluoroborate
[N1,8,8,8]Cl	Methyltrioctylammonium chloride
[N1,8,8,8][NTf_2]	Methyltrioctylammonium bis(trifluoromethylsulfonyl)amide
$NaBF_4$	Sodium tetrafluoroborate
NaCl	Sodium chloride
NH_3	Ammonia
[OMIM]Br	1-Octyl-3-methylimidazolium bromide
[P6,6,6,14][124Triz]	Trihexyl(tetradecyl)phosphonium 1,2,4-triazolide
[P6,6,6,14]Cl	Trihexyltetradecylphosphonium chloride
[P6,6,6,14][NTf_2]	Trihexyltetradecylphosphonium bis(trifluoromethylsulfonyl)amide
[PF_6]$^-$	Hexafluorophosphate
[TEA][HSO_4]	Triethylammonium hydrogen sulphate

Symbols

a, b	Equipment cost constants
$\alpha_r^i, \beta_{pq}^{ij}$	Orthonormal constant coefficients
$BEI_z^{BF_3}$	Lumped background impact of production of boron trifuoride
$BEI_z^{[BMIM]Cl}$	Lumped background impact of production of sodium tetrafluoroborate
BEI_z^{el}	Lumped background impact of production of electricity
$BEI_z^{Et_2O}$	Lumped background impact of production of dethyl ether
$BEI_z^{LiPF_6}$	Lumped background impact of production of lithium hexafluorophosphate
BEI_z^{mat}	Lumped background impact of production of construction materials

$\mathrm{BEI}_z^{\mathrm{NaBF_4}}$	Lumped background impact of production of sodium tetrafluoroborate
$\mathrm{BEI}_z^{\mathrm{NaF}}$	Lumped background impact of production of sodium fluoride
$\mathrm{BEI}_z^{\mathrm{th}}$	Lumped background impact of production of thermal energy
$\mathrm{BEI}_z^{\mathrm{wat}}$	Lumped background impact of production of water
$\mathrm{BEI}_z^{\mathrm{wwt}}$	Lumped background impact of wastewater treatment
BOD	Biological oxygen demand
BP	Boiling point
$CAPEX$	Capital expenses
C_{Con}	Contingency charges
C_e	Cost of equipment item e
C_{Eng}	Engineering and construction cost
C_{FC}	Fixed capital cost
C_{FCP}	Fixed cost of production
$\mathrm{CF}_{e,z}$	Characterisation factor of elementary flow $e \in E$ in impact category $z \in Z$
C_{GPO}	Cost of general plant overhead
C_{Land}	Land cost
C_{Main}	Cost of maintenance
COD	Chemical oxygen demand
C_{OL}	Cost of operation labour
C_{RM}	Raw materials cost
C_{Sal}	Cost of salaries
C_{Sup}	Cost of supervision
C_{Tax}	Cost of taxes and insurance
C_U	Utilities cost
C_{VCP}	Variable cost of production
$\mathcal{D}_\mathrm{f}$	Set of processes immediately downstream of foreground process f
DOC	Dissolved organic carbon
D_z	Total variance of environmental impact for an indicator z

D_{z_i}	Partial variance from individual parameter i for a specific indicator z
$D_{z_{ij}}$	Partial variance from binary parameters i and j for a specific indicator z
e	Equipment type cost exponent
η, δ	Ionic liquid stoichiometry parameters
$\mathrm{EF}_{\mathrm{f},e}$	Elementary flow $e \in E$ exchanged between foreground process f and ecosphere
$\mathrm{EF}_{p,e}^{\mathrm{nom}}$	Nominal value of elementary flow elementary flow $\mathrm{EF}_{p,e}$
$\mathrm{EF}_{p,e}$	Elementary flow $e \in E$ exchanged between background process p and ecosphere
EI_z	Overall environmental impact in category $z \in Z$
ϵ	Relative error
F_e	Equipment item installation factor
$\Delta H_{\mathrm{f[BMIM]Cl}}$	Heat of formation of [BMIM]Cl
HEN	Heat exchanger network
ΔH_f	Heat of formation
$\Delta H_{\mathrm{f[BMIM][BF_4]}}$	Heat of formation of [BMIM][BF_4]
ΔH_L	Lattice energy
$ISBL$	Onsite expenses
$\mathrm{LCI}_{p,e}^{\mathrm{down}}$	Total inventory of elementary flow $e \in E$ from immediate downstream process $p \in \mathcal{D}_{\mathrm{f}}$ and all processes downstream of p in process tree
$\mathrm{LCI}_e^{\mathrm{tot}}$	Total life-cycle inventory of elementary flow $e \in E$
$\mathrm{LCI}_{p,e}^{\mathrm{up}}$	Total inventory of elementary flow $e \in E$ from immediate upstream process $p \in \mathcal{U}_{\mathrm{f}}$ and all processes upstream of p in process tree
$\hat{\mu}_{\mathrm{EI}_z}$	Sample mean of environmental impact EI_z
MW	Molecular weight
N	Sample size
n_m	Cation parameter
n_x	Anion parameter
$OPEX$	Operating expenses
$OSBL$	Offsite expenses

ρ	Density
p, q	Cation and anion oxidation states
$\rho_{[\mathrm{BMIM}][\mathrm{BF_4}]}$	Density of [BMIM][BF_4]
$\rho_{[\mathrm{BMIM}]\mathrm{Cl}}$	Density of [BMIM]Cl
P_c	Critical pressure
$\rho_{p\to \mathrm{f}}$	Scaling factor for elementary flow $\mathrm{LCI}_{p,e}^{\mathrm{up}}$ in terms of FU
$\rho_{\mathrm{f}\leftarrow p}$	Scaling factor for elementary flow $\mathrm{LCI}_{p,e}^{\mathrm{down}}$ in terms of FU
ΔP_R	Pressure drop in reactor
PUR	Purge split ratio
P_{VF}	Pressure in vacuum flash tank
ΔP_W	Pressure drop in washer
R^2	Coefficient of determination
$\sigma_{p,e}^{\mathrm{EF}}$	Standard deviation in log-normal distribution of elementary flow $\mathrm{EF}_{p,e}$
$\hat{\sigma}_{\mathrm{EI}_z}$	Sample standard deviation of environmental impact EI_z
$SO_z\%$	Normalised Sobol index of an indicator z
SO_{z_i}	Sobol index of an individual contribution for variable i for a specific indicator z
$SO_{z_{ij}}$	Sobol index of an binary contribution for variables i and j for a specific indicator z
$SO_{z_{Ti}}$	Total Sobol index for variable i for a specific indicator z
SS_{res}	Residual sum of squares
SS_{tot}	Total sum of squares
T_c	Critical temperature
TOC	Total organic carbon
T_{VF}	Temperature in vacuum flash tank
U^c	Indicator score in Pedigree matrix approach
$\mathcal{U}_{\mathrm{f}}$	Set of processes immediately upstream of foreground process f
U_{POT}	Potential energy
$\boldsymbol{\varphi}$	Vector of uncertain background flows

V_c	Critical volume
$\varphi_r(y_i), \varphi_p(y_i), \varphi_q(y_j)$	Orthonormal basis functions
$\boldsymbol{\omega}$	Vector of uncertain foreground parameters
z	Environmental indicator

Chapter 1

Introduction

With the continuous growth in population and standards of living, the energy and material consumption continues to grow, leading to the depletion of non-renewable resources and the release of harmful emissions. In 2018, energy consumption globally grew at a rate that is almost twice the rate of 2010, accompanied by an acceleration in the release of harmful greenhouse gas emissions [1, 2]. This in turn leads to unsustainable living conditions due to the ever increasing negative impacts on our planet, society and finite resources that put future generations at risk. Thus, there is an urgent need for solutions that can drive sustainable development.

1.1 Post World War II

The end of the Second World War marked the beginning of a new era in human history. By the end of the 20^{th} century, the population doubled to over six billion, and the world economy increased by more than 15 times [4]. Since 1960, industrialisation and oil consumption have been increasing rapidly, and the number of automobiles has increased more than 17-fold by the end of 1996. This era has also seen a significant increase in urbanisation. Between 1950 and 2000, the population living in urban areas increased from 30% to 50%. Overall, this has led to a continuously growing demand for energy and chemicals, driven by the rising standards of living. As a result, human activity has not only polluted the environment on an unprecedented scale but also resulted in several industrial accidents, which have had severe impacts on both humans and the environment [5, 6].

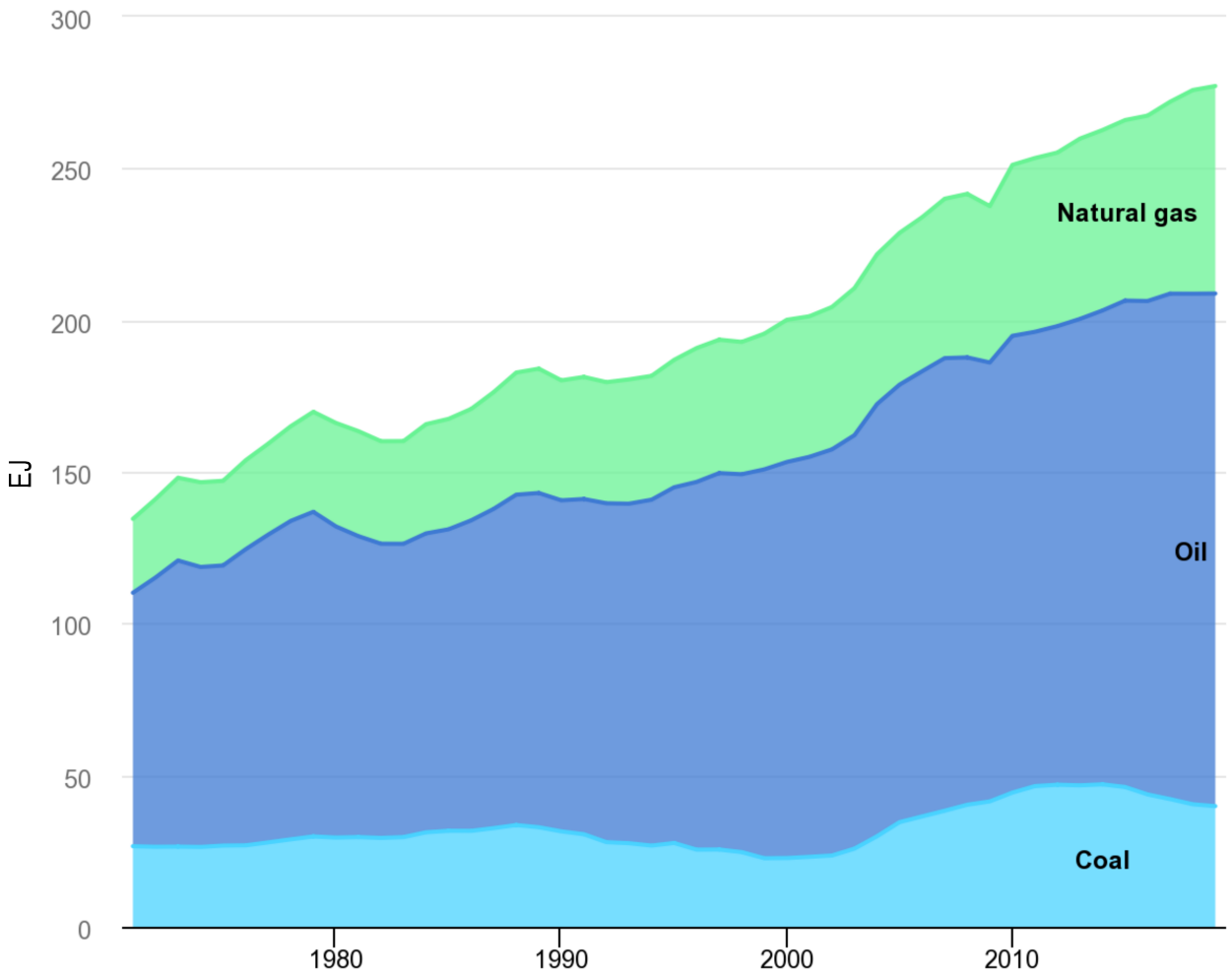

Figure 1.1: Global energy consumption from fossil fuels by source between 1971 and 2019.[3]

Between 1950 and today, global energy consumption increased to a total of more than 173,000 terawatt-hours. As of today, the world's three largest sources of energy are oil, coal, and gas, which are fossil fuel and together account for around 85% of the total energy supply [7, 8]. Figure 1.1 shows the increasing energy consumption from fossil fuels between 1971 and 2019. As a result, the world's cumulative carbon dioxide emissions from fossil fuels jumped from 231 billion tonnes in 1950 to 1.65 trillion tonnes in 2019. Currently, the United States and China contribute almost 40% of the global carbon emissions [7]. Additionally, around 11 billion tonnes of solid waste and 400 million tonnes of hazardous waste are produced globally every year, and more than 1.3 million square kilometres of forests have been lost since 1990 due to deforestation and land use [9]. Other environmental changes include a decline in global freshwater supply and an increase in other types of air pollutants, such as particulate matter and sulphur-based

compounds, all of which can pose a danger to humans' well-being and the life on the planet we live on.

As carbon dioxide emissions and other greenhouse gases build up in our atmosphere, the effects of global warming become increasingly more dangerous to our habitat. Global warming and its subsequent impacts, such as sea level rise, can increase the severity and frequency of many natural disasters such as storms, floods, and droughts [10]. In addition, it can be a driver for communicable diseases that are sensitive to temperature and cause respiratory diseases, such as asthma, which are more common in summer months [11]. Similarly, hazardous waste can cause health issues such as chemical poisoning, neurological diseases, and cancer [12]. Moreover, deforestation causes the loss of habitat for many species, which in turn leads to species extinction and loss of biodiversity. Therefore, avoiding such impacts by reducing energy consumption, cutting environmental emissions, and eliminating waste can make positive changes to society and the environment and enable sustainable development.

1.2 Sustainable development

As industrialisation started to grow at an accelerated rate in the mid-20th century, growing concerns about the environmental impacts and the imminent ecological crisis these activities can cause led to the emergence of the concept of sustainable development. In 1968, Garret wrote a letter, namely "The Tragedy of the Commons," where he argued that if humans act independently, focusing on their own interests only, they will eventually act against their common interests, which consist mainly of their habitat and its finite resources [13]. According to him, people need to change the way they consume common resources to avoid future disasters. In 1972, the United Nations (UN) Conference on the Human Environment took place in Stockholm. This was the first time the UN conference focused on environmental issues, and the goal was to determine the common goals and principles required to guide the world and protect the environment. Efforts to forge a common path for a sustainable future culminated in the publication of the Brundtland report by the World Commission on Environment and Development in 1987.

The most recognised definition of sustainable development first appeared in the Brundtland

report, "development that meets the needs of the present without compromising the ability of future generations to meet their own needs" [14]. The main objectives of the reports were to re-evaluate the critical issues of the environment and to develop an action plan, call for an international act to form channels of collaboration and work on policies that support sustainable development, and increase the level of awareness and understanding of the global crisis at the individual and institutional levels. The report also functioned as a basis for the Rio Declaration in the Conference on Environment and Development in 1992, also known as the Earth Summit in Rio de Janeiro. The document consisted of 27 principles that could provide a guide for countries to create policies that advance sustainability and environmental conservation [15].

In 2015, efforts led by the UN and its stakeholders concerning the environment and sustainability resulted in the adoption of 17 Sustainable Development Goals (SDG), which were set by the United Nations General Assembly [16]. Climate action, sustainable cities and communities, and responsible consumption and production are examples of the SDGs, the common purpose of which is to achieve a sustainable life for future generations. It was clear that, after decades of industrialisation, economic growth at the expense of ecological conservation and social rights could not last forever. Therefore, herein, sustainability refers to maintaining the balance between three interconnected pillars: environment, economy, and society. While many government tools can be used, such as policy changes, all efforts need to be combined with innovative technological approaches to promote substantial change that can help achieve sustainability [1]. One such solution is the development of technologies that reduce energy consumption and environmetnal emissions. This can be done at different levels ranging from the factory scale, through the optimisation of technological systems, to the molecular scale, by replacing or changing the chemistry within the units. An example of the latter is the use of "green" chemicals.

1.3 Early sustainability indicators

Green chemistry refers to the design of chemicals and processes to reduce or eliminate the use or generation of hazardous substances. The origins of the idea date back to 1990, in response to the

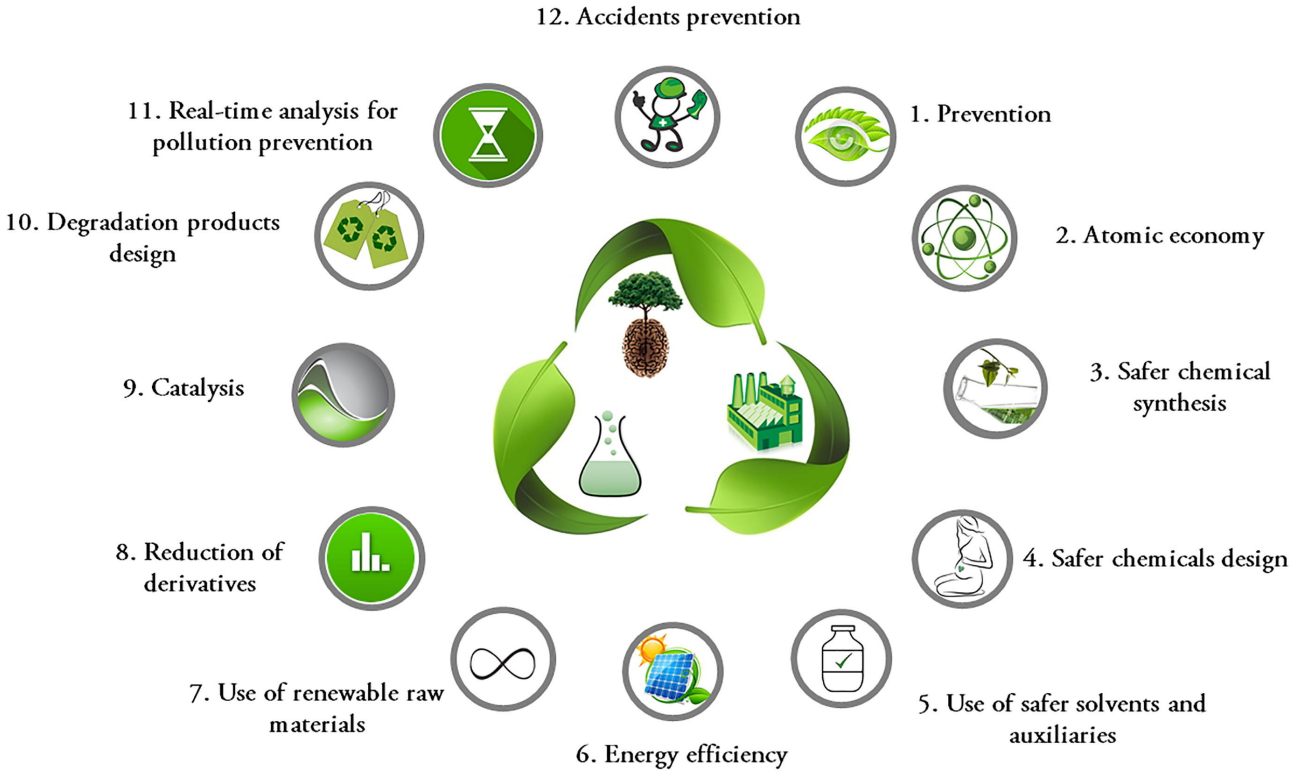

Figure 1.2: The 12 principles of green chemistry.[18]

Pollution Prevention Act, which hs the goal of preventing, controlling, and reducing air pollution through changes in production, operation, and use raw materials [17]. The 12 principles of green chemistry were published in 1998. Green chemicals, therefore, refer to chemicals that meet one or more of the 12 principles.

The 12 principles, as illustrated in Figure 1.2, are based on four main concepts that are meant to guide researchers regarding the practices and concepts to keep in mind when designing a chemical or process. The main concepts are based on the following suggestions: using chemicals that reduce the amount of waste produced, using non-toxic or low-toxicity chemicals, using non-fossil fuel resources or renewable feedstocks, and using chemicals that reduce energy in the process.

An example of a green chemical in our everyday lives is water. It is inherently safe, readily available without the need for processing or manufacturing, and is not derived from fossil fuels. Another example is supercritical CO_2, which is non-toxic, non-flammable, non-reactive, and inherently safe. Although attractive, they also have their shortcomings, which may limit their uses. For example, water is difficult to purify as a solvent and has a high enthalpy of evaporation;

therefore, it can increase energy consumption in separation units, which in turn increases both cost and carbon emissions [19]. Similarly, supercritical CO_2 is considered a poor solvent because of its low polarity [20]. In addition, the high pressure of supercritical fluid systems, in general, makes them expensive to use compared to other technologies. These issues can make them unattractive since they may cancel out their green benefits.

Although green chemistry principles and measures are good preliminary sustainability indicators, which can be used to identify green chemicals during the early stages, they are rather qualitative and limited in scope, e.g. focus on a few aspects such as the improvement they make in certain processes and their toxicity, rather than taking a holistic view of their sustainability considering their entire life cycle. Therefore, the greenness of these chemicals during processing does not necessarily mean they are sustainable. To address this, more comprehensive methods that can quantify their performance in different sustainability dimensions, i.e., economic, environmental and social, using computational tools such as LCA should be used instead.

1.4 Ionic liquids (ILs)

ILs can be defined as salts with melting temperatures below 100 °C, and most ILs are liquids at room temperature [21]. They are relatively new chemicals that have been studied extensively in the last two decades. Their unique properties make them attractive in a wide range of applications such as synthesis [22], extraction [23], working fluids [24], lubricants [25], and electrolytes [26], to name a few. In addition, ILs have long been claimed to be green due to their low vapour pressure and also because of the high thermal and chemical stabilities for most ILs [27–29]. Their low vapour pressure minimises their losses during processing and the thermal and chemical stabilities for most ILs allow them to operate within a wide range of temperatures and mix with many chemicals without being altered or decomposed.

ILs are usually made of an organic cation and inorganic anion. There are numerous cations and anions that can be combined to form ILs which make them more customizable and versatile. Also, under atmospheric conditions, these salts tend to have a wide liquidus range, i.e., the difference between melting temperature and boiling temperature, which differentiates

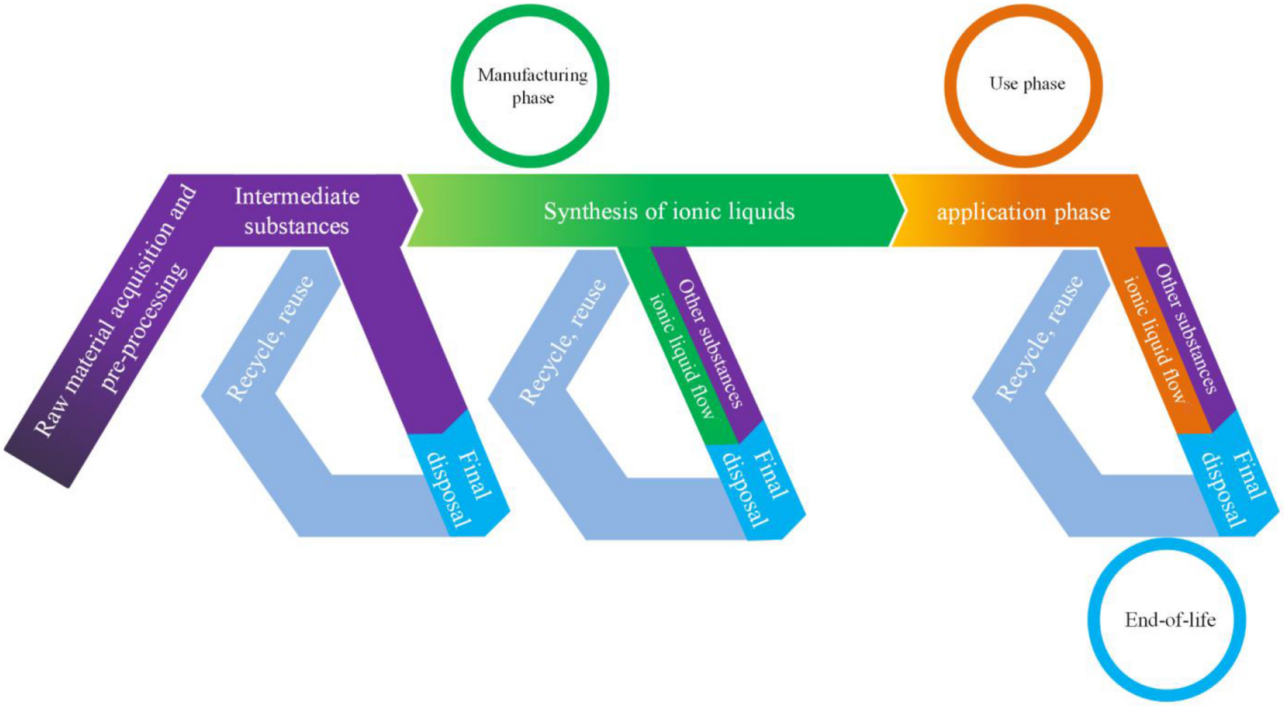

Figure 1.3: Schematic representation of ionic liquids from a life cycle perspective.[32]

them from molecular solvents, in addition to a wide range of other attractive properties, such as non-flammability, biopolymer solubility, catalytic activity, and high ionic conductivity, which is a key property of ILs and common to all of them [30, 31].

ILs, therefore, could have potential to replace conventional chemicals as green alternatives. However, as mentioned earlier, to accurately evaluate the sustainability of ILs, or any other chemical, their entire life cycle, including their production, needs to be considered. This is necessary to ensure that the issues avoided in one stage, e.g., the use phase, are not shifted to other stages of the life cycle, e.g., the production phase, as shown in the schematic of Figure 1.3.

1.5 ILs economic and environmental concerns

ILs are a promising class of green chemicals, but their sustainability from a life-cycle perspective is controversial because of economic and environmental factors. First, the high cost of most ILs is considered a limiting factor [33]. Second, there is an environmental burden caused by the use of volatile organic chemicals (VOC) in IL manufacturing [34] and by the toxicity [35] and low biodegradability [36] of some ILs and their ionic constituents [37] when released to

the environment. Additionally, the synthesis of ILs is complex and requires many steps [38]. Generally, not only does multi-step synthesis reduce the overall yield and add to the operating expenses, but it can also generate a large amount of waste.

Research on IL technologies, although active, is still generally at an early stage. Therefore, there is relatively limited information available for most of them, which hinders efforts to fully evaluate them economically and environmentally. Also, out of the few available ones at commercial scale such as the ISOALKY and BASIL processes by Chevron and BASF [39, 40], respectively, no techno-economic or LCA studies are published. Additionally, there are hundreds of thousands of possible ILs, not to mention the hundreds of applications where they can be used. Because of a lack of data, combined with limited access to confidential information regarding the few commercialised ones, state-of-the-art research on their economic and environmental performance is scarce and limited to only a few ILs and applications [32].

Moreover, the few available studies, which will be discussed in the following Chapter, have shortcomings that need to be addressed. For example, they use different approaches and levels of detail in an inconsistent manner to conduct the assessments, e.g., for comparing alternatives which include ILs. This includes oversimplified models and using estimations inconsistently to bridge the gaps in data, leading to potentially erroneous results. Additionally, several economic and environmental metrics are used in the comparative studies, which makes it difficult to make a decision based on the results obtained, especially when there are trade-offs. Finally, ILs are emerging chemicals from different sources, and thus, considering their variety is important not only to improve the interpretation but to ensure better decisions are made regarding their applications. However, the existing studies either omit the use of uncertainty analysis or use only a few scenarios, rather than accounting for detailed technical parameters.

Unfortunately, the inconsistency and application of inappropriate methods can lead to varying results, which defeats the purpose of the assessment. Therefore, without clear guidance for conducting such assessments in a detailed and consistent manner that can be used under all circumstances, the assessments will be challenging to perform and trust, and the number of assessments will remain scarce compared to the immense number of possible ILs and applications. This may slow down their progress in terms of their technological readiness and commercialisation

because these assessments play a big role in the early stages of design [41].

1.6 Research objectives

The goal of this project is to develop a systematic computer-aided for the consistent and complete economic and environmental assessment of ILs. It aims to address the shortcomings of existing approaches used for evaluating the economic and environmental performance of ILs and to answer the central research question, "how sustainable are ILs as alternatives to conventional technologies?"

The novel combination of case studies, methods, and tools used in this research project is intended to achieve the following objectives:

- To develop a systematic framework for the holistic and consistent economic and environmental assessment of ILs.
- To address multi-criteria problems in comparative economic and environmental assessment of ILs with several conflicting metrics using appropriate sustainability-based decision-making approaches.
- To enhance the framework by incorporating a systematic approach to uncertainty analysis, utilizing computer-aided methods and tools.
- To apply the developed methods on multiple case studies, which includes evaluating the economic and environmental performance of different ILs compared to conventional chemicals in selected applications.

The remainder of this thesis is organised as follows. In Chapter 2, a literature review is presented regarding the sustainability assessment of ILs. Specifically, the chapter provides background concerning the two main classes of ILs and their synthesis, state-of-the-art sustainability assessment of ILs, the types of methods used, and the gaps that need to be addressed. The chapter concludes with a brief overview of the main contributions of the thesis. In Chapter 3, the general methodological framework used throughout this thesis for evaluating the economic

and environmental performance of ILs is elaborated. The main contributions of this thesis are presented in Chapters 4 to 6. Finally, Chapter 7 ends this thesis with concluding remarks and future work. The Appendices include all the supplementary material.

Chapter 2

Sustainability Assessment of Ionic Liquids

This chapter discusses the sustainability assessment of ILs and is organised as follows. First, an overview of ILs and their classes are provided. Then, the current state of research regarding the sustainability of ILs in terms of their economic and environmental aspects is reviewed. Finally, the state-of-the-art methods and tools used for evaluating the sustainability of ILs are discussed, which is the main subject of the thesis. All sustainability assessment methods utilized in the literature concerning ILs, ranging from simple metrics to integrated holistic approaches, are reviewed. The chapter concludes with research gaps and highlights the contributions of the research work documented in this thesis, through which these gaps are addressed.

2.1 ILs Classification and Synthesis

ILs can be classified, due to their versatility and the huge possible number they can be made of, in many ways. One way to categorize them is via synthesis into PILs and AILs [42]. Simply put, PILs are produced by combining a Bronsted acid and a Bronsted base unlike AILs which are synthesized by transferring an alkyl group to the cation followed by anion exchange. One of the challenges in using AILs is their high cost due to the complex synthesis procedures required to prepare them, e.g., the anion exchange step alone requires multiple washing steps for removing

impurities like halides and generates salt waste, leading to higher resource consumption and more generated waste, not to mention the expensive raw materials such as the metal salts used to make them. Their cost can sometimes be 20 times higher than conventional solvents, which is a major factor that could limit their use in industry [43]. Most PILs, however, are synthesised in one step after obtaining the required raw materials, and in some cases, these raw materials are available at low prices. The following subsections will discuss and review both IL classes.

2.1.1 Protic ionic liquids (PIL)

As menioned earlier, PILs represent a class of ILs made of a Bronsted acid and a Bronsted base. A Bronsted acid is defined as a proton donor and a Bronsted base is a proton acceptor. The term proton in this definition refers to a hydrogen ion. This can be illustrated in Reaction R2.1, where AH and B are the Bronsted acid and base, while HB^+A^- is the desired IL. The most common cations and anions used in PILs are shown in Figures 2.1 and 2.2, respectively.

$$AH + B \rightleftharpoons HB^+A^- \tag{R2.1}$$

Because of their distinctive structure and simple synthesis, PILs found their way into many applications. An example is lignin extraction from biomass using ILs, which has become more attractive in the last few years. Several studies have used PILs to extract lignin from different biomass sources [44–47]. Reis et al. studied the pretreatment of cashew apple bagasse using 2-hydroxyl-ethylammonium acetate and found that up to 95.8% of the lignin can be removed with a 8.7% w/w biomass to solvent ratio. Verdía et al. used Miscanthus giganteus with 1-butylimidazolium hydrogen sulphate and reported over 90% lignin yield using an IL-water mixture of 80% IL/20% water.

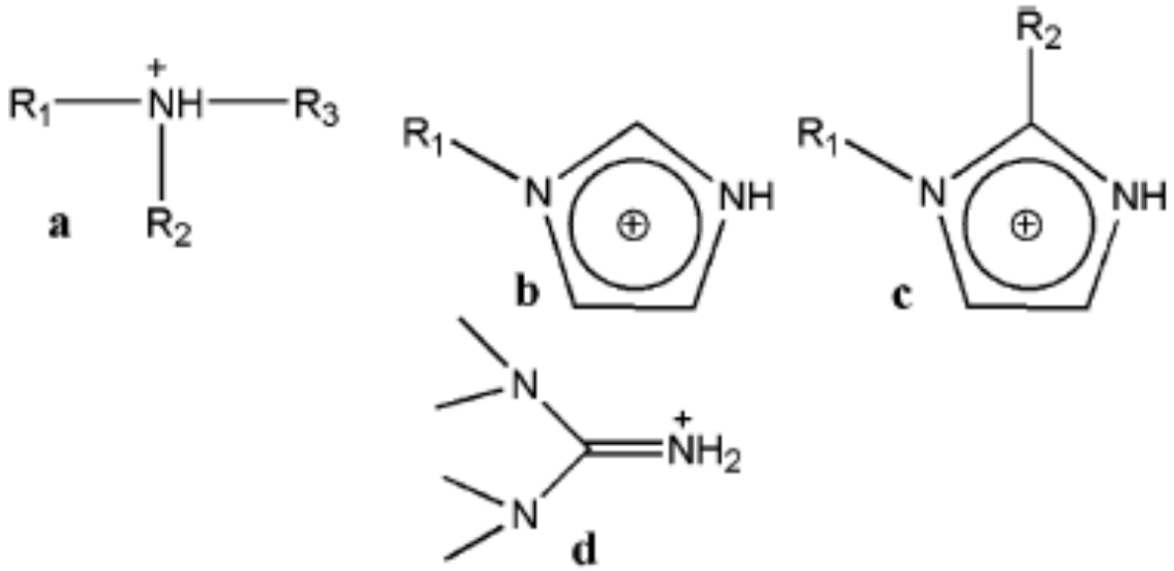

Figure 2.1: Representative PIL cations: (a) ammonium cations, (b) 1-alkylimidazolium cations, (c) 1-alkyl-2-alkylimidazolium cations, and (d) 1,1,3,3-tetramethylguanidinine. Adapted from Greaves and Drummond [48]

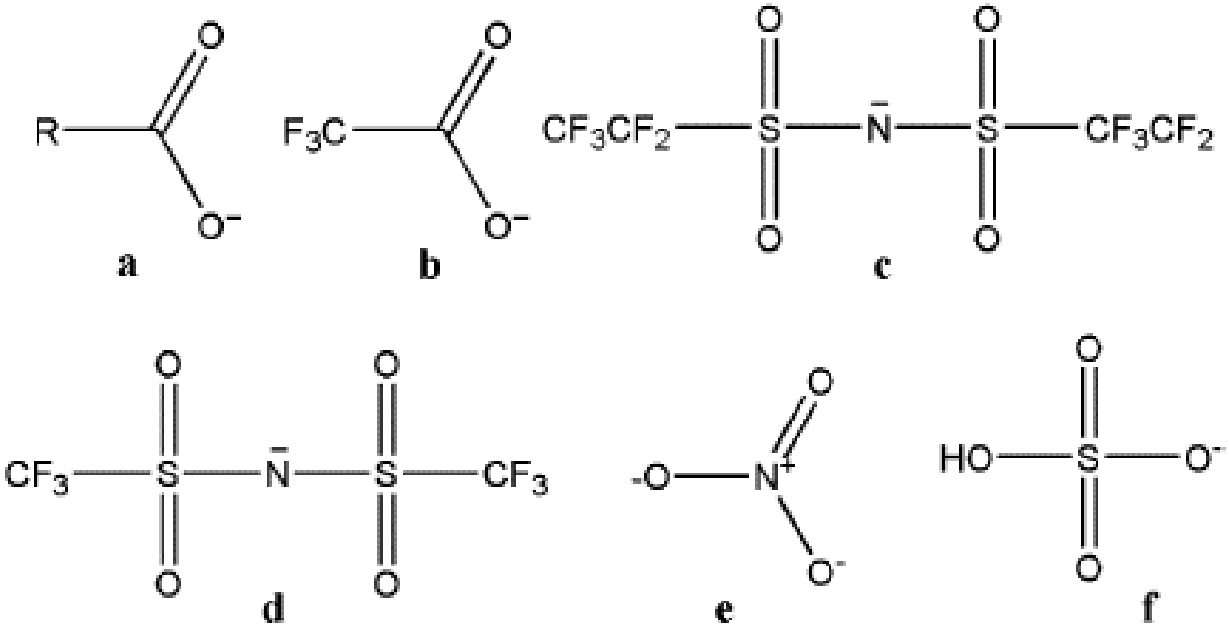

Figure 2.2: Representative PIL anions: (a) carboxylates, (b) trifluoroacetate (TFA), (c) bis(perfluoroethylsulfonyl)imide (BETI), (d) bis(trifluoromethanesulfonyl)imide (TFSI), (e) nitrate, and (f) hydrogen sulphate.[48]

PILs are also used in fuel cell applications, as highlighted in the works of Lee et al. [49], Yasuda and Watanabe [50], and Rana et al. [51]. Another application of interest is their use as lubricants, as illustrated in the works by Qu et al. [25] and Kondo [52]. In addition, PILs can be used as catalysts and solvents in organic synthesis for many types of reactions [53, 54], as solvents in chromatography [55], and in other biological applications [56].

2.1.2 Aprotic ionic liquids (AIL)

AILs, on the other hand, have a broader range of cations that they can be comprised of. The cation types include all the cations used for PILs but all substituents are other than hydrogen, e.g., tetraethylammonium, on the protonated site. The cations used for AILs can be categorised into the following groups: five-membered heterocyclic; six-membered and benzo-fused heterocyclic; ammonium, phosphonium, and sulphonium based; functionalised imidazolium; and chiral as shown in Figure 2.3 [57]. Five-membered heterocyclic cations include imidazolium, pyrazolium, triazolium, thiazolium, and oxazolium. 1-butyl-3-methylimidazolium $[BMIM]^+$ and 1-ethyl-3-methylimidazolium $[EMIM]^+$ are the most commonly studied cations in this category. Six-membered heterocyclic cations have aromatic characteristics. They include one of the most studied cations, pyridinium, and other less studied cations, such as viologen-type, benzotriazolium, and isoquinolinium. Tetraalkylammonium, tetraalkylphosphonium, and trialkylsulphonium based salts, in general, have decreasing melting points with increasing alkyl chain length. Because of their varying properties, such as melting point, viscosity, and stability, they are often used in a wider range of applications compared to the other types of AILs, with tetraalkylammonium as the most studied among them.

Functionalised imidazolium is another class of cations where a functional group is covalently attached to the cation to enlarge the number of applications by expanding and customising the properties for specific applications. Another new class of cations is chiral cations, which are made from chiral molecules or through asymmetric synthesis. However, this class is still in its early stage in terms of synthesis development and application.

Just like cations, many anions can be used to make up AILs. Examples of anions are acetate, tosylate, thiocyanate, hexafluorophosphate $[PF_6]^-$, tetrafluoroborate $[BF_4]^-$, chloride, and alkyl sulphate. Similarly, the choice of anion is based on the properties desired for the application of interest.

The synthesis of AILs can generally be achieved in two steps: the synthesis of the precursor salt with the desired cation and the anion exchange. However, sometimes the latter may not be required if the former step provides the desired IL, e.g., 1-butyl-3-methylimidazolium chloride [BMIM]Cl from 1-methylimidazole with 1-chlorobutane. The synthesis of the salt with the desired cations can be performed with alkylation by nucleophilic substitution using haloalkanes or dialkyl sulfates as alkylating agents for the alkylation of amines, phosphines, or sulphides. However, the reaction temperature and time required for a high yielding alkylation depend on the alkylating agent. For example, reactions with chloroalkanes are the slowest and require high temperatures since they are the least reactive halides [58]. In the second step, the anion exchange, there are generally two methods: through the reaction of halide salts with Lewis acids or by anion metathesis. An example of the former is the preparation of chloroaluminates using aluminium chloride ($AlCl_3$) and chloride salts such as 1-ethyl-3-methylimidazolium chloride [EMIM]Cl. This reaction takes place simply by mixing the two reactants, but it is highly exothermic and needs to be conducted under cooling to remove excess heat and keep at low temperatures below 100 °C to avoid decomposition. In the second method, anion metathesis, two salts exchange their anions using specific techniques depending on the desired IL and whether it is water-soluble or water-immiscible. An example is the preparation of [EMIM]$[PF_6]$ from [EMIM]Cl and hexafluorophosphoric acid ($NaPF_6$) with sodium chloride as a by-product. Reactions R2.2–R2.3 illustrate the steps for the case of AILs prepared from haloalkanes followed by anion exchange with metal salts, where RX is the haloalkane, B is the cation precursor, $[RB]^+X^-$ is the halide IL, MY is the metal salt with the desired anion, $[RB]^+Y^-$ is the desired IL, and MX is the halide salt byproduct.

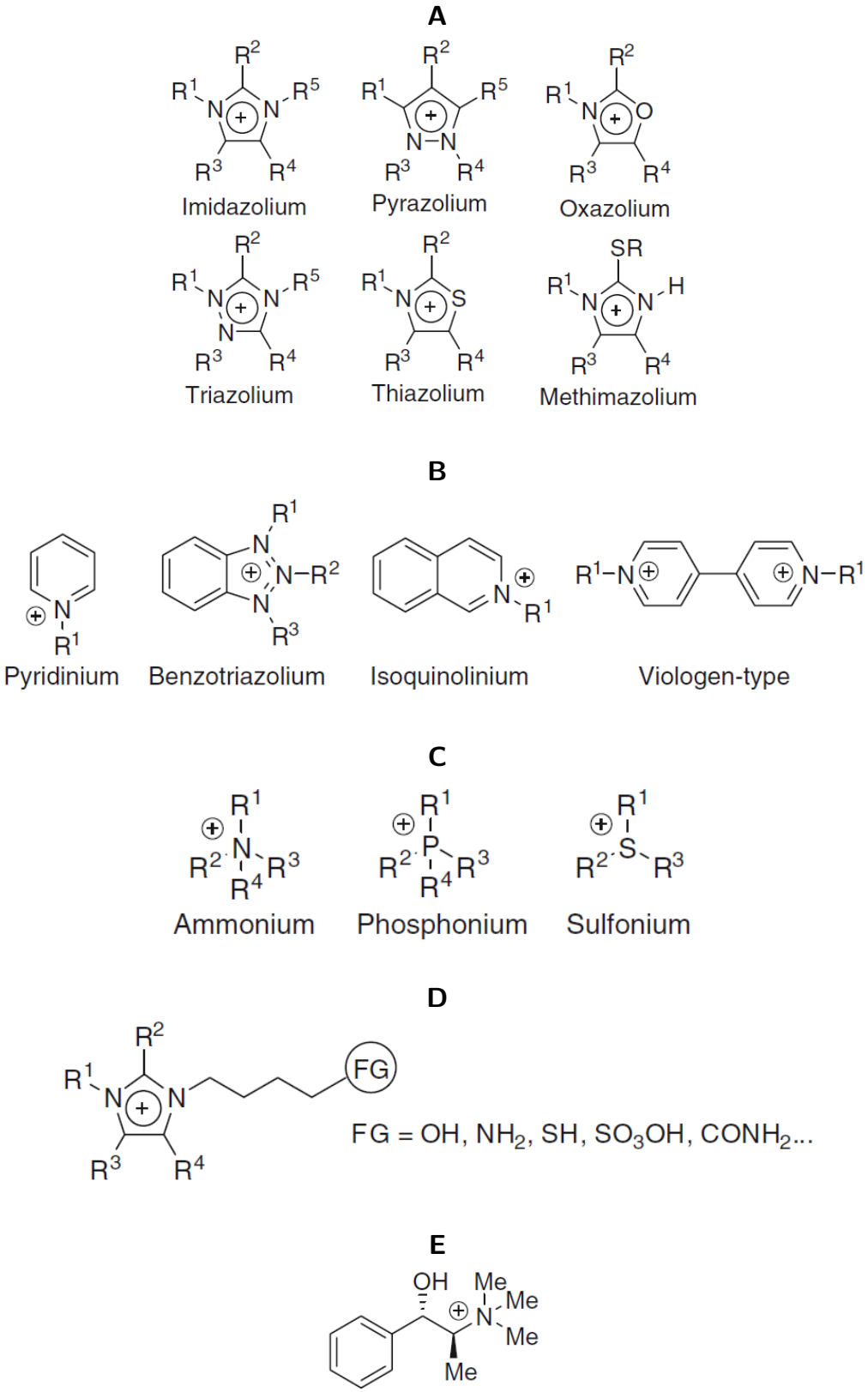

Figure 2.3: Representative AIL cations: (A) five-membered, (B) six-membered, (C) ammonium, phosphonium, and sulphonium, (D) functionalized imidazolium, and (E) chiral ((1S, 2R)-(+)-N,N-dimethylephedrinium).[57]

$$RX + B \longrightarrow [RB]^+X^- \tag{R2.2}$$

$$[RB]^+X^- + MY \rightleftharpoons [RB]^+Y^- + MX \tag{R2.3}$$

Like PILs, there is a growing number of potential applications where AILs can be advantageous over conventional chemicals. For example, AILs can be used in bioprocessing [59], organic synthesis [60], and as electrolytes [61]. Additionally, they can be used in separation technologies. For example, Meindersma et al. [62] tested several AILs for the extraction of aromatics from aliphatics. Accordingly, 4-methyl-N-butylpyridinium tetrafluoroborate [mebupy][BF_4], 4-methyl-N-butylpyridinium methyl sulphate [mebupy][CH_3SO_4], and 1-butyl-3-methylimidazolium tetrafluoroborate [BMIM][BF_4] exhibited the highest performance. Another example is their use in carbon capture, as reported by Li et al. [63], who tested pure and mixed AILs for CO_2 sequestration. It was found that both pure AILs and mixtures are capable of effectively absorbing CO_2 and are easily regenerated. In addition, AILs have been used to remove metals from hydrocarbons. An example is the work of P.J. Corbett et al. [64], who tested a range of AILs to remove metals, like sodium ions, from diesel, and an extraction of up to 99.1% was achieved.

2.2 Economic and Environmental Sustainability of ILs

Generally, there are two approaches for sustainable chemistry. One is making chemical reactions and processes more sustainable, and another by using chemistry to drive sustainability which is the case with ILs. From the discussion above, it is evident that ILs may have a great potential to replace conventional chemicals. However, their economics and environmental performance need to be considered when compared with their conventional counterparts before they can be considered for full commercialisation. In this section, two aspects of sustainability, i.e., economic and environmental aspects, will be reviewed.

2.2.1 Economic performance of ILs

It is well known that the economic aspects of any process are weighted heavily in all feasibility studies before introducing new technologies to the market. It is also an essential component in most comparative studies. As mentioned earlier, one of the potential limitations of the use of ILs is their high cost. However, they have an advantage over their conventional counterparts in that they can be easily recycled during processing due to their low vapour pressures, which results in easier separation and minimal solvent losses. This lowers the consumption of fresh solvent, and hence, can compensate for the high cost. Therefore, it is necessary to assess the economics of manufacturing ILs, and also using them in processing applications when comparing alternatives. The use phase is especially important since it determines the recyclability of ILs and hence the overall amount required.

A good example is an early work by Klein-Marcuschamer et al. [65] where they investigated the economics of using IL for the pretreatment of lignocellulosic biomass. It was concluded that, for the process to be feasible, both IL price and biomass loading need to be reduced while IL recycling needs to be increased. Another techno-economic study by Sen et al. [66], investigated the use of [EMIM]Cl for biomass pretreatment, and the cost of the ILs ($10/kg) was the major contributor to the total cost, which was related to the amount and price of fresh IL used. It was concluded that unless the price of IL is lowered, alternative process configurations need to be developed to lower the consumption of the solvent (0.31 IL/biomass wt%) for the process to be economically feasible. Although these examples are focused on the use of ILs in biorefining applications, and not inclusive of all available economic studies on ILs, many papers reviewing the use of ILs in other technologies such as carbon capture and biodeisel production had similar conclusions, emphasizing the challenge of the high prices of ILs [67, 68].

It is clear from both studies that IL price plays a major role in the economic feasibility of the process. However, the prices of ILs could be a limiting factor under the following scenarios: when the IL prices are derived from their production in small quantities instead of their large-scale production considering economy of scale, and when the ILs are produced in high purity, which may not be necessary for all applications. Both factors can increase the price significantly, and this may affect the outcome of the feasibility study. For example, Chen

et al. [69] conducted an economic assessment to estimate the cost of IL when produced in bulk. A scale-up procedure was used to simulate the industrial process for manufacturing two ILs, triethylammonium hydrogen sulphate [TEA][HSO_4] and 1-methylimidazolium hydrogen sulphate [HMIM][HSO_4]. The lowest reported cost for [TEA][HSO_4] was \$1.24/kg, which was lower than the selling price of acetone and ethyl acetate. Furthermore, the authors suggested that the cost of PILs can be simply estimated from the cost of the acid and the base used to make them and their molecular weights. Although this may be too general, it can be used to get a quick estimation early in the feasibility stage.

Since the work of Chen et al., the idea of inexpensive ILs has gained momentum and more research concerning their economics has been conducted. For example, George et al. [70] investigated the both the performance and the economics of biomass pretreatment using the inexpensive ILs studied by Chen et al. and compared it to a different system using 1-ethyl-3-methylimidazolium acetate [EMIM][OAc], a relatively expensive AIL. The authors concluded that the use of the former not only enhances the process, e.g., by raising the decomposition temperature for higher thermal stability, but can also compete with the cheapest pretreatment chemicals, such as ammonia in terms of pretreatment efficiency and cost effectiveness. This result indicates that ILs can be attractive for large-scale commercialisation. Another study, by Chiappe et al. [71], reported that cost-effective biodiesel from microalgae can be produced using inexpensive PILs. According to the authors, the cost of biofuel from microalgae can be a barrier to large-scale production since it is expensive compared to fossil fuels. However, by using low-cost switchable PILs, the cost of microalgae fuels can be reduced by 75%.

2.2.2 Environmental impact of ILs

The economic assessment results from the examples above are promising and show that ILs can be economically feasible and have the potential to replace existing solvents. However, there have been concerns about the environmental characteristics of ILs for several reasons. One reason is that most ILs are manufactured using lengthy and complex procedures. This is accompanied by the use of conventional solvents, thus shifting the burden upstream, i.e., moving the impacts from the use phase to the production phase. Another reason is that, although ILs usually

have low vapour pressure and usually are chemically stable, they are environmentally stable after disposal, i.e., higher lifetimes and higher exposure [72]. Since most ILs are non-volatile at atmospheric conditions, they end up entering aqueous streams. For this reason, toxicity and bioaccumulation data are required to assess their viability.

Although there were a couple of techno-economic studies on biomass pretreatment using ILs, none have reported their LCA. However, other applications of ILs have reported their LCA. An example is the study by Zhang et al. [34] where the authors compared the use of [BMIM][BF_4] with other conventional solvents, like acetone and water, for the production of cyclohexane and reported the environmental impacts of the different solvents. It was found that [BMIM][BF_4] had the highest footprint in most impact categories including global warming potential. Similarly, Alviz et al. [73] compared the environmental impact of 1-butyl-3-methylimidazolium bromide [BMIM]Br and toluene for the production of acetylsalicylic acid. Since [BMIM]Br is manufactured via a complex and lengthy synthesis route, the results showed a higher ecological footprint for [BMIM]Br, which is more than twice that for toluene. However, when the authors considered another case for the recovery of [BMIM]Br, which is an advantage of using ILs, its impact had been reduced and was lower in several impact categories than toluene at a recovery rate of 89–98%. This result shows that the benefits from the recyclability of ILs may compensate for the initial environmental footprint of manufacturing them.

One of the first experimental studies concerning the biodegradability of ILs was conducted by Gathergood and Scammells [36] using CO_2 evolution tests. They prepared ILs with properties recommended for enhancing biodegradation. The experimental results showed that the most biodegradable ILs on their list, [BMIM][BF_4] and 1-butyl-3-methylimidazolium hexafluorophosphate [BMIM][PF_6], were on the passing level of 60% CO_2 evolution for a biodegradable chemical. In another study, by Neumann et al. [74], nine ILs were evaluated for anaerobic degradation, which is a suitable biodegradation test for waste water treatment processes in the absence of oxygen, using HPLC-UV, and eight out of nine exhibited no change in the initial concentration. This indicates that ILs generally tend to degrade slower than conventional chemicals.

As for the ecotoxicity of ILs, numerous studies have tested and reported their toxicity on several organisms such as bacteria, yeast, and algae. For example, in the study by J. Cornmell et al.

[75], two water-immiscible ILs, trihexyltetradecylphosphonium bis(trifluoromethylsulfonyl)amide [P6,6,6,14][NTf_2] and methyltrioctylammonium bis(trifluoromethylsulfonyl)amide [N1,8,8,8][NTf_2], and two chloride-based ILs, trihexyltetradecylphosphonium chloride [P6,6,6,14]Cl and methyltrioctylammonium chloride [N1,8,8,8]Cl, were tested for their toxicity to microbial cells using Fourier transform infrared analysis. The results showed that all of them caused changes in the spectral fingerprints of the cells with varying degrees. In another study, thirty mice were exposed to 1-octyl-3-methylimidazolium bromide [OMIM]Br to test its toxic effects [35]. The results showed damage to the mouse caused by acute exposure, which resulted in the release of antioxidants in the livers. These few examples show that ILs can be toxic and detrimental to the health of humans and other living species.

Because of the results above and other unknown potential impacts, it is necessary to conduct an environmental assessment of ILs early in the design stage. Considering both economic and environmental performance ensures that the chemicals are not only economically viable but also environmentally benign, enabling more robust and sustainable application. In the following sections, the different assessment methods used to evaluate the sustainability of ILs are reviewed and analysed.

2.3 Sustainability assessment of IL

Sustainability mainly revolves around three interdependent pillars: environment, economy, and society. To improve existing processes and products and to design better alternatives, their sustainability needs to be measured using a combination of experimental data and sustainability assessment methods and tools.

According to Devuyst et al., sustainability assessment is defined as "a tool that can help decision-makers and policy-makers decide which actions they should or should not take in an attempt to make society more sustainable" [76]. In the last decade, the number of articles on ILs has been growing. However, only a few reports have investigated their sustainability using various tools and methods. Generally, the tools used to evaluate the sustainability of ILs can be categorised into metrics-based and holistic approaches, which consist of conventional economic

assessment, environmental (LCA), and integrated approaches. These will be discussed in detail next.

2.3.1 Sustainability metrics

Metrics or indicators are values that are based on defined equations used to measure the quality of a specific indicator, e.g. mass and energy indicators. These metrics are simple to use, can be applied to a wide scope, are quantifiable, and allow for tracking trends [77]. One of the earliest metrics developed is the E-factor, which is an environmental metric that quantifies the amount of waste generated per kilogramme of product as shown in Equation 2.1 [78]. It accounts for the actual waste produced in the process, including the waste from chemicals not involved in the production, such as solvents and catalysts, and can be applied to processes with individual or multiple steps. Atom economy (Equation 2.2) is another environmental metric that is used to measure the amount of reactant that ends up in the final product, using theoretical stoichiometric relations and yields. Products with the lowest stoichiometric amount of waste and by-products are given the highest scores. Unlike the E-factor, atom economy is only applied to single steps and therefore is narrower in scope. Both the E-factor and atom economy have been used as the basis to derive other mass-based metrics and address specific aspects of reactions, e.g., solvent intensity and carbon economy, which measure the amount of solvents used to produce a chemical and the relative amount of carbon in the final product compared to its reactants.

$$\text{E-factor} = \frac{\text{actual mass of total waste}}{\text{actual mass of product}} \tag{2.1}$$

$$\text{Atom Economy} = \frac{\text{molar mass of product}}{\text{molar mass of reactants}} \tag{2.2}$$

Because of their simplicity and convenience, these tools have been widely used to measure and describe the sustainability of various chemical reactions involving ILs [79–85]. To assess the sustainability of 1-alkyl-3-methylimidazolium ILs, Maggel et al. [80] used the E-factor and atom economy to give a score to several different laboratory-scale synthesis routes. Since mass-based scores are not enough to address the problem, and due to a lack of other data, such as energy requirements, the authors included qualitative tools, such as the Strengths, Weaknesses, Opportunities and Threats analysis (SWOT), to combine their mass-efficiency scores with the 12 green principles as well as current and future strengths and weaknesses. However, the combined use of these metrics, e.g. atom economy and E-factor, for measuring the sustainability aspects of processes may lead to overemphasising or double counting some characteristics, e.g., amount of waste. In addition, energy-intensive atom-efficient processes may end up requiring more materials and producing more waste and emissions than an energy-efficient, low atom economy process if, for example, fossil fuels are used to power the process. This can lead to eliminating less atom-efficient alternatives that may be more sustainable than the apparently atom-efficient ones.

Another metric of interest that can be used in parallel with the metrics mentioned above is the cumulative energy demand (CED) [86]. CED measures the total amount of primary energy used in all the processes leading to the final product. This is another common tool that is widely adopted [87–90]. According to Kralisch et al. [91], CED is an indicator of all environmental impact categories, i.e., environmental issues, except for human health and ecotoxicity. Although this may be true in some cases, e.g., where one source of energy is used and assuming all processes are 100% atom-efficient, most products are manufactured using different energy mixes, which can greatly affect their results. Additionally, when mass flows are not accounted for when comparing different products, it is implicitly assumed that these products may use the same raw materials and quantities, and thus, their impact on resources would be equal.

To address these issues, all possible environmental impacts and economic factors need to be characterised and quantified independently. It is worth noting that the simple metrics discussed earlier did not cover economic aspects, and economic assessments have been usually conducted in isolation of other sustainability aspects, i.e., environment and society. Additionally,

all parameters that may affect the overall result need to be considered. For example, quantities and costs of starting materials are not enough to characterise the economics of a product because there are other factors, such as type of equipment, utilities, production rate, recycling, and reaction yield, that should be accounted for. Similarly, all environmental impacts beyond human toxicity and ecotoxicity, such as global warming potential and ozone depletion, need to be considered for full environmental assessment since they also contribute to environmental damage. This can be addressed using holistic approaches, as discussed next.

2.3.2 Holistic approaches

Unlike metrics that use simplified equations to relate an input variable to specific indicators in one or more of the sustainability pillars, holistic approaches refer to one or more of the following:

1. Approaches that consider all input variables and parameters that may affect an indicator in a sustainability domain, e.g., cost determined from a full economic assessment.

2. Approaches where multiple impacts or characteristics in a sustainability domain are considered simultaneously, e.g., using multiple environmental impact categories for environmental assessment.

3. Approaches where two or more sustainability characteristics are integrated to assess different sustainability dimensions simultaneously.

The holistic methods used in the literature for the sustainability assessment of ILs can be further categorised into conventional assessment, life cycle assessment and integrated assessment, where economic and environmental performance are analysed simultaneously.

Conventional economic assessment

A conventional economic assessment refers to the current practices performed by industries and governments to evaluate the economic feasibility of products and services. This is usually conducted by evaluating the various expenses linked to making the desired product. Generally, there are two types of expenses: capital expenses (CAPEX), which are those required to start

operating the plant, like the cost of equipment and start-up; and operating expenses (OPEX) incurred during the operation of the plant, like raw materials, utilities, maintenance, and auxiliary components. Additional parameters, like plant lifetime, interest rate, depreciation, and tax rate, are provided or assumed to complete the assessment.

Such assessments are needed to support the research efforts on ILs and to help make an informed decision about whether they are economically feasible. An example is the work of Sen et al. [66], estimating the CAPEX and OPEX of producing sugars from biomass hydrolysis using [EMIM]Cl. The authors assumed the production rate as a basis and also used a combination of different costing models for the cost of equipment, e.g., the power law for most equipment with a correlation from the literature for other equipment. Another example is the work of Ruth et al. [92], comparing the cost of retrofitting IL-supported membranes to that of amine scrubbing for carbon capture in a power plant. The authors estimated the marginal change in the CAPEX and OPEX due to retrofitting while keeping everything else unchanged.

Although the economic assessment was conducted with varying models and assumptions because a lot of data are lacking at this stage, the results can still be used initially to inform researchers about the feasibility of using ILs for specific applications. However, there are many IL applications other than the examples mentioned above, for which economic viability needs to be evaluated in parallel with their environmental assessment.

Environmental life-cycle assessment (LCA)

To investigate the environmental performance of a product, their impacts in the form of emissions and resource depletion need to be quantified and characterised. LCA is a standardised environmental assessment tool that has been used widely and consists of four phases: goal and scope, inventory analysis, impact assessment, and interpretation. Furthermore, LCA considers the full life cycle of a product, which includes the extraction of raw materials (cradle), production (gate), use and end of life (grave), and in some cases, recycling for reuse. Therefore, when conducting a cradle-to-grave assessment in comparative LCA, it is ensured that the basis on which different alternatives are compared is the same. Additionally, by visualising the different life-cycle stages of a product at the same time, all environmental issues along the chain can be

identified early on for better decision-making.

Regardless of its benefits, there are only a few studies that conducted LCA on ILs [32]. Moreover, these studies can have varying scopes aligned with the different goals of the assessments. For example, the goal of the work by Zhang et al. [34] was to compare [BMIM][BF_4] to other solvents to produce cyclohexane, and the process included in their study was the production of solvent (cradle-to-gate). However, in a study by Peterson [93], the goal was to compare the full life cycle of ILs as a co-fluid with CO2 in refrigeration, and thus, the scope included the use and disposal (cradle-to-grave).

Since ILs are relatively new solvents, data about their production and use are scarce. Therefore, most studies use a combination of known data with various estimation tools to bridge the gap. To estimate missing mass flows for the LCA of [BMIM]Cl, Huebschmann et al. [94] used lab-scale data. In another work, Farahipour and Karunanithi [95] used a combination of data from the literature and simulations for [BMIM][OAc]. Similarly, for missing energy flows, Cuellar Franca et al. [96] used thermodynamic models for the synthesis of trihexyl(tetradecyl)phosphonium 1,2,4-triazolide, while Zhang et al. [34] combined process simulation with reported data for [BMIM][BF_4].

To translate mass and energy flow into impacts, a characterisation method is needed to link them to environmental issues such as global warming potential. Since each of the IL LCA studies had a specific goal, different characterisation methods were used, and different impact categories were selected. For example, Kralisch et al. [91] selected toxicity and energy as indicators, for which toxicity data were used in addition to CED as a characterisation method. Moreover, Righi et al.[97] selected multiple impact categories as indicators, and a more comprehensive characterisation method was used, which is CML 2001.

Finally, in the interpretation step, once results are generated, an uncertainty analysis, i.e., investigates the uncertainty of different variables, is conducted to test the robustness of the results. This is especially important for emerging chemicals such as ILs with low technological readiness levels, and hence, a high degree of uncertainty. However, most of the studies use sensitivity analysis with limited scenarios as an alternative to full uncertainty analysis. An example is the work of Zhang et al. [34], where sensitivity analysis in the form of a range of

values was applied to replace the missing data for intermediate chemicals. Another example is the work of Huebschmann et al. [94], where sensitivity analysis was used to identify key process parameters with the highest impact on LCA results. Although convenient, this simplified approach to uncertainty analysis is limited and does not capture the full range of uncertain scenarios because it does not account for all uncertainties throughout the whole supply chain. For example, uncertainties in LCA assessments may come from all processes leading to the final product and accounting for them is necessary for completeness. Thus, including full uncertainty analysis is crucial in the decision-making process, especially when comparing chemicals that are quite similar in terms of their impacts.

As stated earlier, there is a gap between the number of possible IL applications and the number of their reported LCA results. This is in large part due to a lack of LCA data because ILs are novel chemicals and only a few commercial processes are known, for which such data are inaccessible. Additionally, using different approaches can lead to varying results. For example, a simplified approach based on stoichiometric calculations and not account for process parameters that have an impact on mass and energy flows would have different results than a full assessment that accounts for such variables.

Integrated approaches

As mentioned earlier, sustainable development requires bringing the different elements of sustainability together when comparing alternatives. However, when different criteria are considered, it turns into a multi-criteria decision-making problem, which requires certain analytical tools or weighting methods to solve.

One of the earliest studies that considered different aspects of ILs was the work of Kralisch et al. [38]. The authors compared different solvent options for the different stages of synthesising [BMIM]Cl by looking at their CEDs, human health impacts, ecosystem impacts, and prices. Both CEDs and prices were quantified, whereas the environmental impacts were qualitatively analysed. Although some options can be easily eliminated if their performance is worse than others in all indicators, options with trade-offs need a basis on which they can be ranked before a decision can be made.

One way to solve this problem is by using weighting factors. To compare the environmental and economic performance of different biomass pretreatment options using ILs, Morales used CED, operating cost, and investment cost with equal weighting factors on their normalised values to find the optimal choice [90]. This implies that all indicators have the same weight. In reality, this is not the case because preferences for certain criteria may give them more weight and affect the results obtained for the optimal choice. To avoid such issues, an optimisation procedure combining partial ranking was used by Kralisch et al. [91], with preferences varied to determine the different scenarios under which different optimal results are obtained. Although this method solves the problem of predefining preferences, it still fails to provide a solution that is optimal under all scenarios, since it is preference-based. To address this issue, a relationship between the different criteria or a common goal needs to be established to turn the multi-objective problem into a single-objective problem.

When tackling sustainability problems, multiple interdependent factors need to be looked at wholly rather than individually. For example, most decisions made in industry are economically driven, and thus, can undermine the environmental consequences resulting from such decisions. While this is true, their activities can have impacts on other areas outside their system, such as the environment and society, which are equally important for sustainable development. This instability in other systems can affect the economics of the company, e.g., because of the scarcity of raw materials due to external effects. Therefore, it is necessary to capture these external effects when conducting an economic assessment.

In addition, the integrated approaches reviewed so far have only used a limited number of environmental indicators, which do not cover all the known environmental impacts. What this may fail to address is the possibility of shifting an impact from one category to another. It is critical to ensure that a proposed alternative does not solve an existing issue by creating another one. Therefore, a full assessment of environmental performance using LCA with a broad set of categories covering a wide range of environmental issues is required.

2.4 Thesis contributions

This thesis addresses the gaps identified above by developing a systematic computer-aided framework that integrates life cycle assessment (LCA) and life cycle costing (LCC) with detailed process modelling and simulation. It also incorporates advanced decision-making tools, and approaches to enhance the evaluation of ILs in terms of economic and environmental metrics while promoting the adoption of life-cycle thinking. The developed methods are applied to relevant IL case studies, where different types of ILs are evaluated and compared to conventional chemicals in the context of specific applications.

By assessing ILs use in representative case studies, this research project will focus on two types of ILs: protic alkylammonium ILs and aprotic dialkylimidazolium ILs. Out of the many types of ILs discussed in the literature, these two types were chosen for the following reasons. First, unlike AILs, protic alkylammonium ILs and PILs in general, are not as complicated to synthesise and can simply be made from the transfer of a proton from a Brønsted acid to a Brønsted base, which could have a positive effect on their cost and environemntal impacts. Second, aprotic dialkylimidazolium ILs are considered one of the most studied types of ILs due to their additional beneficial properties, allowing them to be used in many disparate applications. Additionally, due to the complex synthesis of many ILs and the lack of data, the work was limited in scope to the production phase and their performance in selected applications.

In Chapter 3, the methodological framework used throughout this thesis is explained. The framework combines both process design and modelling methods with conventional economic and life-cycle assessments. The former involves a scale-up process of the experimental procedure followed by modelling using process simulation software to quantify the mass and energy flows that are needed as inputs in the assessment stage. The latter is then performed using mathematical programming tools that translate these inputs into economic and environmental indicators.

Chapter 4 presents a novel case study where the general framework established in Chapter 3 is applied. It addresses the importance of developing alternative, cleaner routes for producing ILs. The study compares two routes for producing 1-butyl-3-methylimidazolium tetrafluorob-

orate [BMIM][BF_4], namely metathesis and a halide-free method, using both economic and environmental indicators. The assessment is based on their industrial processes, which are designed using a scale-up procedure from their corresponding experimental procedures. The study is further extended to include the use of [BMIM][BF_4] in fuel desulfurization. Here, both routes of producing [BMIM][BF_4] are compared with conventional fuel desulfurization solvents in both the production phase and the use phase. This Chapter is based on the peer-reviewed paper below: Baaqel, H.; Hallett, J. P.; Guillén-Gosálbez, G. Chachuat, B. (2021). Sustainability assessment of alternative synthesis routes to aprotic ionic liquids: the case of 1-butyl-3-methylimidazolium tetrafluoroborate for fuel desulfurization. ACS Sustainable Chemistry Engineering, 2022, 10, 1, 323–331.

Chapter 5 builds on the framework presented in Chapter 3 to include a method for solving multi-criteria problems, which is applied using a relevant case study. Here, a weighting method based on monetization is used to quantify the cost of environmental impacts in the form of externalities. This method stresses the importance of accounting for both direct and indirect costs to estimate the true cost of chemicals. The case study compares two PILs, namely triethylammonium hydrogen sulphate [TEA][HSO_4] and 1-methylimidazolium hydrogen sulphate [HMIM][HSO_4], with two conventional biomass pretreatment solvents. The evaluation is conducted in both the production phase and the use phase, which considers the biomass pretreatment application. This Chapter is based on the peer-reviewed paper below: Baaqel, H.; Díaz, I.; Tulus, V.; Chachuat, B.; Guillén-Gosálbez, G. Hallett, J. P. (2020). Role of life-cycle externalities in the valuation of protic ionic liquids – a case study in biomass pretreatment solvents. Green Chemistry, 22(10), 3132-3140.

In Chapter 6, the methodological framework presented in Chapter 3 is improved by including uncertainties from different sources that may arise when conducting an LCA of ILs. This approach emphasises the importance of accounting for uncertainties from both background and foreground processes, especially when comparing ILs with a high degree of similarity in terms of their economic and environmental performance. Essentially, the chapter presents an improved framework that involves a detailed uncertainty analysis. The framework also includes a method for improving uncertainty analysis using advanced sensitivity analysis approaches to help

identify key uncertainty parameters, which can be used to further guide research efforts. The framework is demonstrated using a case study that compares [BMIM][BF_4] and [BMIM][PF_6]. The material of this Chapter is based on a working manuscript.

Finally, Chapter 7 ends the thesis with conclusions and perspectives on future work.

Chapter 3

Methodological Framework of Ionic Liquid Sustainability Assessment

This chapter will describe the general methodological framework that will be used throughout this thesis to meet the outlined objectives. The framework consists of the following main components: the life cycle assessment (LCA), the life cycle costing (LCC) and the process system design. An advantage of the framework detailed below is to ensure that both LCA and LCC being consistent in terms of system boundaries, and material and energy flows. The following sections describe the methods and approaches that are used in each of these components.

3.1 Life cycle assessment (LCA) and life cycle costing (LCC)

For sustainability assessment, there is a need for a tool that can check and measure the performance of the core elements, i.e., environment, economy, and society, using consistent methodologies and guidelines to ensure these components are addressed properly. In addition, to perform a full evaluation of products, the system boundaries need to encompass everything related to or associated with the product under investigation. This includes everything from its production to its end-of-life disposal and treatment. Theoretically, even R&D activities early in the design stage should be included whenever possible since such activities are linked

to that product. These requirements can be met with the use of life cycle sustainability assessment (LCSA) [98]. This is a holistic life-cycle framework that consists of three assessment methods: life-cycle assessment (LCA), life-cycle costing (LCC), and social life-cycle assessment (S-LCA) corresponding to the environmental, economic, and social components of sustainability, respectively. The application of S-LCA currently poses many challenges in practice, e.g., choice of indicators and aggregation detail, which are not widely agreed upon in addition to several other limitations, e.g., subjectivity in qualitative data, as discussed in the S-LCA guidelines by UNEP [99]. Additionally, its impacts are still not well defined and there is little information regarding the S-LCA cause-effect chain models for characterising impact accurately [100, 101]. Finally, many of the social impacts depend largely on company's behaviours, which can also vary significantly by its geographic location further complicating S-LCA of ILs at low TRL. Therefore, this work will focus only on the environmental (LCA) and economic (LCC) counterparts, which are discussed next.

3.1.1 Life cycle assessment (LCA)

LCA is the most common environmental assessment method that follows the ISO 14040 standard [102] and has been used by many organisations, including governments, and in various industries for decision-making [103–107]. LCA methodology consists of four phases: goal and scope, inventory analysis, impact assessment, and interpretation. These phases are used to identify the purpose of the LCA study, from which the boundaries are defined, data are collected, and impacts are characterised for analysis and recommendations. In this work, SimaPro software is used to help collect and analyse LCA results [108]. The following section discusses each of these phases in detail.

Goal and scope

An LCA is a simplified model of a real system. To address this issue, the goal and scope need to be defined in a way that ensures consistency throughout. The goal sets the basis on which the remaining phases are formed. When the goal is defined, the application and audience need to be stated, in addition to the purpose.

In the scope, the functional unit, system boundaries, and allocation modelling are defined. The functional unit sets the reference upon which the comparisons of LCA results are based. This is usually chosen such that it reflects the function that the product fulfils. For example, if a comparison is made between two fuels, the functional unit would be one unit of distance travelled, and so on. For system boundaries, the parts of the system included in the study are specified, which mainly depends on the goal. For example, if the goal is to compare similar products with common processes used during their life cycle, only those parts that are uncommon are included. Additionally, the geographical coverage, i.e., what geographical area or region the data represent is also specified. Finally, in processes where there are multiple products, an allocation is used to distribute the environmental impacts between products, which is usually conducted using a physical or economic basis. The former is usually used when the economic values of the products have the same order of magnitude, while the latter is used when the other products have negligible economic value.

Inventory analysis

In this step, the data for all the mass and energy flows are collected. This is the most demanding step because it requires a substantial amount of time and resources to gather the data. Furthermore, the data quality and completeness are key to obtaining reliable results.

Generally, there are two different types of data: foreground data and background data. Foreground data are the data of the system under the control of the decision-maker, whereas background data are those of systems where the decision-maker has no influence and commonly precede those of the foreground system and are already available, e.g., in the literature. In this work, background data will be obtained from the ecoinvent database [109], which is one of the most common LCA databases because it provides reliable, transparent, and accessible data, which are critical for a robust LCA assessment.

One of the main issues with conducting a LCA for ILs is that many processes required for preparing their precursors are inaccessible or unavailable in the literature. To address this, process modelling and simulations are used to collect missing data. Process simulation has been used in many studies of LCA for ILs [93, 95, 97, 110] because it has many advantages, such as

convenience and speed of obtaining results, compared to conventional methods, such as field surveying, where it is infeasible in most cases, e.g., due to data protection. Additionally, to ensure all processes leading to the production of the ILs are considered in the evaluation, a synthesis tree needs to be created. This helps identify missing processes early on, which ensures consistency and completeness of the evaluation.

Synthesis trees can be constructed using a synthesis route that can be obtained from different sources, e.g., handbooks, articles, and patents. Additionally, because of their complexity, most ILs have multiple synthesis routes reported in the literature. However, at this stage, efforts should focus on commercial synthesis routes, or those that can be used on an industrial scale.

However, emissions and waste treatment data are often estimated using proxy data. Using proxy data is a simplified LCA method where data for similar processes or those with similar characteristics are adapted and used to bridge the gap. In this work, the guidelines developed by Hischier et al. [111] are used because they are the same guidelines used in some ecoinvent processes, thus ensuring consistency. The proxy data and methods of obtaining them are presented in Table 3.1.

Impact assessment

In the impact assessment phase, the data collected in the inventory analysis phase need to be linked to environmental impacts and quantified using environmental mechanisms and severity factors. This is referred to as classification and characterisation, both of which depend on the characterisation model used.

In the classification step, the substances released or extracted from nature are linked to one or more environmental issues. For example, carbon dioxide is linked to global warming while other substances, like 1-Chloro-1,1-difluoroethane CFC 142b, are linked to both global warming and ozone layer depletion. Once this step is complete, the quantified emissions and inputs are characterised.

In the characterisation step, the emissions data and inputs are converted to environmental impacts using characterisation factors. These factors usually refer to the impact severity of the substance relative to a reference substance. Environmental impact categories include, but are

Table 3.1: Proxy data used in LCI

Data category	Proxy data	Proxy method
Air emissions	Raw materials	0.2% by mass of inflows are assumed to be vaporized
	Cooling water	4% by volume of total cooling water are assumed to be vaporized
	CO_2	90% by mass of carbon in the waste stream is assumed to be completely burned in waste treatment to produce CO_2 as per the following complete combustion equation: $C_\alpha H_\beta O_\gamma + (\alpha + \frac{\beta}{4} - \frac{\gamma}{2})O_2 \longrightarrow \alpha CO_2 + \frac{\beta}{2} H_2O$
Water emissions	COD	The chemical oxygen demand (COD) or total oxygen consumed is assumed to be equivalent to the amount of oxygen needed to react with the amount of carbon remaining in the waste stream after treatment, which is assumed to be 10% of total carbon
	BOD	For the worst-case scenario, the biological oxygen demand (BOD), which is the oxygen consumed due to biological aerobic digestion by organisms, is assumed to be equivalent to the amount of COD
	TOC	The total organic carbon (TOC) is assumed to be equivalent to 10% of the total carbon in the waste stream, which is the amount of carbon remaining after treatment
	DOC	For the worst-case scenario, the dissolved organic carbon (DOC) is assumed to be equivalent to TOC

not limited to, global warming, human toxicity, water use, resource scarcity, ozone depletion, and acidification. In some models, these impacts can further be grouped into fewer high-level protection areas such as human health and ecosystems.

Here, ReCiPe 2016 [112] is used as the characterisation model. ReCiPe is considered the most recent and harmonised LCA impact assessment tool. The substances in ReCiPe are linked to 17 midpoints that include categories like global warming, toxicity, ozone depletion, and land use, and the severity of their impacts are determined from widely used environmental models. In addition, different impact factors are developed for three different cultural perspectives representing different time horizons, which are the individualist, hierarchist and egalitarian perspectives, from the most optimistic to the most precautionary, respectively. Some of the advantages of using ReCiPe are the set of impact categories, which are considered the broadest among other approaches and rely on impact mechanisms which are globally applicable in terms

of environmental fates and ecosystems.

Interpretation

The final phase in LCA is the interpretation, where the following steps are conducted. First, a hotspot analysis is performed to identify the parts or processes in the system with the highest contributions to environmental impacts. This is used later to make recommendations for improvements. Second, data variation and uncertainties are addressed by uncertainty analysis using approaches like Monte Carlo simulations.

Uncertainties can generally be categorized into two types: foreground uncertainties and background uncertainties. Foreground uncertainties refer to those of data from processes which the LCA modeler can control, unlike background uncertainties which come from processes over which the LCA modeler has no control, and usually retrieved from LCA databases such as ecoinvent. This framework focuses on the latter since they are readily available from the LCA database ecoinvent, which is used throughout this thesis. However, foreground uncertainties need also be accounted for whenever feasible for a complete assessment, and Chapter 6 is dedicated to dealing with these uncertainties using an advanced uncertainty and sensitivity analyses framework to enhance decision-making. Note that different LCA databases and software may address these uncertainties differently, e.g., it could be easier to address foreground uncertainties in GaBi than by using SimaPro with ecoinvent, and hence different approaches maybe required for the comprehensive handling of these uncertainties.

Data uncertainties in the background arising from varying sources, differing quality, and estimations are assessed using the Pedigree matrix proposed by Weidema [113]. In this method, a score $U_{\mathrm{D},i}$ is given from 1 to 5 based on five criteria: reliability, completeness, temporal, geographical, and technological differences. Every combination of scores for the criteria gives a standard deviation value. These values, in addition to a basic uncertainty factor $U_{\mathrm{D,b}}$, are then added up to obtain the geometric standard deviation σ_k. The data are assumed to follow a log-normal distribution:

$$\sigma_k = \exp \sqrt{\ln(U_{\mathrm{D,b}})^2 + \sum_{i=1}^{5} \ln(U_{\mathrm{D},i})^2} \tag{3.1}$$

All the uncertainties starting from the first process are propagated throughout using a Monte Carlo simulation built in SimaPro.

3.1.2 Life-cycle costing (LCC)

LCC refers to any of the methods and tools that are used to estimate the total economic cost of a product or a process over its entire life cycle. Total cost is made up of capital expenses (CAPEX) and operating expenses (OPEX) [114]. The cost of the IL in this work is estimated using the total annualized cost (TAC), which consists of OPEX and annualized CAPEX. The latter represents the annual cost of paying off the fixed capital investment of a plant over its entire lifespan; herein, 330 days of operation a year (equivalent to 7,920 hours) and a 10-year lifetime are assumed. CAPEX covers all costs related to planning, constructing, and commissioning a plant and consists of fixed capital and working capital. However, since working capital is returned at the end of plant life, it is not considered here. Additionally, cost of decommissioning at the end of plant life is omitted in this work, assuming that revenues from depreciated value of equipment material will make up for it. OPEX covers all costs related to operating a plant and consists of variable costs of production and fixed costs of production. Table 3.2 elaborates on what is included for each of these components, how they are calculated, and their contribution to the overall cost. The included costs are selected according to the guidelines of Towler and Sinnott [115]. Fixed capital consists of onsite expenses (ISBL), offsite expenses (OSBL), engineering costs, and contingency charges. ISBL is the main component of the fixed capital cost and the other components are calculated as percentages of ISBL. Generally, there are three approaches for estimating ISBL:

1. Rapid estimation: this method relies on data for existing plants or sections thereof.

2. Factorial method estimation: this method relies on the cost of major equipment and the

remaining components are estimated as factors of the total major equipment cost.

3. Detailed estimation: this is a rigorous method that is usually done later in the final stage of plant design.

Table 3.2: Breakdown of cost estimation. Estimations of offsite capital costs, engineering and construction costs, contingency charges, supervision, salaries, maintenance, land, taxes and insurance, and general plant overhead were obtained from Towler and Sinnott [115]

CAPEX, C_{CAPEX}
Fixed capital, C_{FC}:
Onsite capital costs, C_{ISBL}
Equipment cost
Offsite capital costs, $C_{\mathrm{OSBL}} = 40\%\ C_{\mathrm{ISBL}}$
Engineering and construction costs, $C_{\mathrm{Eng}} = 10\%\ (C_{\mathrm{ISBL}} + C_{\mathrm{OSBL}})$
Contingency charges, $C_{\mathrm{Con}} = 15\%\ (C_{\mathrm{ISBL}} + C_{\mathrm{OSBL}})$
OPEX, C_{OPEX}
Variable cost of production, C_{VCP}:
Raw materials, C_{RM}
Utilities, C_{U}
Fixed cost of production, C_{FCP}:
Operation labour, $C_{\mathrm{OL}} = 720,000\ \mathrm{US\$_{2020}}$[a]
Supervision, $C_{\mathrm{Sup}} = 25\% C_{\mathrm{OL}} = 180,000\ \mathrm{US\$_{2020}}$
Salaries, $C_{\mathrm{Sal}} = 50\%(C_{\mathrm{OL}} + C_{\mathrm{Sup}}) = 450,000 \mathrm{US\$_{2020}}$
Maintenance, $C_{\mathrm{Main}} = 3\%\ \mathrm{C_{ISBL}}$
Land, $C_{\mathrm{Land}} = 1\%(\mathrm{C_{ISBL}} + \mathrm{C_{OSBL}})$
Taxes and insurance, $C_{\mathrm{Tax}} = 1.5\%\ C_{\mathrm{FC}}$
General plant overhead, $C_{\mathrm{GPO}} = 65\%(C_{\mathrm{OL}} + C_{\mathrm{Sup}} + C_{\mathrm{Sal}} + C_{\mathrm{Main}})$

[a]Based on 4.8 operators per shift with three shift positions and an average salary of $50k per operator.

In this work, I use the factorial method because industrial data for most IL technologies and their production processes are inaccessible or not known. In addition, the purpose of this work is to obtain economic and environmental data based on preliminary process flow diagrams, and thus, detailed estimation is not appropriate at this stage. Using this method, C_{ISBL} can be calculated from Equation 3.2.

$$C_{\text{ISBL}} = \sum_{e \in \text{Equipment}} F_e C_e \tag{3.2}$$

with:

C_e, cost of equipment item e

F_e, equipment item installation factor

Due to a lack of data, the cost of equipment is calculated from the correlation in Equation 3.3.

$$C_e = a + bS^e \tag{3.3}$$

with:

a,b, constants

e, equipment type exponent

S, size parameter

Capital costs are inflated to reflect up-to-date costs using the cost indices, as shown in Equation 3.4.

$$\text{Cost}_{\text{new}} = \text{Cost}_{\text{old}} + \frac{\text{Cost index}_{\text{new}}}{\text{Cost index}_{\text{old}}} \tag{3.4}$$

The inflation rate is set using the Chemical Engineering Plant Cost Index, one of the most commonly used published composite indices, which was developed based on four main components: process equipment, construction labour, buildings, and supervision and engineering.

For variable costs of production, like utilities and raw materials cost, data from various sources, like the ecoinvent database [109] and iea statistics [116], are used in this work. The prices from ecoinvent represent a global and long-term average (mostly five years). The mass and energy flows and the type of utility are determined from the simulation results.

3.2 Process system design

The scope of this thesis encompasses all processes related to the production and use of ILs. To conduct such an assessment, all environmental and economic data related to these processes need to be collected. However, if these data are missing or not available, they need to be obtained from process modelling and simulations, as discussed next.

3.2.1 Process synthesis and design

Process synthesis is a step during process design where different process parts or functions are selected and interconnected to define and build a flowsheet [117]. Once the main functions and units are identified, detailed process design is conducted, where design parameters are determined to optimise the flowsheet, e.g., optimal separation sequence. Process synthesis and design represent a bilevel decision-making problem and are interconnected because one cannot be decided until the other is decided. Therefore, the process synthesis-design problem is combinatorial and there are multiple higher-level decisions, which each contain lower-level decisions. The approaches used to solve this problem generally fall under three categories: heuristic-based, mathematical techniques, and hybrids using a combination of the former [118]. The first approach is based on a set of rules and the experience of the engineer, whereas the second is based on a mathematical superstructure representation of all possible flowsheets, where an objective is optimised, e.g., profit maximisation and energy minimisation. Since each assessed IL involves many processes leading up to its production while balancing detail and time efficiency, the heuristic-based approach is used in the present work. This forms an appropriate starting point for initial assessment, after which further optimisation using mathematical approaches can be used when necessary. The following steps are used to generate a flowsheet of a process

for which data is missing.

First, an industrial process is obtained from the literature, if available. The process description should be detailed enough to allow for a complete process flowsheet. However, in many cases, especially for emerging chemicals like ILs, such information is either unavailable or inaccessible. In this case, a process flowsheet needs to be generated from scratch, and to accomplish this, process information must be collected, including design, units, and conditions, in the following order:

1. An industrial production pathway is obtained from the literature, e.g., Ullman's encyclopaedia. These references usually list the most common synthesis routes for common products with a description of how they are produced industrially.

2. When no industrial processes are available, which is the case for most ILs, a lab-scale process is used. Here, a scale-up procedure of the most common lab process is applied to produce a flowsheet that is suitable for industrial use.

Depending on the process information and data availability, one or more of the following guidelines, which represent the hierarchy of process design proposed by Douglas [119], are used in the following order to create and complete a flowsheet:

1. Decide whether the process is batch or continuous. There are several guidelines that determine whether the process is batch or continuous. The main two guidelines are related to operational issues and production rates. For example, if the reaction is slow, i.e., takes hours or days, a batch process is used. In addition, if the production rate is low, i.e., less than 1 x 10^6 lb/yr, a batch process is preferred. The case studies throughout this work evaluate the commercial production of ILs, i.e., at a large scale, with an output of over 10 x 10^6 lb/yr. Additionally, if there is any batch operation, implicit intermediate tanks are used to ensure an overall continuous steady-state process.

2. Draw the structure of the process. This starts with a conceptual design from reaction information using only feeds as inputs and products as outputs, then progresses gradually to a process block diagram after identifying the tasks needed to make the desired product.

For example, the main tasks needed to produce [TEA][HSO_4] from the reaction of 1-methylimidazole and sulfuric acid are reaction and separation. In the reactor, the 1-methylimidazole and sulfuric acid are mixed and converted to [TEA][HSO_4], which is the product. Since reactants in most reactions are not converted 100%, e.g., due to impurities or side reactions, and also due to the use of solvents in some processes, a separation operation is used as a second stage in the process to isolate the product, [TEA][HSO_4] in this case, from excess water used a solvent.

3. Add a recycling structure. The unused materials are recycled for the most efficient material use. In the example of above, the excess water is recycled to minimise waste and reduce fresh water consumption.

4. Add a separation structure. In this step, a strategy is used for designing a separation sequence when a process produces more than one product. Usually, the most volatile component, i.e., the lowest boiling point (BP), is separated first, followed by the second most volatile, and so on. For example, an IL and water mixture in the liquid state are separated by removing water (BP = 100°C) since it has a lower BP than IL. Different types of separators can be used depending on the mixture, its components, and its phases, so more than one type of separation operation may be needed in the same process. For example, a crystallizer is used to separate solid-liquid mixtures while extraction columns are used to separate liquid-liquid mixtures using a solvent system, and so on.

5. Add a heat exchanger network (HEN). Conventionally, the structure of a HEN is determined using pinch analysis [120]. The approach begins first by identifying the hot, cold, and utility streams. Hot streams are streams that need to be cooled down, while cold streams are those that need to be heated up, and utility streams are external streams that are either hot or cold. These are used to supplement or extract excess energy not supplied by the HEN. Then, thermal data, such as inlet and outlet temperatures, heat capacities, and enthalpy difference, are extracted for each stream, and a minimum temperature difference is determined. Temperature-enthalpy diagrams are constructed, known as composite curves, from which the minimum energy required for heating and cooling by utilities and

a minimum number of heat exchangers can be determined. However, instead of using this approach, heat integration is automated using process modelling and mathematical programming tools that optimise both energy and cost, which is discussed in the next subsection.

3.2.2 Process modelling and simulation

After designing the process, it is modelled and simulated to collect necessary data such as the mass and energy flows. In this work, integrated computer-aided tools are used for process modelling and simulation. Commercial simulators, such as Aspen HYSYS and Aspen Plus, based on a sequential modular approach are used for generating and simulating the desired flowsheet. Both tools allow the user to model the different units and overall process for simulating plant operations.

They also have large built-in chemical databases that contain chemicals pure and mixture properties. However, since ILs and novel chemicals are not readily available in their databases, and there is insufficient experimental data, some methods are used for modelling their thermo-physical and mixture properties. Throughout this work, the missing properties are filled in using the following procedure. First, literature-based data obtained from experiments are prioritised because they provide the most reliable data. An example is ILThermo, which is an online database for ILs [121]. The remaining properties can be obtained using various approaches. One such approach involves semi-empirical models derived from group contribution methods. Group contribution methods generally use molecular structures to predict different properties based on the principle that organic groups always behave the same way in different molecules. Examples of where a group contribution method was used include the work of Valderrama and Rojas to estimate the physiochemical properties of ILs [122] and the work of Gardas and Coutinho to predict the viscosity of ILs [123]. Alternatively, the missing properties can be obtained using computational methods and tools based on thermodynamic and quantum chemistry simulations such as COSMO-RS and COSMO-SAC.

Since energy flows can have a significant impact on the economic and environmental results of ILs, enthalpy of formation estimation is necessary for calculating the heat of reaction,

which affects the calculation of the energy requirement. For the heat of formation, the molecular structure of the cation and anion are first drawn and optimised in molecular modelling and graphics software such as ArgusLab, an open-source software, which is used in this work. The structure is then processed using a quantum chemistry tool like MOPAC, an open-source software, also considered here for the charge density profile and calculating the enthalpy of formation. The heat of formation is then calculated from the Born-Haber cycle, as shown in Equation 3.5 below [124].

$$\Delta H^{\circ}_{f_{\mathrm{IL}}} = \Delta H^{\circ}_{\mathrm{f_{cation}}} + \Delta H^{\circ}_{\mathrm{f_{anion}}} - \Delta H_{\mathrm{L}} \tag{3.5}$$

where ΔH_{L} is the lattice energy calculated from Equation 3.6 below [125].

$$\Delta H_{\mathrm{L}} = U_{\mathrm{pot}} + \left[p\left(\frac{n_{\mathrm{m}}}{2} - 2\right) + q\left(\frac{n_{\mathrm{x}}}{2} - 2\right)\right] RT \tag{3.6}$$

where n_{m} and n_{x} are parameters that depend on the nature of the cation and anion, respectively. They are equal to three for monoatomic ions, five for linear polyatomic ions, and six for non-linear polyatomic ions. p and q are the oxidation states of the cation and anion, respectively, and U_{pot} is the potential energy, which is calculated from Equation 3.7 as follows:

$$U_{\mathrm{pot}} = \eta\left(\frac{\rho_{\mathrm{m}}}{M_{\mathrm{m}}}\right)^{1/3} + \delta \tag{3.7}$$

where ρ_{m} is the density and M_{m} is the molecular weight of the IL, while η and δ are coefficients that depend on the stoichiometry of the IL. Finally, the remaining properties can be estimated from the software's built-in property estimation methods, e.g., using the built-in property constant estimation system in Aspen HYSYS.

Finally, while the first four steps of the process synthesis are done manually, heat integration is automated through the use of either the MINLP approach presented by Yee and Grossmann

[126] or similar models based on a stage-wise superstructure. Herein, the energy use and capital expenses of the HEN are optimised simultaneously. Once these models are solved, the minimum required utilities, number and areas of heat exchangers, and the HEN configuration are obtained.

Chapter 4

Economic and Environmental Assessment of the Combined Production and Use of the Ionic Liquid 1-Butyl-3-Methylimidazolium Tetrafluoroborate in Fuel Desulfurization

Abstract

In this chapter, the methodology outlined in the previous chapter is applied to a case study where a one-pot, halide-free production route to 1-butyl-3-methylimidazolium tetrafluoroborate [BMIM][BF_4] is compared against metathesis and two conventional fuel desulfurization solvents, namely acetonitrile and dimethylformamide. Halide-free synthesis is predicted to reduce the cost and environmental impacts associated with the production of [BMIM][BF_4] by two- to five-fold compared to metathesis. By including the use phase of the solvents in fuel desulfurization and accounting for the uncertainty in background data, halide-free [BMIM][BF_4] consistently exhibits the lowest cost and environmental impacts, while dimethylformamide is worst in class. As well as demonstrating the influence of synthesis routes on the sustainability, these results

highlight the need to perform detailed process modelling and include the use phase of solvents for more comprehensive lifeconomic and environmental assessments.

4.1 Context and problem definition

As discussed in Chapter 2, the metathesis route required for making an AIL with the desired anion is complex, and concerns have been raised over the resulting IL purity [127, 128]. For instance, the presence of halides may greatly alter an IL's physical properties [129, 130], or cause catalyst deactivation and poisoning [131, 132]. A purification step, therefore, becomes necessary to remove the halides and obtain the desired purity. This step increases the complexity and cost of the synthesis of AILs, potentially hampering their large-scale production. In response to this, i.e., to tackle chloride impurities, which are undesired from an application point of view, halide-free routes have been developed [57]. By avoiding unnecessary purifications steps, these routes could potentially minimise waste and unnecessary intermediate reactants, reducing cost and environmental impacts . One such route is the direct synthesis of 1,3-disubstituted imidazolium tetrafluoroborate that avoids the anion exchange step altogether [133].

The overall sustainability performance of AILs remains unclear because the impact of their synthesis may not be as sustainable as their subsequent use within a process [134, 135]. Conventional synthesis pathways for the most common AILs are complex, while the use of VOCs as part of these pathways, either directly as raw materials or indirectly as solvents, raises concerns about their environmental performance. Therefore, further studies are required to quantify their environmental impact more accurately.

LCA methodology quantifies the environmental burdens of products across their entire life cycle, from resource extraction (cradle) to use (gate) and disposal (grave) [136]. Although LCA has been conducted for a wide range of chemicals [137], it has been scarcely applied to ILs [138]. Furthermore, most LCA studies of ILs rely on simple models, such as stoichiometric and heat of formation calculations or approximations, rather than detailed first-principles process models [34, 38, 96, 139, 140]. The latter addresses the shortcomings of the former by accounting for many missing parameters, such as process efficiency, utilities, and material losses, not to mention enabling process optimisation by applying mass and heat integration. Additionally, previous reports focus on conventional IL synthesis routes. In contrast, alternative synthesis procedures, such as halide-free synthesis, have remained largely unexplored. A recent comparative LCA

of two PILs using detailed process modelling has also highlighted the need to include the use phase of solvents in the analysis to ensure a meaningful comparison [141].

One potential application for ILs is the removal of sulphur compounds from fuels, which remains an ongoing challenge in the oil refining industry due to ever more stringent regulations. Besides causing catalyst poisoning in automotive catalytic converters, sulphur oxides emitted by fuel combustion have deleterious effects on human health and ecosystems [142–144]. Conventional solvents for oxidative desulfurization of fuels using liquid-liquid extraction include acetonitrile and dimethylformamide (DMF) [145]. ILs are an attractive alternative to these organic solvents because of their low volatility, ease of recycling, and high thermal stability, while their high tunability may enable tailor-made solvent extractions [146]. In particular, imidazolium ILs, such as 1-butyl-3-methylimidazolium tetrafluoroborate [BMIM][BF_4], can attain higher desulfurization levels than traditional hydrodesulfurization [147].

For the first time, this case study compares the economic and environmental performance of [BMIM][BF_4] with that of the conventional fuel desulfurization solvents, namely acetonitrile and DMF. The analysis considers the metathesis and one-pot halide-free synthesis routes of [BMIM][BF_4] by building on published experimental protocols and data [133, 148] in combination with detailed process modelling for quantifying the cost and environmental impacts of IL production on an industrial scale. Furthermore, the analysis covers both the production phase and the use phase of the solvents. This methodology is detailed in the following section, followed by the results and conclusions.

4.2 Materials and methods

Inventory and cost data for the production of [BMIM][BF_4] via both routes (metathesis and halide-free) are currently unavailable in commercial LCA databases. To bridge this gap, detailed process models were developed by scaling up the available experimental procedures [133, 148]. This is a standard approach for predicting the performance of processes at a low technology-readiness level [149]. The same strategy is applied to model the production of various precursors of [BMIM][BF_4], for which data are also missing—synthesis trees for [BMIM][BF_4] are shown in

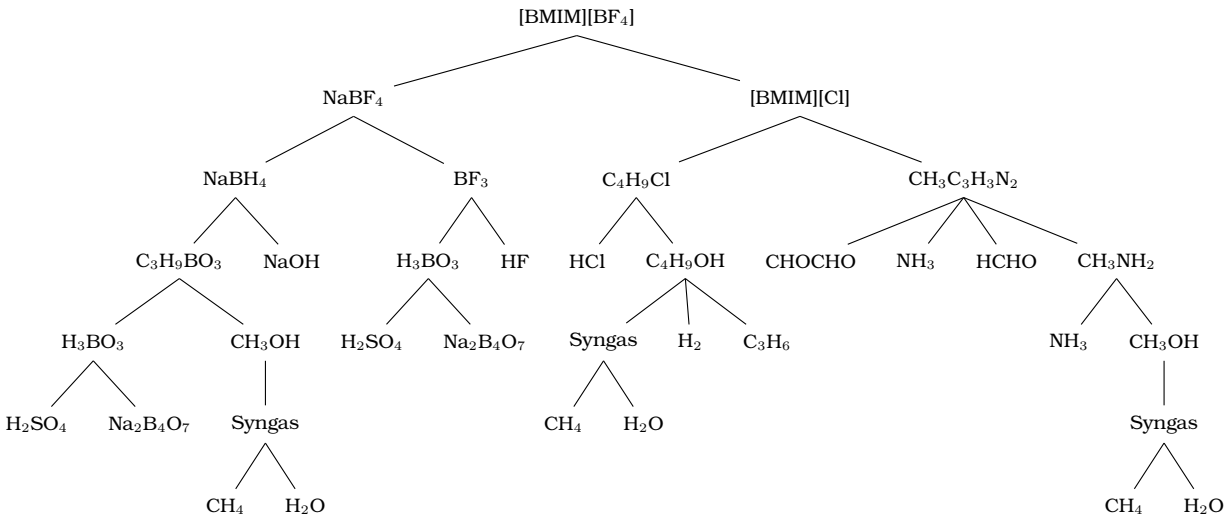

Figure 4.1: Synthesis tree of [BMIM][BF_4] using the metathesis route

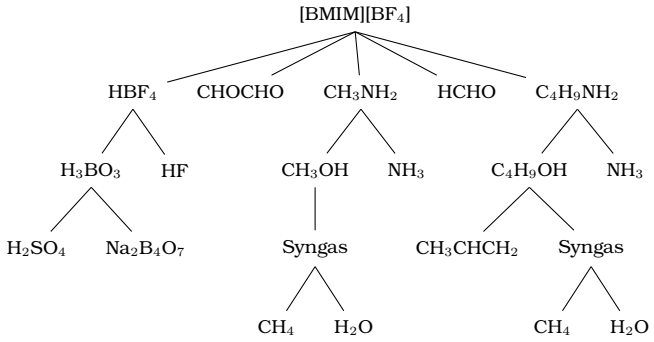

Figure 4.2: Synthesis tree of [BMIM][BF_4] using the halide-free route

Figures 4.1 & 4.2. The relevant process models and the methods and tools used to conduct the assessment are described in the following subsections.

An important difference between the metathesis and halide-free routes is that the former process yields an aqueous solution of [BMIM][BF_4], whereas the latter results in an aqueous solution of [BMIM][BF_4] with 1,3-Di-N-butylimidazolium tetra uoroborate [BBIM][BF_4] and 1,2,3-trimethylimidazolium tetra uoroborate [MMIM][BF_4] in a 5:4:1 molar ratio (details below). However, given the small difference in key physical properties caused by the change in cation (see Appendix A), the behaviour of the IL mixture shall herein be assimilated to a different technical grade of [BMIM][BF_4] regarding its desulfurization efficiency. A confirmation of this performance similarity can be found in the work of Souza et al. [133].

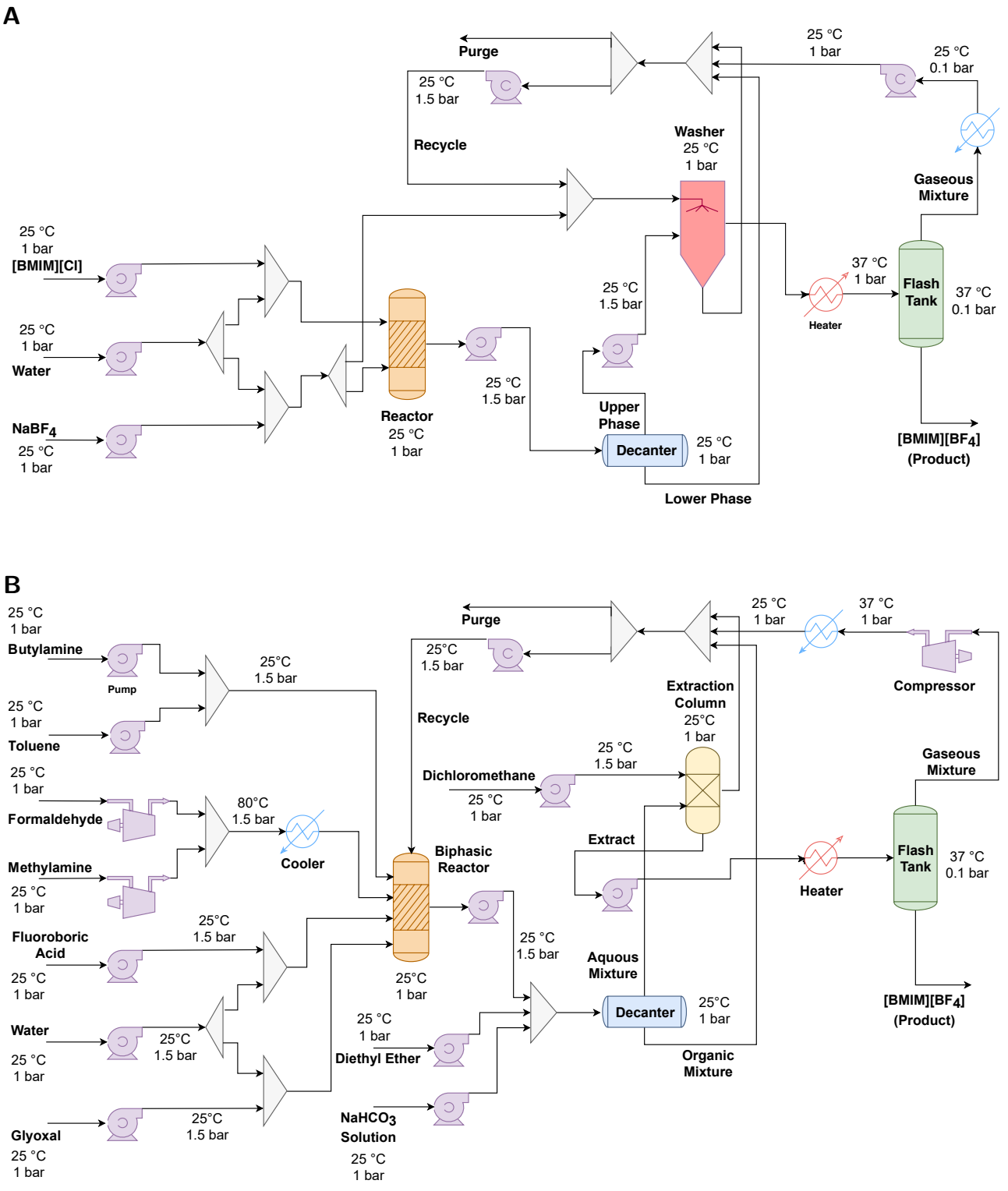

Figure 4.3: Process flow diagrams for the production of [BMIM][BF_4] from the metathesis route (A) and the halide-free route (B).

4.2.1 Modelling of AIL production processes

The process simulations for both synthesis routes of [BMIM][BF_4] were conducted in Aspen HYSYS® (version 9). The relevant process models are detailed next.

[BMIM][BF_4] production via the metathesis route The synthesis of [BMIM][BF_4] proceeds via anion exchange between 1-butyl-3-methylimidazolium chloride [BMIM]Cl and sodium tetrafluoroborate $NaBF_4$, producing solid sodium chloride (NaCl) as a by-product—see Reaction R4.1. The scaled-up manufacturing process (Figure 4.3A) is based on the experimental procedure described by Chen et al. [148]. [BMIM]Cl is mixed with an excess of $NaBF_4$ under atmospheric conditions. The reaction mixture is separated into an upper phase, which contains the main aqueous product with impurities and a lower phase containing solid NaCl and undissolved $NaBF_4$. The upper phase is sent to a 3-stage washer using $NaBF_4$ solution to remove impurities. In the final step, [BMIM][BF_4] is separated from water in a vacuum flash vessel, resulting in aqueous [BMIM][BF_4] with 25 wt% water content.

$$[\mathrm{BMIM}]\mathrm{Cl} + \mathrm{NaBF_4} \longrightarrow [\mathrm{BMIM}][\mathrm{BF_4}] + \mathrm{NaCl} \tag{R4.1}$$

The production process of the [BMIM]Cl precursor (Figure A.1) is based on the experimental procedure reported by Baba et al. [150]. It starts by mixing 1-methylimidazole in toluene with excess 1-chlorobutane and running the reaction at 112 °C under atmospheric pressure. [BMIM]Cl is separated in a vacuum flash vessel from toluene and other unreacted materials, which are returned to the reactor.

The precursor 1-methylimidazole is synthesised using the Debus-Radziszewski method (Reaction R4.2)[151]. Glyoxal, formaldehyde, methylamine, and ammonia react in equimolar ratios and condense to form water and 1-methylimidazole. This reaction takes place at 50–100 °C in water with a yield between 60–85%.

$$(\mathrm{CHO})_2 + \mathrm{CH_2O} + \mathrm{CH_3NH_2} + \mathrm{NH_3} \longrightarrow \mathrm{H_2C_2N(NCH_3)CH} + \mathrm{H_2O} \tag{R4.2}$$

LCA inventories for this synthesis were previously estimated by Righi et al. [97]. Because of a lack of details about the process configuration and operating conditions and the fact that neither process water nor cooling water was reported, these inventories could not be used here. Instead, a scaled-up process is developed (Figure A.2) using the standard method by Douglas [119], which is consistent with the modelling methodology of ionic liquid production. Equimolar amounts of the four reactants are mixed in water at 25 °C under atmospheric pressure. This mixture is pressurised to 3 bar and then cooled down to 80 °C before entering a biphasic reactor, where it reacts at 80 °C and 2.5 bar to form the 1-methylimidazole and water with 75% conversion. The outlet liquid stream from the reactor is depressurised to 1.5 bar and heated up to 98 °C using steam, then feeds into a flash drum to separate the aqueous mixture of 1-methylimidazole from the unreacted feed products and steam in the flashed gas. The outlet gas stream from the reactor is mixed with this flashed gas and recycled back to the reactor. This recycled stream is cooled down to 25 °C and compressed to 3 bar, and a 10% purge is applied.

Finally, the production of 1-chlorobutane (Figure A.3) starts by reacting 1-butanol with an excess of hydrochloric acid at 120 °C [152]. The reaction mixture is cooled down to 25 °C and sent to a flash vessel tank, where the vapour phase containing mainly hydrochloric acid is separated. Next, the liquid phase is reheated to 69 °C and sent to a second flash vessel, where 1-chlorobutane is isolated from the residual 1-butanol and excess water.

[BMIM][BF_4] production via the halide-free route. This alternative synthesis route of [BMIM][BF_4] (Figure 4.3B) is based on the experimental procedure developed by Souza et al. [133]. Equimolar amounts of n-butylamine in toluene, formaldehyde, methylamine, glyoxal, and fluoroboric acid are reacted under atmospheric conditions to directly produce [BMIM][BF_4]—see Reaction R4.3. Diethylether and saturated sodium bicarbonate are added to the reaction mixture, which is then separated into an aqueous phase containing the IL and an organic phase. The aqueous phase is sent to an extraction column, where the desired IL is separated using dichloromethane. The remaining impurities are removed in a final vacuum flash vessel resulting in a mixture of [BMIM][BF_4], [BBIM][BF_4], and [MMIM][BF_4] in a 5:4:1 molar ratio with 25 wt% water content.

$$CH_2O + C_2H_2O_2 + C_4H_{11}N + CH_3NH_2 + HBF_4 \longrightarrow [BMIM][BF_4] + 3H_2O \quad \text{(R4.3)}$$

Fluoroboric acid is synthesised by reacting hydrogen fluoride with a boric acid solution at 80 °C under atmospheric pressure (Figure A.4). The conversion of this exothermic reaction is close to 100%.

Physical property estimation [BMIM][BF_4], [BBIM][BF_4], [MMIM][BF_4], [BMIM]Cl, 1-methylimidazole, fluoroboric acid, boric acid, sodium bicarbonate, and $NaBF_4$ are currently unavailable in the Aspen HYSYS database; hence, pseudo-components were created to estimate their properties. The methodology is described in Chapter 3, while the complete set of properties is reported in Tables A.1–A.9 in Appendix A. Physical properties, such as densities, were retrieved from the literature [121]. Critical properties and normal boiling points of the ILs were estimated using the group contribution method established by Valderrama and Rojas [122]. Properties of the other pseudo-components were estimated from their molecular structure using the Aspen HYSYS built-in property constant estimation system. The heat of formations were determined via quantum calculations.

4.2.2 Economic assessment

The production cost of [BMIM][BF_4] was estimated via the total annualised cost (TAC) of the scaled-up processes. The TAC is expressed on a per-weight basis of solvent or a per-weight basis of desulfurized fuel, in agreement with the chosen functional unit in the environmental assessment (see below). The costing method presented by Towler and Sinnott [115] was applied for the TAC, which adds up the OPEX and the annualised CAPEX—see the full methodology in Chapter 3 and Table 3.2. The inflation rate was set based on the Chemical Engineering Plant Cost Index. The costs of raw materials and utilities were sourced from ecoinvent 3.5[109] and are listed in Table A.10, while the CAPEX and other OPEX data relative to the production of [BMIM][BF_4], [BMIM]Cl, 1-chlorobutane, and fluoroboric acid are reported in Tables A.11–A.20.

For consistency, all of these costs are expressed in US$2020 using currency conversion and inflation factors.

4.2.3 Environmental assessment

The LCA follows the ISO 14040 principles and was conducted using the SimaPro software (version 9.0) interfacing with ecoinvent 3.5[109].

1. Goal and scope The goal of the analysis is two-fold: (i) to compare two production routes for the synthesis of [BMIM][BF_4] and (ii) to compare the performance of [BMIM][BF_4] with that of acetonitrile and DMF for fuel desulfurization. The functional units are defined as "1 kg of solvent" according to objective (i) and "1 kg of desulfurized fuel" to encompass the use phase according to objective (ii). A cradle-to-gate scope is adopted in response to both objectives, which includes all processes from raw material extraction to the actual solvent production and use, but excludes any further processing or waste management after the solvent use. Furthermore, it is assumed that [BMIM][BF_4] is the single product of both process alternatives, so no allocation is needed, and the geographical location is chosen as Europe.

2. Life-cycle inventory (LCI) The mass and energy flows for the two production processes of [BMIM][BF_4], and the associated precursors, are predicted via process simulation in Aspen HYSYS because they are unavailable in ecoinvent. These are combined with inventory data gathered from ecoinvent for the background processes to quantify the life-cycle inventories of [BMIM][BF_4]. A complete list of the foreground inventory flows, expressed for the functional unit of "1 kg of solvent", can be found in Tables A.21–A.25.

3. Life-cycle impact assessment (LCIA) The LCI entries are converted into environmental impacts using the ReCiPe 2016 methodology [112]. These impacts are first categorised into 18 midpoint indicators, including global warming, toxicity, ozone depletion, and land use, and then further aggregated into three endpoint categories: the damage areas of resources, human health, and ecosystems quality. Furthermore, the assessment follows the hierarchist perspective, which is based on the cultural theory of scientific agreement and adopts a medium timeframe of 100

Table 4.1: Fuel desulfurization data for functional unit conversion

solvent type	**fuel type**	**solvent-to-fuel ratio**	**extraction efficiency**	**solvent loss**	**solvent make-up**	**ref.**
[BMIM][BF_4] metathesis	light fuel oil	$1.40\,\mathrm{kg\,kg^{-1}}$	55%	0.3%	$0.008\,\mathrm{kg\,kg^{-1}}$	[157]
[BMIM][BF_4] halide-free	light fuel oil	$1.40\,\mathrm{kg\,kg^{-1}}$	55% ±5%	0.3%	$0.008\,\mathrm{kg\,kg^{-1}}$	[157]
acetonitrile	gasoil	$0.94\,\mathrm{kg\,kg^{-1}}$	82%	5%	$0.058\,\mathrm{kg\,kg^{-1}}$	[158]
dimethylformamide	gasoil	$1.14\,\mathrm{kg\,kg^{-1}}$	92%	13%	$0.160\,\mathrm{kg\,kg^{-1}}$	[158]

years for environmental impacts. The complete ReCiPe midpoint and endpoint results are given in Tables A.26 & A.27 for the functional unit of "1 kg of solvent", respectively.

Expressing these environmental impacts in terms of the second functional unit of "1 kg of desulfurized fuel" entails the application of conversion factors that reflect the need for solvent makeup based on process performance for sulphur extraction. The applied conversion factors consider the extraction efficiency, solvent-to-fuel ratio, and percentage loss, as summarised in Table 4.1 with the corresponding data sources, which are based on 99.5% sulphur removal, so the sulphur content of the desulfurized fuel is below 0.5 wt% [153]. To make up for the lack of process data for IL solvent loss, a percentage loss is estimated from the IL solubility in fuel oil [154]. Because the solubility of [BMIM][BF_4] in aromatics is much higher than in aliphatic molecules and cycloalkanes [155], it is assumed that the desulfurized fuel only contains aromatics to stay conservative. The resulting estimate of 0.3% solvent loss is obtained by averaging the solubilities of [BMIM][BF_4] in benzene, toluene, o-xylene, m-xylene, and p-xylene [156].

4. Interpretation and uncertainty analysis The final phase of LCA entails checking that the conclusions are well-substantiated, typically using uncertainty quantification. Regarding the multiple sources of uncertainty that can affect the calculations herein, the focus remains on uncertainty in background inventory data. This uncertainty arises from a combination of factors and is modelled using the Pedigree matrix [113, 159] in SimaPro (cf. Chapter 3). Specifically, the life-cycle inventory entries are assumed to follow log-normal distributions with standard deviations resulting from the aggregation of uncertainty factors (Tables A.21–A.25). Each of these factors is quantified based on several data quality indicators describing the reliability, completeness, temporal correlation, geographical correlation, technological state, sample size,

and expert judgement related to the data. The uncertainty in the life-cycle inventory entries is propagated to the environmental impacts using Monte Carlo sampling in SimaPro. Finally, an additional 5% uncertainty factor was applied to the desulfurization efficiency of the halide-free [BMIM][BF_4] (cf. Table 4.1). This factor represents 10% of the 53% (wt%) fraction of [BBIM][BF_4] and [MMIM][BF_4] in the aqueous IL solution.

4.3 Results and discussion

4.3.1 Economic assessment

The bar chart in Figure 4.4 compares the production costs of [BMIM][BF_4] with those of acetonitrile and DMF on a per-weight basis to reflect current commercial practice for solvent. The production cost of [BMIM][BF_4] using the halide-free method ($6.4/kg) is predicted to be nearly half that of the metathesis route ($11.8/kg). Notably, the contributions of the annualised CAPEX and fixed OPEX to both production costs are negligible in comparison to the variable OPEX—the corresponding figures can be found in Appendix A. The difference in variable OPEX is attributed to the high price of $NaBF_4$, which is used as a reactant and in the washing steps—none of the $NaBF_4$ is recycled in this process after it has been used and contaminated with impurities. Overall, feedstock procurement contributes about 98% of the variable OPEX for the metathesis route, and reduces down to 59% in the halide-free synthesis, where utility costs for compression (electricity) contribute a significant 40%. Nevertheless, even the production cost of halide-free [BMIM][BF_4] remains about 4-fold higher than those of acetonitrile ($1.57/kg) and DMF ($1.75/kg). This large difference is a result of the relatively inexpensive raw materials required for these organic solvents. The production of acetonitrile from propylene ($1.20/kg) and ammonia ($0.56/kg) via the Sohio process is slightly cheaper than the production of DMF from dimethylamine ($1.57/kg) and CO ($0.72/kg).

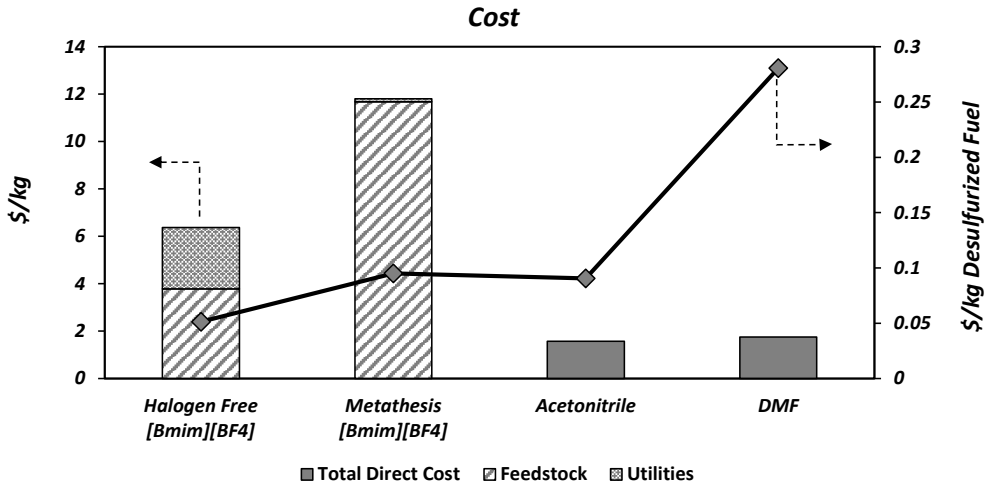

Figure 4.4: Cost comparison of [BMIM][BF_4] and organic solvents. Annualised CAPEX values are not shown since they make up less than 0.05% of the total cost.

A radically different picture emerges after accounting for the use phase of the solvents. The superimposed line chart in Figure 4.2 compares the use costs of [BMIM][BF_4] with those of acetonitrile and DMF on a per-weight-of-desulfurized-fuel basis to reflect the variation in process performance for sulphur extraction across the range of solvents (cf. Table 4.1). Notably, halide-free [BMIM][BF_4] becomes the cheapest option ($0.05/kg desulfurized fuel), while metathesis [BMIM][BF_4] becomes comparable with acetonitrile ($0.09/kg desulfurized fuel) and significantly cheaper than DMF ($0.28/kg desulfurized fuel). These results are explained by the reduction in the amount of IL solvent makeup required to extract the same amount of sulphur from sour fuel compared to the more volatile organic solvents, recalling that the makeup of IL is 7 and 20 times lower than the makeup of acetonitrile and DMF, respectively.

4.3.2 Environmental assessment

The bar charts in Figure 4.5 summarise the LCA results for all three endpoint damage categories—human health, ecosystem quality, and resources—on a per-weight basis of solvent. The complete set of midpoint and endpoint indicators for all four solvents are reported in Tables A.26 & A.27. Note that the midpoints and endpoints are complementary in the sense that the indicators at the midpoint level have stronger relation to environmental flows with low uncertainty, while those at the endpoint level provide better information on the environmental relevance of the

mass and energy flows, and easier to communicate, but with higher uncertainty due to higher aggregation level of the characterization factors.

The production of [BMIM][BF_4] via the halide-free route greatly alleviates the damage on human health (79%), ecosystem quality (80%) and resources (67%) compared to the metathesis route. Such improvements are the result of a shorter synthesis tree (compare Figures 4.1 & 4.2) and fewer processing steps (compare Figures 4.1A & 4.1B). Producing the precursors in the metathesis route is by far the main hotspot, making up over 95% of the impacts in all three damage areas. The precursors in the halide-free process are also contributing over two-thirds of the endpoint impacts, followed by utilities (mostly electricity), with a share between 24–31% in each damage area. But regardless of the selected [BMIM][BF_4] route, the production of acetonitrile or DMF is predicted to have lower impacts in all three damage areas. For instance, DMF has a lower impact than metathesis [BMIM][BF_4] on human health, ecosystem quality, and resources by 90%, 91%, and 80%, respectively. Only under the resource damage area is halide-free [BMIM][BF_4] comparable to acetonitrile, but still significantly worse in other damage areas or in comparison to DMF. Notably, the values of several midpoints of [BMIM][BF_4] vary from those reported by Zhang [34]. This is mainly due to the reaction yields, heating and cooling requirements, separation efficiency, waste, and emissions, all of which are not accounted for in the simplified version. This holds not only for IL production but also for their precursors.

The main impacts on human health caused by the production of any of the solvents are attributable to particular solvent precursors: for [BMIM][BF_4] via metathesis, the production of $NaBF_4$ (65%) and [BMIM]Cl (32%); for halide-free [BMIM][BF_4], fluoroboric acid (31%), butylamine (21%), and dichloromethane (12%); for acetonitrile, propylene (34%) and ammonia (26%); and for DMF, dimethylamine (50%) and carbon monoxide (26%). The main midpoint contributions to this endpoint damage area, for either [BMIM][BF_4] routes, are global warming and fine particulate matter formation. Global warming is mostly caused by CO_2 emissions from burning fossil fuels, such as coal and natural gas, for heat and electricity production. Particulate matter formation is mainly attributed to sulphur dioxide, emitted either from sulphuric acid production, which is needed to make boric acid, or by fossil fuel combustion for electricity generation, and to particulate matter with diameters ¡ 2.5 µm, which are emitted by lignite

combustion for electricity generation.

The production of the solvent precursors also cause the largest impacts on ecosystem quality: in the case of [BMIM][BF_4] via metathesis, the production of $NaBF_4$ (51%) and [BMIM]Cl (45%); for halide-free [BMIM][BF_4], fluoroboric acid (25%) and butylamine (23%); for acetonitrile, propylene (37%) and ammonia (25%); and for DMF, dimethylamine (54%) and carbon monoxide (22%). The largest midpoint contributions to this endpoint damage area, for either [BMIM][BF_4] routes, are global warming (>50%), acidification, terrestrial ozone formation, and water consumption. Terrestrial acidification is mostly caused by sulphur dioxide (>75%) emitted from sulphuric acid production. A majority of the ozone formation impacting terrestrial ecosystems in [BMIM][BF_4] via metathesis is attributed to toluene emissions (67%) as part of the production of [BMIM]Cl, while in halide-free [BMIM][BF_4], it is attributable to NOx emissions (85%) from transportation activities. Lastly, water consumption is mainly associated with hydroelectricity production.

Over 99% of the impacts caused by either [BMIM][BF_4] routes concerning the resource damage area are due to fossil fuel scarcity. In the metathesis route, these impacts are mostly attributed to the production of [BMIM]Cl (56%) and $NaBF_4$ (42%) precursors. In the halide-free synthesis, they are associated with the production of butylamine (29%), diethylether (15%), glyoxal (13%), and fluoroboric acid (13%) precursors. Such resource depletion is, to a large extent, caused by the use of natural gas for the production of methanol, electricity, and other utilities (>45%) and crude oil for the production of fossil-intensive chemicals such as ethylene and propylene (>45%). Regarding acetonitrile, 77% of the impact on resources is attributed to propylene production and another 14% from ammonia production—using natural gas feedstock. For DMF, dimethylamine production from methanol and ammonia makes up 65% of the impact on resources, and carbon monoxide contributes another 21%.

The superimposed line charts in Fig. 4.5 represent the solvent impacts on a per-weight-of-desulfurized-fuel basis. As with the economic assessment earlier, accounting for the use phase of solvents depicts a completely different outcome from the bar charts, whereby [BMIM][BF_4] is now competitive with acetonitrile and DMF under all three damage areas. The halide-free synthesis of [BMIM][BF_4] is even predicted to reduce all endpoint environmental damages by

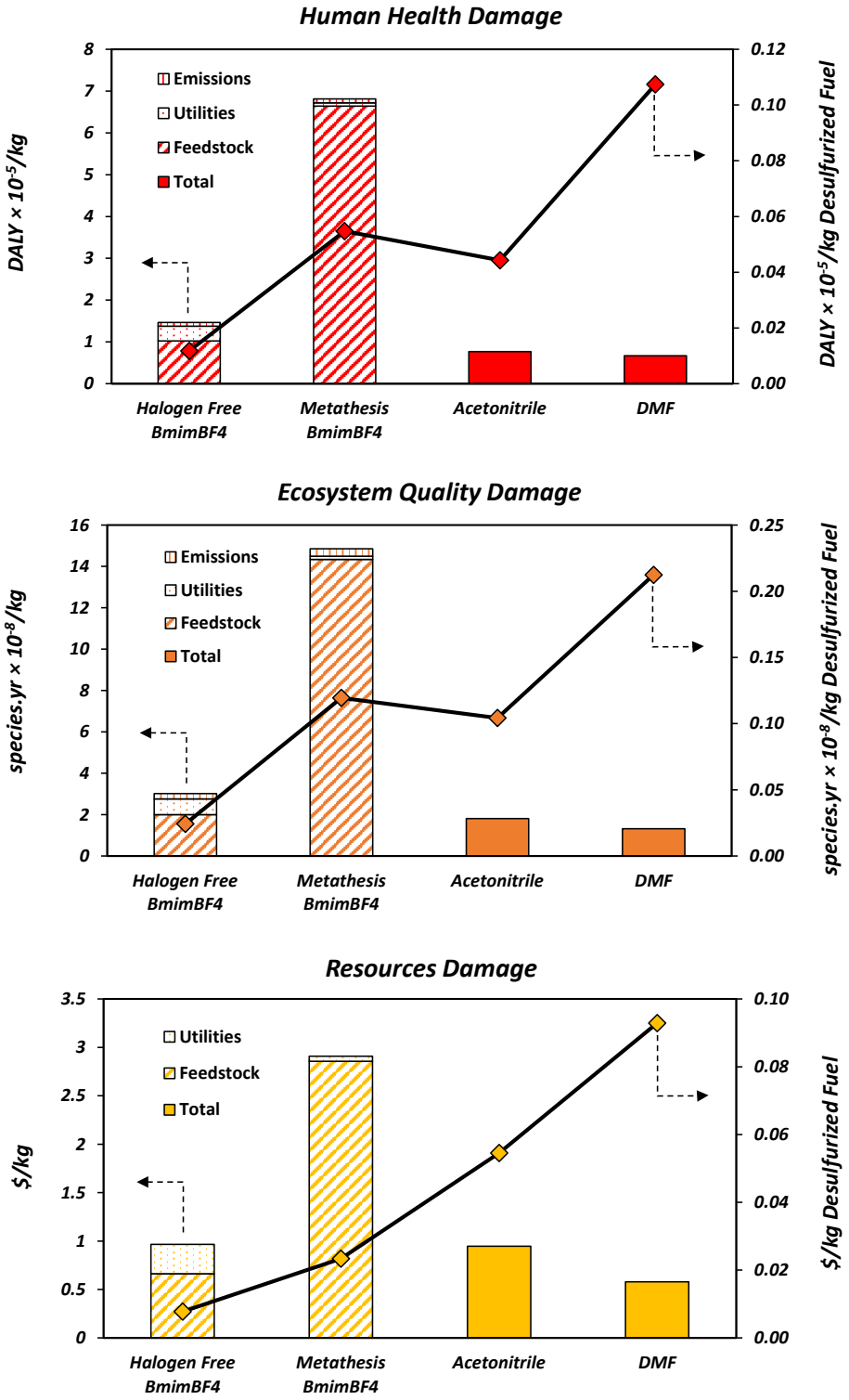

Figure 4.5: LCA comparison of [BMIM][BF_4] and organic solvents.

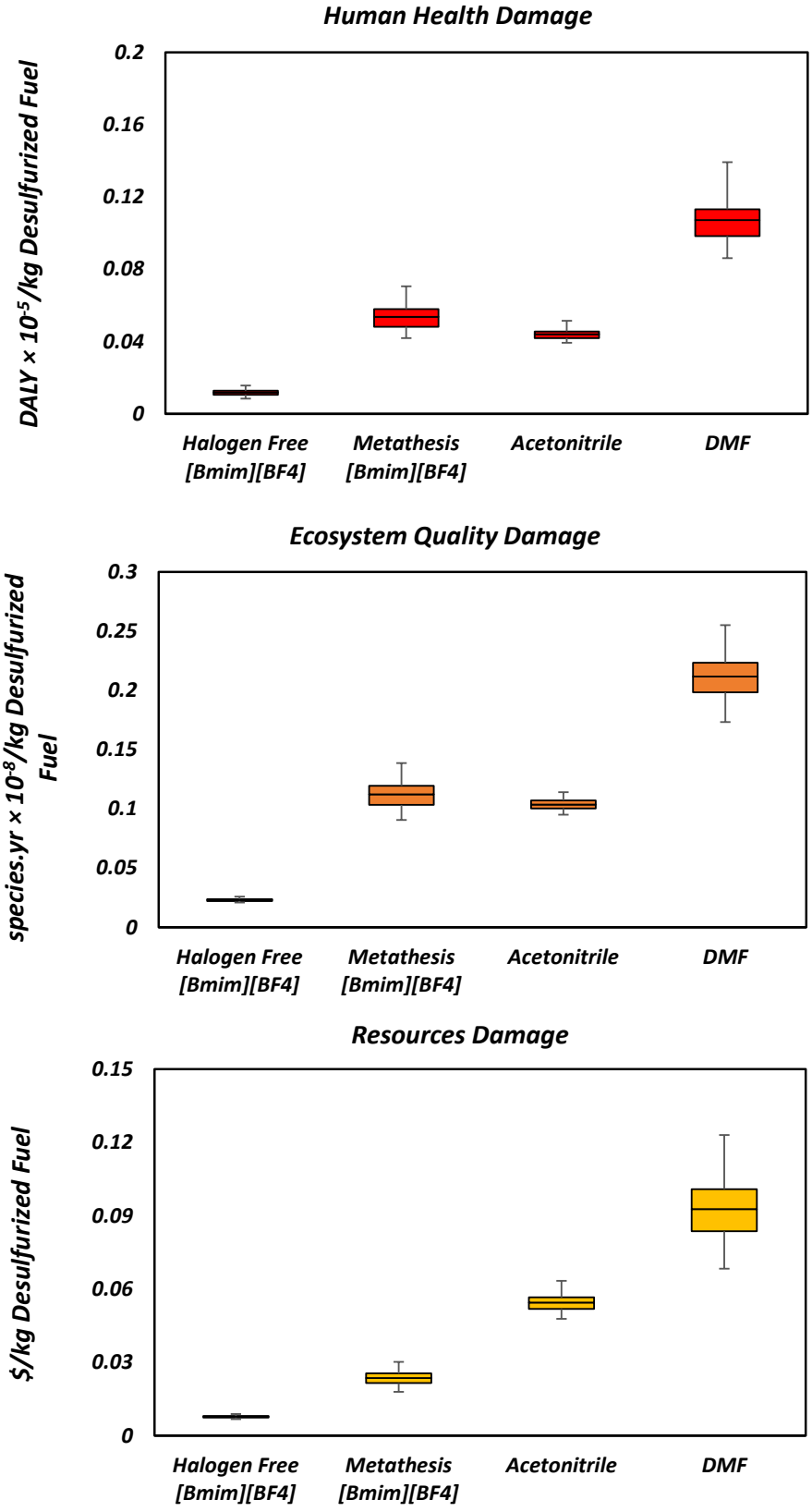

Figure 4.6: LCA uncertainty analysis results.

3.5- to 5-fold compared to acetonitrile and by 8- to 9-fold compared to DMF. This trend, which is consistent with the economic comparison in Fig. 4.4, can again be explained by the reduction in the amount of [BMIM][BF_4] needed to extract the same amount of sulphur from sour fuel compared to the more volatile organic solvents (Table 4.1). It is robust in the sense that 0.3% solvent loss for [BMIM][BF_4] corresponds to a conservative estimate based on the IL solubility in the fuel, which is a worst-case scenario.

To strengthen the conclusions of this environmental assessment, the box plots in Fig. 4.6 show the variations in the predicted endpoint indicators by propagating uncertainty in the background inventory data. The central line inside each box represents the median scenario. The upper and lower ends of the box represent the 25^{th} and 75^{th} percentiles, respectively, and the whiskers extend the box to include all the data within the 95% highest-posterior density interval. Halide-free [BMIM][BF_4] consistently exhibits the lowest environmental impacts across all four solvents and all uncertainty scenarios, while DMF is consistently worst in class. By contrast, the impact ranges of [BMIM][BF_4] via metathesis and acetonitrile present significant overlaps for the damage areas of human health and ecosystems quality—the probability of acetonitrile causing less environmental damage in these two areas is 83% and 66%, respectively. Conversely, acetonitrile consistently causes more damage to resources than [BMIM][BF_4]. A follow-up analysis, therefore, can consider the combined monetized cost of externalities and direct production cost for each solvent.[141]

4.4 Conclusions

A major impediment to the commercialisation of ILs in fuel desulfurization is the high production cost caused by their relatively complex synthesis procedures. Simpler synthesis routes for ILs may not only help reduce their production costs but reduce the overall cost of fuel desulfurization and make them attractive in multiple applications. Industrial applications of ILs have also been hindered by the lack of life-cycle assessments regarding their large-scale deployment.

This chapter presents an economic and environmental assessment of a one-pot, halide-free production route to [BMIM][BF_4] against the metathesis route and two conventional fuel

desulfurization solvents, namely acetonitrile and DMF. The halide-free route can halve the production cost of [BMIM][BF_4] using metathesis. This alternative route may reduce the environmental impacts associated with the production of [BMIM][BF_4] by three- to five-fold. Nevertheless, by omitting the use phase of solvents, the volatile organic solvents, acetonitrile and DMF, emerge as cheaper and cleaner options by the nature of their feedstock and their simpler synthesis trees.

Including the use phase in the assessment draws a radically different picture, whereby halide-free [BMIM][BF_4] consistently outperforms the volatile organic solvents for fuel desulfurization due to its superior sulphur extraction efficiency and recyclability. Even [BMIM][BF_4] produced via metathesis, despite showing the highest production cost and environmental impacts on a per-weight basis, becomes competitive with acetonitrile and superior to DMF, both economically and environmentally, on a per-weight-of-desulfurized-fuel basis. The cost and environmental impacts of [BMIM][BF_4] for fuel desulfurization might even be lower in practice because the assessment used a conservative estimate of the solvent losses. In future work, this analysis can be further refined by accounting for other parameters such as the effect of solvent viscosity, extraction time, and temperature.

This case study also demonstrates, using a specific application like fuel desulfurization, that ionic liquids can be more sustainable in their combined production and use phases than conventional organic solvents. It further highlights the value of using detailed process modelling with LCA studies for more accurate results because it accounts for critical parameters that are usually omitted using short-cut methods. However, one shortcoming of the proposed framework is that, with multiple economic and environmental indicators, it does not address multi-criteria problems, especially if applied to case studies with clear trade-offs. Therefore, appropriate weighting methods need be used in order to draw conclusions and facilitate decision-making.

Chapter 5

Coupling Monetization with Economic and Environmental Assessment of the Combined Production and Use of the $[HSO_4]^-$-Based Ionic Liquids in Biomass Pretreatment

Abstract

As an answer to the multi-criteria problem when comparing different technologies with multiple sustainability indicators and trade-offs, this chapter explores combining the concept of monetization with detailed process simulation and LCA to estimate the true cost of ionic liquids. Hence, all sustainability indicators merge into a single score to facilitate decision-making. A case study on four solvents used in biomass pretreatment is conducted: triethylammonium hydrogen sulphate [TEA][HSO_4], 1-methylimidazolium hydrogen sulphate [HMIM][HSO_4], acetone from fossil sources, and glycerol from renewable sources. The results show that the total monetized cost of production accounting for externalities can be more than double the direct costs estimated using conventional economic assessment methods. The ionic liquid [TEA][HSO_4] is found to have the lowest total cost, while the renewable solvent glycerol presents the highest total cost. This case study highlights the need for monetizing environmental impacts to estimate the true

cost of ILs and address multi-criteria analysis problems in their sustainability assessment. It is expected that this methodology will be incorporated into future research and development of sustainable ILs.

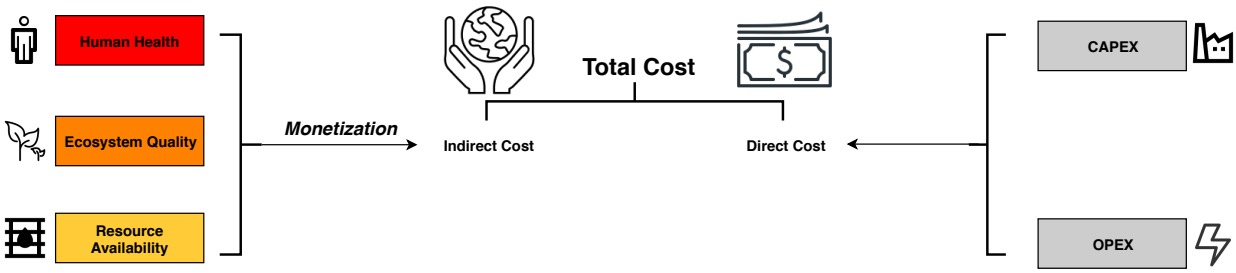

Figure 5.1: Monetization framework for quantifying the cost of externalities.

5.1 Context and problem definition

The standard approach to economic assessment often disregards indirect costs due to environmental externalities, namely impacts that occur as part of a product's life cycle and incur a cost for their mitigation. Such externalities need to be taken into account as indirect costs alongside direct production costs to reflect a product's true cost [160, 161]. For instance, natural phenomena such as global warming can have adverse effects on both human health and ecosystem quality, both of which carry indirect costs. Poor health can affect an individual's capacity to perform certain tasks, which leads to the loss of productivity or the need for health care [162]. Similarly, anthropogenic impacts on ecosystem quality may be reversed through environmental remediation projects [163].

Because most decisions are economically driven, it is of paramount importance to account for the externalities associated with the production and use of ionic liquids to compare them fairly with their non-ionic counterparts. Additionally, when comparing alternatives in LCA with environmental impact trade-offs, a weighting method is usually used in the weighting phase to convert different impacts with different units into a single score. There are several weighting methods suggested to tackle this issue, which include monetary valuation, panel, and distance-to-target methods. [164]

Monetary valuation—monetization in short—converts social and environmental impacts into currency Figure 5.1. It has been used to determine the cost of non-market goods in various sectors including energy systems to estimate the environmental damage cost of a specific energy

mix [165], health care systems to quantify the benefits of informal care [166], and insurance systems to predict the demand by homeowners after a disaster [167]. It has also been used in the weighting phase of LCA to evaluate trade-offs [168–170]. The advantages of monetization have been discussed in several papers, and it appears to be the preferred weighting method over the panel and distance-to-target methods for two main reasons [164, 171, 172]. First, unlike monetization, panel methods are based on individual preferences, such as experts and politicians rather than the public, while distance-to-target methods weigh the impacts using the ratio between the current level of the impact and a target level, which is based on rule ethics rather than utilitarian ethics. Second, in addition to ranking options from a welfare perspective, monetization makes it possible to inform decision-makers on whether the benefits from certain policies exceed the costs.

Herein, we combine LCA and monetization to quantify the *true* cost of ionic liquids for the first time. The focus is on [TEA][HSO_4] and [HMIM][HSO_4], two widely used protic ionic liquids in biomass pretreatment for their lignin solvating power [30], which we compare against acetone and glycerol regarded as the business-as-usual solvents [173–177]. The analysis starts with an environmental impact assessment of the solvents using LCA. These environmental impacts are then turned into currency via monetization and combined with the direct production costs to yield a total monetized cost.

5.2 Materials and methods

We consider four solvents for biomass pretreatment: two conventional solvents, acetone, and glycerol, that are produced industrially; and two PILs, [TEA][HSO_4] and [HMIM][HSO_4], for which only experimental synthesis procedures are currently available.

Glycerol and acetone are both market products. Their price and LCA data are readily available, e.g., from the ecoinvent 3.5 database,[109] where over 90% of the acetone is co-produced with phenol by the cumene process, while about 80% of the glycerol is a by-product of the biodiesel manufacturing process. Respectively 28% and 10% of the environmental impacts generated by these processes are then allocated to acetone and glycerol. Note that environmental

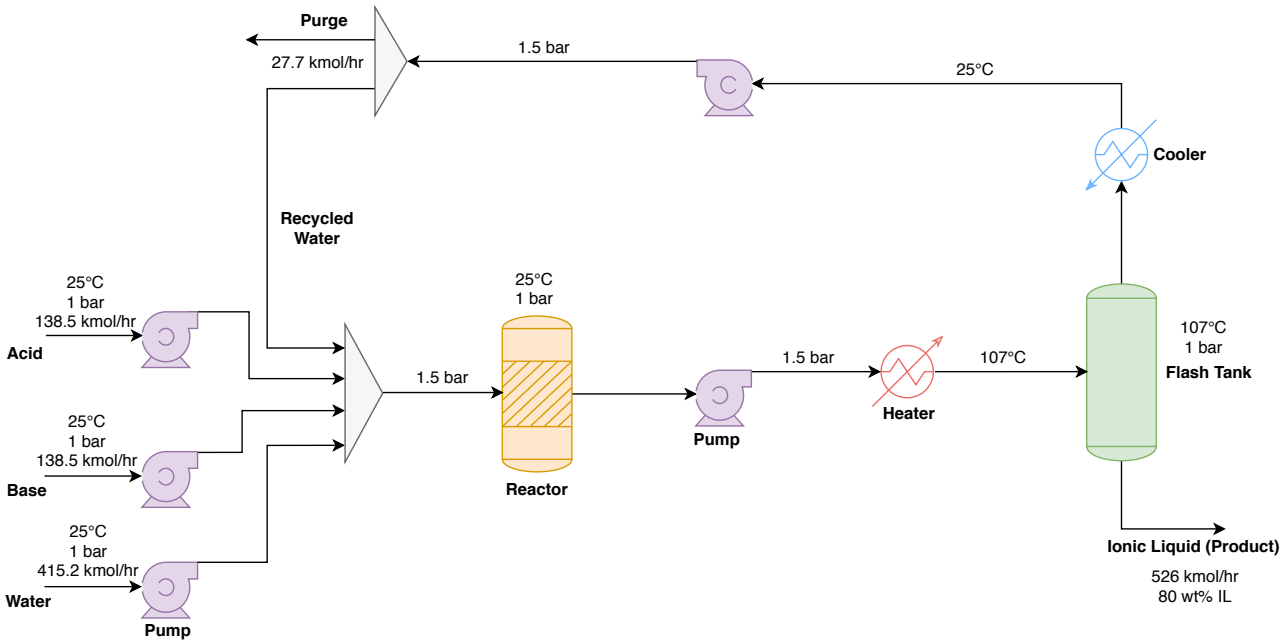

Figure 5.2: Process flow diagrams for the production of the protic ionic liquids.

impacts of acetone and glycerol are allocated based on economic allocation, and hence, changes in market prices could change the results.

To circumvent the lack of data for both ionic liquids, detailed process models are developed by scaling up the available experimental procedures. The process model as well as the methods and tools used to conduct the assessment are detailed in the following subsections.

5.2.1 Modelling of protic ionic liquid production processes

The process simulator Aspen HYSYS v9.0 is used to model the production processes of the ionic liquids [TEA][HSO_4] and [HMIM][HSO_4].

Ionic liquid production The ionic liquids of interest are synthesised through the transfer of a proton from a Brønsted acid to a Brønsted base [48]. The bases triethylamine and 1-methylimidazole are used for the synthesis of [TEA][HSO_4] and [HMIM][HSO_4], respectively, in combination with sulphuric acid. The synthesis trees for both ILs are shown in Figures 5.3 & 5.4. The scaled-up manufacturing process (Figure 5.2) is adapted from the work by Chen et al. [69]. Equimolar amounts of sulphuric acid and base are mixed with water at ambient temperature and pressure to produce an aqueous ionic liquid mixture. Since this acid-base reaction is highly

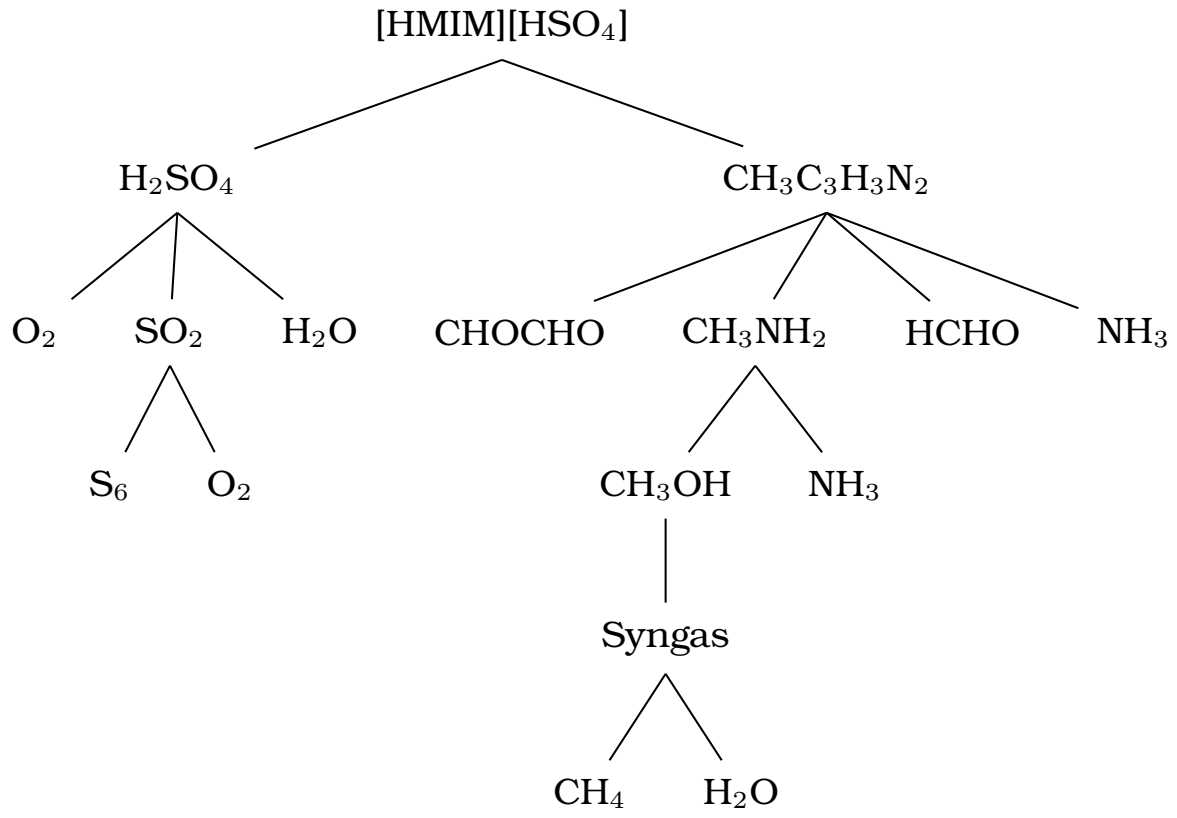

Figure 5.3: Synthesis tree of [HMIM][HSO_4]

exothermic, excess water is added to cool down the mixture and avoid unwanted phase transition, thermal decomposition, or undesired by-product formation. The outlet stream from the reactor is then heated up with steam to remove the excess water in a flash drum. The recycled water is cooled down with cooling water and a 10% purge is applied to prevent the accumulation of impurities.

Physical properties A full list of the properties used is provided in Tables B.1 & B.2 of Appendix B. Pseudo-components are created for [HMIM][HSO_4] and [TEA][HSO_4] as they are unavailable in the database of Aspen HYSYS v9.0. Certain properties such as density are obtained from experiments or the literature [121]. The other properties of both ionic liquids such as critical properties and normal boiling points are estimated using the group contribution method developed by Valderrama and Rojas [122]. Since energy flows can have a significant impact on the economic and environmental assessment of ionic liquids, accurate enthalpies of

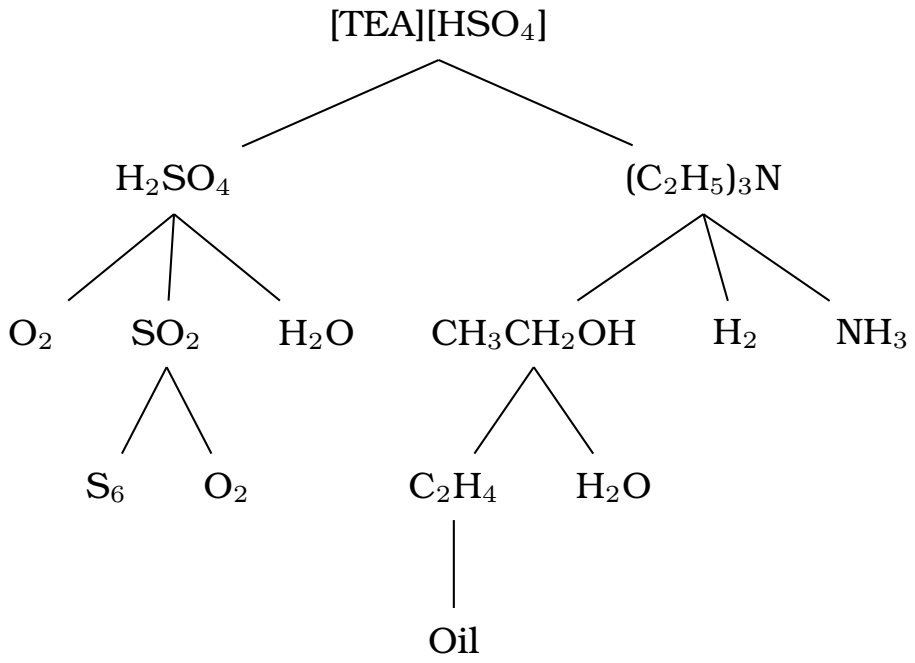

Figure 5.4: Synthesis tree of [TEA][HSO_4]

formation are also needed to calculate the heat of reactions. The detailed methodology used for calculating these enthalpies can be found in Chapter 3.

5.2.2 Functional unit

The economic and environmental assessment below is conducted for a functional unit of "1 kg of solvent", using a per-weight basis to reflect current commercial practice for solvent. By limiting the scope to the production phase of solvent only, this functional unit greatly simplifies the assessment. This approach is also appealing in that it enables the screening of candidate ionic liquids that have not yet been demonstrated at full commercial scale.

In practice, one could also include the use phase of solvent to reflect their actual function. There is indeed considerable variation in the design and operation of biomass pretreatment processes across the range of solvents, e.g., due to differences in lignin solvating power, the heat of regeneration, or solvent degradation [178–180]. A detailed modelling of bespoke pretreatment processes for each solvent is beyond the scope of this work. Instead, we consider three published pretreatment processes to enable an alternative comparison in terms of "1 kg of

biomass". Conversion factors on a weight-of-solvent-makeup-per-weight-of-treated-biomass basis are calculated using the solvent recycling rate, the mass fraction of solvent in the feed mixture, and the solvent-biomass feed ratio in each process: (i) 32 kg ton^{-1} for both ionic liquids using the ionoSolv process [179, 181], (ii) 140 kg ton^{-1} for acetone using the organosolv process with ethanol as a proxy solvent [178], and (iii) 2,500 kg ton^{-1} for glycerol based on a recent process [180]. Further details can be found in Section B.4 of Appendix B. This preliminary comparison furthermore assumes a similar CAPEX and OPEX for the different processes and neglects any extra solvent or enzyme in the pretreatment.

5.2.3 Economic assessment

The production cost of the ionic liquids is estimated via the total annualised cost (TAC) of the scaled-up processes, following the approach by Towler and Sinnott [115] as delineated in Chapter 3. The TAC is comprised of the OPEX and the annualised CAPEX. The latter represents the annual cost of paying off the fixed capital investment of a plant over its entire lifespan—here assuming 330 days of operation a year (equivalent to 7,920 hours) over a 10 year period. The CAPEX itself consists of equipment costs, offsite costs, engineering and construction costs, and contingency charges. The CAPEX of the main units in each production process is reported in Tables B.4, B.6, and B.8. The inflation rate is furthermore set based on the Chemical Engineering Plant Cost Index. The OPEX consists of fixed production costs, which are associated with operation and labour, and variable production costs associated with the procurement of raw materials and utilities. The former is reported in Tables B.5, B.7, and B.9, and the latter are sourced from ecoinvent 3.5 as given in Tables B.3. Note that the prices of raw materials and utilities represent a five-year global average as mentioned in Chapter 3. All of the costs—including the externalities discussed below—are expressed in USD2019 using currency conversion and inflation factors.

5.2.4 Environmental assessment

The LCA follows the ISO 14040 principles and is conducted using the software SimaPro interfaced with ecoinvent 3.5. In agreement with the functional unit selection above, a cradle-to-gate scope

is adopted that includes the impacts from the raw material extraction to the final product synthesis but excludes the product use phase assuming that the biomass pretreatment is identical for all the solvents. It is furthermore assumed that the production takes place in Europe as the geographical location. Notice that no allocation is required since the processes for producing the ILs (Figure 5.2) do not yield any by-products.

Data for the background processes from the ecoinvent 3.5 database are combined with information about the foreground system, mainly mass and energy flows obtained from the process simulation in Aspen HYSYS. A complete list of the life-cycle inventories (LCI) can be found in Tables B.8–B.9. The proxy data and methods used to quantify the air and water emissions are reported in Chapter 3. To ensure consistency, they follow the guidelines by Hischier et al. [111], which are used for many processes in ecoinvent.

The LCI entries are converted into environmental impact using the ReCiPe 2016 methodology [112]. During this life-cycle impact assessment (LCIA), all of the LCI entries are categorised into 17 midpoint indicators, including global warming, toxicity, ozone depletion, and land use. The severity of these impacts is determined from state-of-the-art environmental models such as the absolute global warming potential for climate change [182, 183], and toxicity potential for human, marine, and terrestrial toxicities [184, 185]. The midpoint indicators are further aggregated into three endpoint (damage) categories: resources, human health, and ecosystem quality. Furthermore, the assessment conducted here follows the hierarchist perspective, which is based on the cultural theory of scientific agreement and adopts a medium timeframe of 100 years for environmental impacts. The complete ReCiPe midpoint and endpoint results are given in Tables B.10–B.11, respectively.

5.2.5 Monetization

Monetization converts environmental impacts into currency. It is routinely used in cost-benefit analysis to support decision-making when both economic and environmental indicators need to be considered simultaneously. After the conversion, all of the economic and environmental metrics may be combined into a single total cost that is readily interpreted or used for comparison basis.

Existing monetary valuation methods often measure an individual's willingness to pay for preventing or mitigating the environmental impacts incurred by an activity.[161] Herein, damages to human health and ecosystem quality are monetized using, respectively, the budget constraint and choice modelling methods.[186] Budget constraint measures the potential economic production of an individual per year in terms of quality-adjusted life-year, a year-based biophysical unit describing human health quality. Though assuming that what is earned must be spent, budget constraint lowers the uncertainty by directly valuing the economic production compared to other valuation methods. Choice modelling measures ecosystem quality based on the economic penalty that an individual is willing to accept for environmental protection. This method is widely used in healthcare programmes as a means to monetize human well-being.[187, 188]

The monetary values of 74k EUR2003/DALY (125.3k USD2019/DALY) and 9.5M EUR2003/species×yr (16M USD2019/species×yr) are used for the monetary valuation of human health and ecosystem quality, respectively [189]. Note that the monetary values were converted . By contrast, resource damages are already expressed in monetary units and do not need conversion. It is worth noting that monetization factors carry wide ranges of uncertainty, e.g., monetary valuation of ecosystem quality ranges between 2.4-23.8M EUR2003/species×yr. However, the focus here is on proving the concept and effectiveness of the monetization weighting method, and hence, only average values are used, and further work to quantify these uncertainties is necessary. Further details on the monetization, currency and inflation factors used can be found in Table B.12.

5.3 Results and discussion

5.3.1 Economic assessment

Figure 5.5 presents the direct production costs per kg of solvent. [HMIM][HSO_4] ($1.46/kg) has the highest cost and [TEA][HSO_4] ($0.78/kg) the lowest one. This large gap between either of the ionic liquids is partly due to the larger number of steps involved in the production of [HMIM][HSO_4] (cf. Figure 5.3 & 5.4) compared to [TEA][HSO_4] and the other solvents. The direct production cost of glycerol is higher than that of [TEA][HSO_4] and acetone because

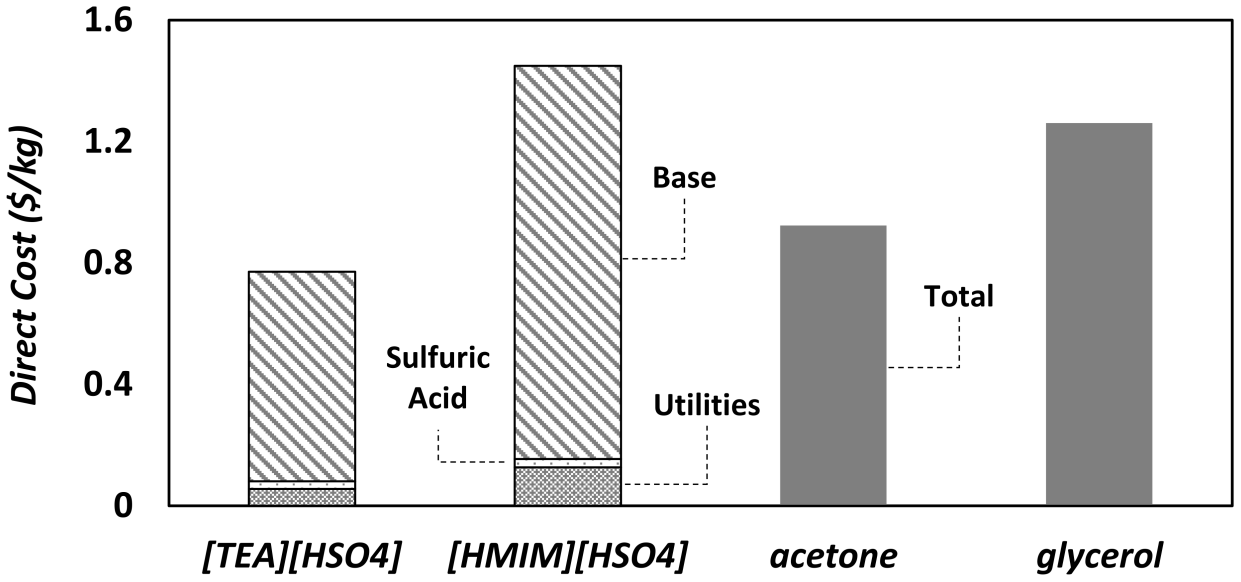

Figure 5.5: Direct costs of solvents. A breakdown of OPEX and CAPEX contributions is shown for the two ionic liquids. Other negligible costs including the annualised CAPEX and other OPEX components such as process water are not shown.

glycerol production uses more expensive starting materials like rapeseed and soybean oils [190].

The OPEX comprises over 90% of the direct production cost of both ionic liquids and the procurement of raw materials makes up most of the OPEX. This finding is consistent with previous reports [69]. The precursors, such as triethylamine ($1.4/kg) for [TEA][$HSO_4$] and 1-methylimidazole ($2.8/kg) for [HMIM][$HSO_4$], are costly, even though this is mitigated by the low cost of sulphuric acid ($0.05/kg). Other variable production costs, such as utilities, are low because the reactions are exothermic, and the separations are straightforward due to the low volatility of ionic liquids. The CAPEX contribution is also relatively small, even though it might be overestimated by considering a lifespan of 10 years which is shorter than the usual lifetime of chemical plants.

5.3.2 Environmental assessment

Figure 5.6 presents the LCA results for all three endpoint impact categories: human health, ecosystem quality, and resources. In the human health category, the impacts of [HMIM][HSO_4] and glycerol are, respectively, 50% and 80% higher than those of [TEA][HSO_4] and acetone. As noted earlier, the production of 1-methylimidazole for [HMIM][HSO_4] is relatively complex

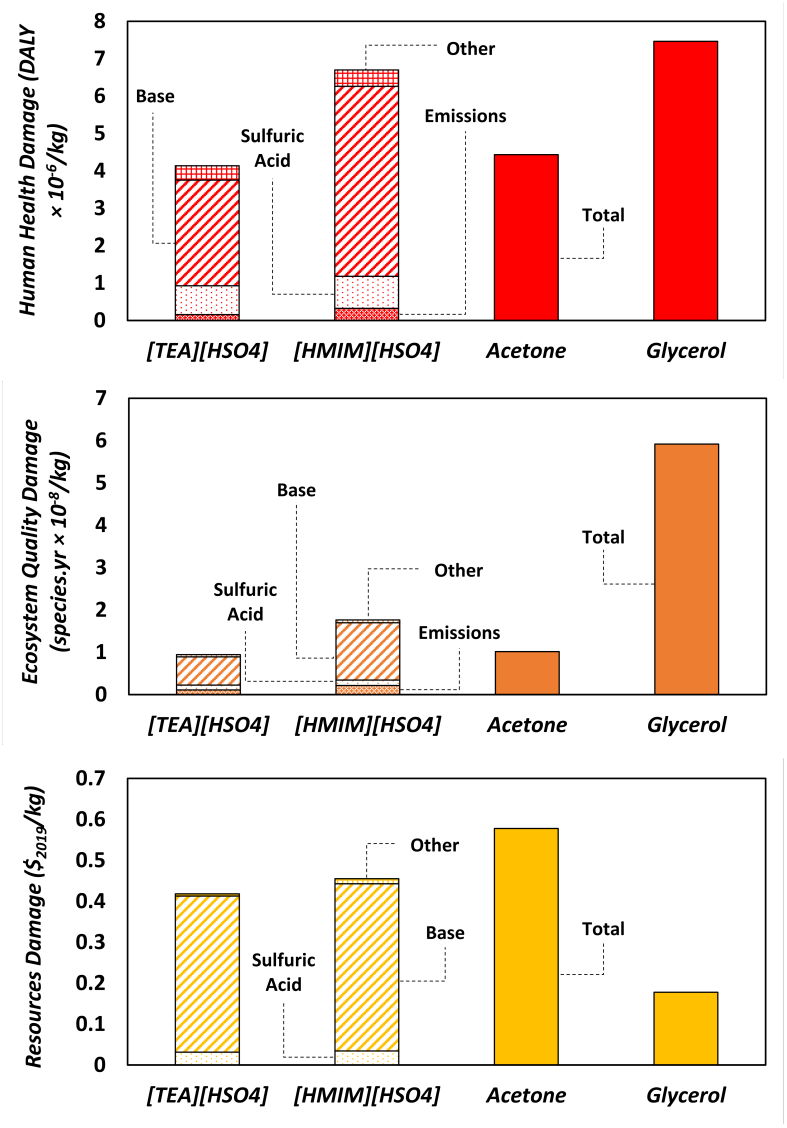

Figure 5.6: Endpoint environmental impacts of solvents. Top: human health; middle: ecosystem quality; bottom: resources. A breakdown into emissions, acid, base, and other contributions is shown for the two ionic liquids.

and requires more steps than triethylamine for $[TEA][HSO_4]$, thus generating more waste and emissions (Figure **??**). This is reflected by the higher scores in multiple human health impact categories such as global warming potential, ozone depletion, and ionising radiation (cf. Table B.10 of Appendix B). Higher emissions in ozone-depleting substances such as chlorofluorocarbons and nitrous oxide, which are used as refrigerants in the production of bulk chemicals (ammonia, nitric acid) and fuels, occur in syntheses involving a greater number of intermediate steps since they become more reliant on heat integration [191]. The major contributor to ionising radiation is nuclear power in the electricity mix.[192] By contrast, the higher impact of glycerol on human

health is linked to the cultivation and processing of crops such as rapeseed and soybean. These processes combined with deforestation usually emit large amounts of pollutants such as CO_2 and particulate matter that are detrimental to human health [193].

The impact of [HMIM][HSO_4] on ecosystem quality is 86% higher than those of [TEA][HSO_4] and acetone, but three-times lower than that of glycerol. The reason behind this is land use as producing 1 kg of glycerol requires almost 100 times more land area than [HMIM][HSO_4], the second largest in this category. The large areas needed for crop cultivation and the related deforestation are responsible for soil damage and loss of habitat for plants and animals [194].

Regarding resource depletion, both [TEA][HSO_4] and [HMIM][HSO_4] have a lower impact than acetone which consumes the largest amount of fossil resources among the solvents. This is because the production of acetone is nearly entirely reliant on fossil resources, whereas the ionic liquids comprise equimolar quantities of base and sulphuric acid, where only the bases are heavily reliant on fossil resources while sulphuric acid requires significantly fewer fossil resources. The slightly higher score of [HMIM][HSO_4] over that of [TEA][HSO_4] is again due to 1-methylimidazole requiring more synthesis steps than triethylamine, leading to higher consumption of fossil resources to cover the energy demand. It is also worth noting that while glycerol has high predicted impacts on both human health and ecosystem quality, its impact on resources is low since it is renewable and uses a minimal amount of fossil resources outside of processing. Production of the Brønsted bases make up the largest impact on resources for both ionic liquids since they are derived from fossil resources. More generally, the bases yield the largest contributions in all three impact categories and should therefore be the primary focus for future improvement.

5.3.3 Externalities and total cost

Figure 5.7 shows the combined monetized cost of externalities and direct cost for each solvent. [TEA][HSO_4] presents the lowest indirect cost and glycerol the highest one. Resource and human health damages are the biggest contributors to the monetized externalities of solvent production, except for glycerol. As noted earlier, this is because acetone and the protic ionic liquids of interest are heavily reliant on fossil resources, whose extraction costs are expected to rise in

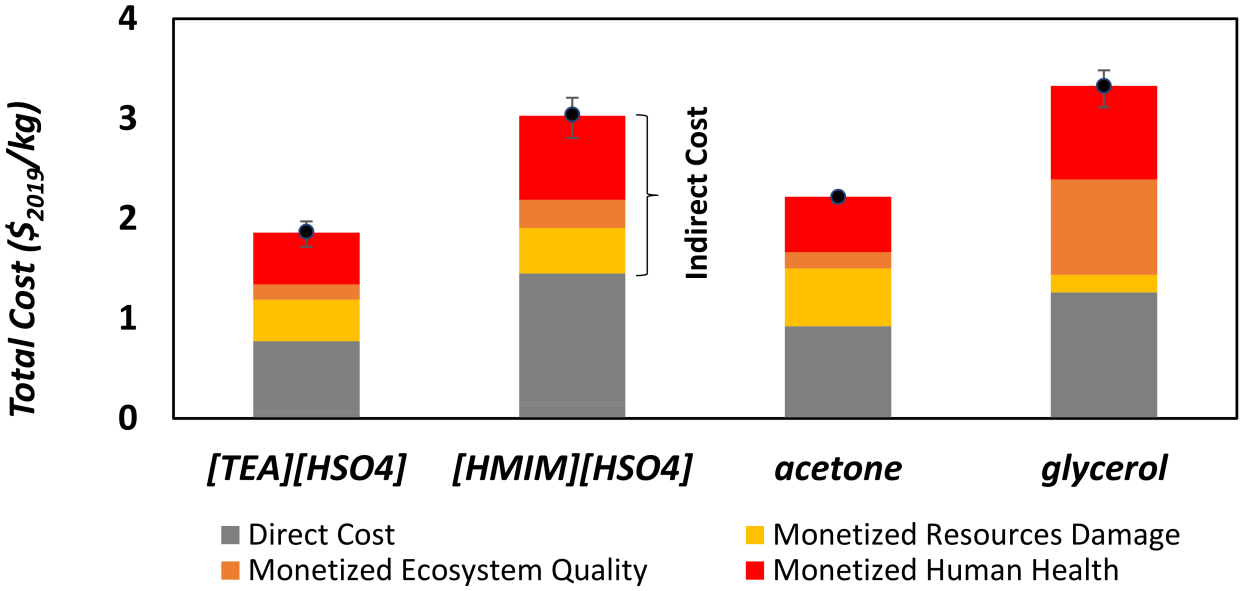

Figure 5.7: Total cost of solvent production combining direct production costs and externalities in terms of human health, ecosystem quality, and resource damages.

the future due to scarcity [195]. [HMIM][HSO_4] has higher externalities than [TEA][HSO_4] and acetone because of its higher impact on human health and ecosystem quality. As for glycerol, it is the substantially higher land use that makes its monetized impact on ecosystem quality, and thus its indirect cost, significantly higher than for the other solvents. This makes glycerol the worst solvent in terms of externalities, even though its direct production cost is lower than that of [HMIM][HSO_4].

Notice that the indirect costs associated with all four solvents are larger than their direct production costs, so the total monetized costs are more than double the production costs. The total cost of glycerol ($3.33/kg) is the highest because of its large externalities (¿$2/kg). It is 10% higher than the total cost of [HMIM][HSO4] ($3.04/kg), 50% higher than that of acetone ($2.22/kg), and nearly 90% higher than that of [TEA][HSO4] ($1.87/kg). In addition, the uncertainty of the estimated externalities is shown in Figure 5.7, where the whiskers correspond to the 25th and 75th percentiles among all the scenarios generated by Monte Carlo sampling. These uncertainty ranges are generally small and do not overlap with each other, apart from those of glycerol and [HMIM][HSO_4] that show a slight overlap. This uncertainty analysis confirms that the estimated externalities are representative, and thus, their comparison is meaningful.

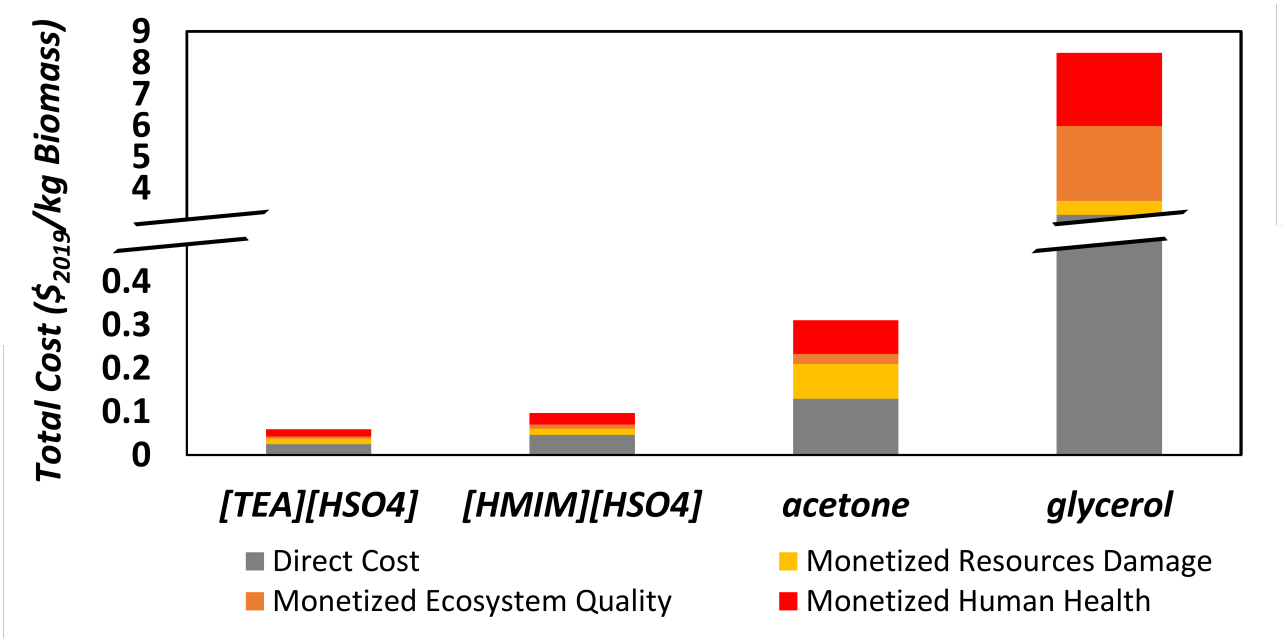

Figure 5.8: Total cost of solvent production on a per-weight basis of pretreated biomass.

Finally, Figure 5.8 reports the total monetized cost per kg of pretreated biomass, for comparison with the costs per kg of solvent in Figure 5.7. Although the applied conversion factors carry a large uncertainty due to the underlying assumptions (cf. Section Functional unit above and Section B.4 of Appendix B), this analysis suggests that the advantages of ILs compared with the other two solvents in terms of costs and environmental impacts might be unequivocal after integrating the use phase. Since the ILs have higher solvating power than acetone or glycerol and enjoy a near 100% recycling rate, the makeup of an IL (32 kg ton^{-1}) is expected to be the lowest in a biomass pretreatment process. By contrast, the relatively poor recycling rate of glycerol (75%) requires the largest solvent makeup (2,500 kg ton^{-1}, about 80 times more than ionic liquids), which combined with its high externalities leads to a much higher total cost. Even with a more favourable recycling rate of 95%, the makeup would still be 16 times larger than ILs. This cursory analysis illustrates that a solvent's use phase can radically change its economic and environmental evaluation.

5.4 Conclusions

Interest in sustainable solvents has increased significantly over the past decades due to a growing awareness of the impact of solvents on pollution and energy consumption in the chemical industry. ILs are uniquely versatile and show great potential for reducing solvent losses and regeneration expenditures, but their widespread application remains hindered by environmental-related concerns in terms of toxicity and biodegradability alongside the suspicion of high production costs. Herein, the primary focus has been on a holistic framework that combines a conventional economic assessment with a cradle-to-gate LCA to determine the total monetized cost of ILs as a basis for comparison with other solvents. This framework relies on detailed models of the production processes of ionic liquids and their precursors to circumvent the lack of cost and LCA data.

A case study in lignocellulosic biomass pretreatment has compared the production of the popular ionic liquids [TEA][HSO_4] and [HMIM][HSO_4] against acetone from fossil resources and glycerol from renewable resources. The economic valuation reveals that [HMIM][HSO_4] has the highest direct cost of all four solvents due to the complex synthesis of its precursor 1-methylimidazole, while [TEA][HSO_4] presents the lowest direct cost—about half of that of [HMIM][HSO_4]. Glycerol is found to have the second highest production cost because rapeseed oil and soybean oil are costly precursors. Adding externalities on top of these direct production costs does not change the comparison radically, but since the indirect costs from these externalities are larger than the corresponding production costs, the total monetized costs of all four solvents end up being more than double their production costs. Glycerol becomes the most expensive solvent in terms of total monetized cost, overtaking [HMIM][HSO_4] due to its high externalities in the human health and ecosystem quality categories. By contrast, the ionic liquid [TEA][HSO_4] is found to have the lowest total cost since its production requires relatively inexpensive materials and follows a simple synthesis procedure, followed by acetone. All of these conclusions are furthermore supported by an uncertainty analysis of the LCA data and monetization factors.

Finally, the results of an initial comparison between solvents on a per-weight-of-treated-biomass basis concluded that the benefits of ionic liquids for biomass pretreatment are likely

to be downplayed by excluding the solvents' use phase. This is because the makeup of ionic liquid in a biomass pretreatment process could be significantly lower than the makeup of other solvents, especially glycerol. Nevertheless, our analysis relies on conversion factors that carry large uncertainty. A recommended follow-up to this work, therefore, entails expanding the valuation to include the use phase of solvents, for instance via detailed modelling of the biomass pretreatment processes themselves.

Overall, this case study demonstrates the need to account for negative externalities in the comparison of solvents. By showing that solvents produced from renewable resources do not necessarily present lower externalities than other solvents derived from fossil resources, including ILs, these results challenge the conventional wisdom stating that ILs are more costly and damaging to the environment. Therefore, a holistic comparison should be used more systematically for future research and development of sustainable solvents.

Chapter 6

Global Sensitivity Analysis in Life-Cycle Assessment of Early-Stage Technology using Detailed Process Simulation: Application to Dialkylimidazolium Ionic Liquid Production

Abstract

The ability to assess the environmental performance of early-stage technologies at the production scale is critical for sustainable decision-making. The previous case studies discussed mainly the nominal results with little focus on uncertainty analysis, i.e., conducting conventional uncertainty analysis with background uncertainties only. This chapter builds on the base framework outlined in Chapter 3 and presents a systematic framework for uncertainty quantification in LCA of emerging technologies using global sensitivity analysis (GSA) coupled with a detailed process simulator and LCA database. This methodology accounts for uncertainty in both the background and foreground LCI and is enabled by lumping multiple background flows, either downstream or upstream of the foreground processes, to reduce the number of factors in the sensitivity

analysis. The goal of this final methodology is to have a complete set of working tools to assess the sustainability performance of ILs. A case study comparing the life-cycle impacts of two dialkylimidazolium ionic liquids is conducted to illustrate the methodology. It is found that failure to account for the foreground process uncertainty alongside the background uncertainty can underestimate the predicted variance of the endpoint environmental impacts by a factor of two. The variance-based GSA then reveals that only a few uncertain foreground and background parameters contribute significantly to the total variance in the endpoint environmental impacts and allows singling out the most relevant lumped background parameters for further analysis. These results emphasise the need for using GSA for more reliable decision-making under uncertainty in LCA.

6.1 Context and problem statement

The LCI stage of LCA entails the collection of data related to the mass and energy flows, from raw material extraction to process emissions and waste. For existing processes, this inventory data may be collected directly onsite or retrieved from environmental databases such as ecoinvent [109]. In many cases, however, inventory data may be lacking due to low technology-readiness of processes or be inaccessible because of confidentiality [196–198]. These inventory gaps can impede the environmental assessment of chemicals, particularly in early development stages [32, 141].

Various approaches have been proposed to bridge the gap in inventory data. Streamlined LCA methods aim to predict the life-cycle impacts of a product from readily available information [199], such as a method that relies on linear regression for predicting the life-cycle impacts of chemicals based on their molecular structure. The approach was refined by including thermodynamic properties and information regarding the sigma-profile of the molecule [200]. These regression models were shown to provide accurate predictions for a range of chemicals, including petrochemicals and their derivatives. However, they can lead to large errors with other chemicals and may fail to accurately predict certain life-cycle impacts, especially impacts that are not directly linked to the descriptors used in the regression models.

Short-cut methods based on stoichiometric yields or simplified models [34, 96] provide an alternative to these simple regression models. Precursor work by Kralisch et al. [38] led to a simplified LCA method combining lab-scale experiment data with proxy data of similar chemicals, as necessary. More recently, Cuéllar-Franca et al. [96] developed an approach for constructing the life-cycle synthesis tree of a chemical by going back to where data for the most basic precursors are available and using stoichiometric and basic thermodynamic calculations where data are unavailable. Although it is convenient to quickly obtain a preliminary estimate, the previous methods may not be suitable for a detailed assessment, especially when comparing products and processes with similar performance indicators. Part of the reason for this is that they omit key process parameters such as heating and cooling duties, process waste and emissions, and process efficiencies.

Detailed process models can support a more reliable environmental assessment to predict the performance of processes at a low technology-readiness level (TRL), for which industrial process data are unavailable [149]. Commercial process simulators such as Aspen HYSYS encompass a wide range of unit operations, provide access to accurate thermodynamic property packages, and facilitate mass and heat integration to model real-life processes. However, these process models can also be subject to large uncertainty [201–203]. Therefore, it is improtant to quantify these uncertainties and propagate them to the predicted inventories, and ultimately, to the predicted environmental impacts.

The ISO 14044 standard stipulates that a sensitivity analysis should be conducted as part of the LCA framework to identify the most important sources of uncertainty but does not recommend a specific technique. A large body of research has thus been devoted to characterising, propagating, and analysing various sources of uncertainty in LCAs, using a range of techniques, over the past few decades [204–207]. Despite this, many LCA studies that build on detailed process simulations simply omit the effects of inventory uncertainties; while many others solely consider uncertainty in the background inventory data [208–210], often formulating probability distributions for the inventories using data quality indicators such as a Pedigree matrix [113, 211]. A more thorough uncertainty analysis requires the foreground inventory uncertainties, such as process operating conditions and thermophysical properties, alongside the background inventory uncertainties.[212] This is especially relevant in comparing processes with similar performance indicators, where the corresponding uncertainty ranges might overlap significantly. Moreover, sensitivity analysis can help clarify the effects of model and process parameters on the predicted foreground inventories, ultimately guiding future experimental work to help reduce this uncertainty.

A popular approach to sensitivity analysis in economic and environmental assessments is one-at-a-time sensitivity analysis (OTSA) [213], which varies the values of the uncertain input parameters one at a time while keeping the remaining parameters constant at a given reference point, resulting in a ranking of the uncertain parameters [214–216]. While this approach often works well for models that are nearly separable in their inputs, the ranking results may be misleading when the level of interactions between the input parameters is more pronounced, a

problem that is exacerbated by larger input domains. These limitations can be overcome by applying global sensitivity analysis (GSA) [217], which accounts for output variations over the entire input domain and can capture interactions between two or more input parameters. GSA methods do not merely rank the uncertain parameters, but also quantify how much each input parameter contributes to the overall output variance.

Nevertheless, the application of GSA in LCAs has remained scarce [206, 211]. Cucurachi et al. [218] proposed a protocol for conducting GSA in LCAs, with a focus on the LCIA stage, and in particular, on uncertainties in the characterisation factors and weighting methods. By contrast, Groen et al. [206] focused on the LCI stage and compared various GSA methods in terms of their effectiveness. Several recent applications of GSA in LCAs include biodiesel production [219], building design [220], geothermal heating networks [221], and advanced photovoltaic cells [222]. A key challenge in these GSA applications is the large number of uncertain input factors, especially when dealing with inventory data [223–225]. This may require a large number of samples to compute reliable sensitivity indices and result in a high computational burden or even become intractable when a detailed process simulator is used to fill in the inventory data gaps, for instance, in early-stage technological assessments. This can also explain why the particular combination between GSA and detailed process simulators remains unclear.

The main objective of this chapter, therefore, is to combine the base framework used throughout this thesis with GSA and uncertainty techniques, including a sampling approach, to provide a complete set of working tools for the sustainability assessment of ILs and similar low TRL technologies. The framework focuses on analysing the combined effects of background and foreground inventory uncertainties. A new methodology is introduced, whereby the uncertain background inventory flows, either downstream or upstream of the foreground processes, are lumped to reduce the number of factors in the sensitivity analysis and improve computational tractability. A practical implementation of this methodology that takes advantage of existing software is also discussed. The methodology is demonstrated in a case study comparing the life-cycle impacts of two dialkylimidazolium-based ILs, namely 1-butyl-3-methylimidazolium tetrafluoroborate [BMIM][BF_4] and 1-butyl-3-methylimidazolium hexafluorophosphate [BMIM][PF_6]. Both ILs have drawn wide interest in the literature, owing to their high solvating capacity and

negligible vapour pressure, including their use as physical separation media [226, 227]. The low TRL of IL production processes motivates the use of a detailed process simulator to scale up their production, and thus, the need to account for foreground data uncertainty.

6.2 Materials and methods

The adopted LCA framework follows the four phases defined in the ISO 14040 standards: (i) goal and scope, (ii) inventory analysis, (iii) impact assessment, and (iv) interpretation. Choices about the system, including the scope, the boundaries of the foreground system, and the functional unit, are made in the goal and scope phase. Environmental flows for all inputs and outputs of each process in the complete process tree are collected during the LCI phase, including raw materials, energy streams, emissions, and waste. Both the foreground and background inventories are then translated into environmental impacts during the LCIA phase through a characterisation method, which is based on scientifically agreed environmental mechanisms with cause-effect pathways, through which substances released in emissions or resource usage can cause environmental damages. Finally, the interpretation phase checks that the conclusions from the impact assessment are well-substantiated before making recommendations, and this is where uncertainty quantification and sensitivity analysis are especially relevant.

Uncertainties in LCA stem from two main sources: (i) uncertain inventory flows into and out of processes within the technosphere or between processes and the ecosphere, and (ii) uncertain characterisation factors linking the ecosphere flows to environmental damages [225]. Given the emphasis on emerging technologies, the main focus involves those uncertainties arising through the LCIs, which are subsequently distinguished as foreground and background uncertainties. The former refers to uncertainties affecting the low TRL processes in the foreground system, where detailed process models are used to circumvent the gap in inventory data from state-of-the-art databases such as ecoinvent [109]. These uncertain parameters include operating conditions, thermodynamic and physical properties, separation yields, and reaction rates, which translate to uncertainties related to the flows exchanged between the foreground system and the rest of the technosphere, or with the ecosphere. By contrast, background

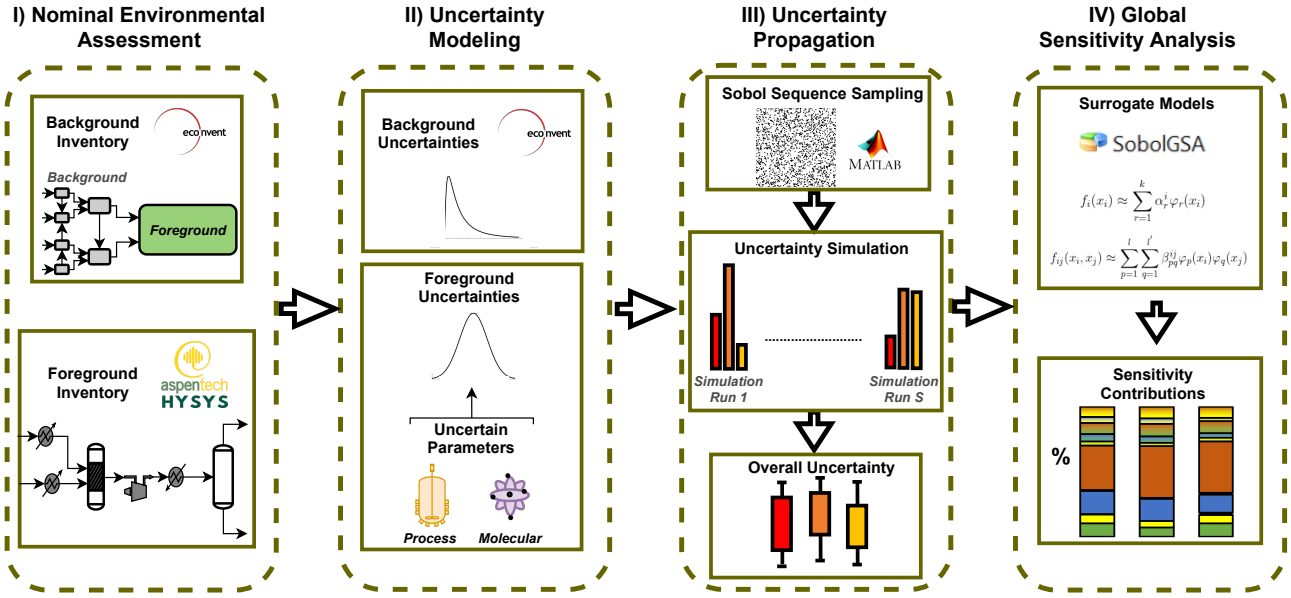

Figure 6.1: Methodology conceptual framework.

uncertainties are linked to the background processes and supply-chain activities, translating to further uncertainties in the flows between processes in the technosphere and ecosphere.

The proposed methodology for uncertainty propagation and analysis in LCA is summarised in Figure 6.1. Considering the emphasis on emerging technology, a key novelty involves the effects of combining the background and foreground inventory uncertainties on the predicted environmental impacts. The framework starts with a nominal environmental assessment (Step I), incorporating available LCA database information (e.g., background processes) with detailed process modelling to bridge inventory gaps (e.g., foreground processes). The next two steps require characterising and modelling the background and foreground uncertainties (Step II) before discretising and propagating these uncertainties using quasi-Monte Carlo sampling techniques (Step III), where each uncertainty realisation is propagated through both the background and foreground inventories, and ultimately through to the environmental impacts. The resulting impact uncertainty ranges are apportioned back to individual uncertain background and foreground factors as sensitivity indices (Step IV), using surrogate models trained on the sampled uncertainty scenarios to drive a variance-based GSA. Another key novelty entails lumping multiple background inventories to reduce the dimensionality and improve the tractability of GSA in this context. The following subsections provide more details about the main steps.

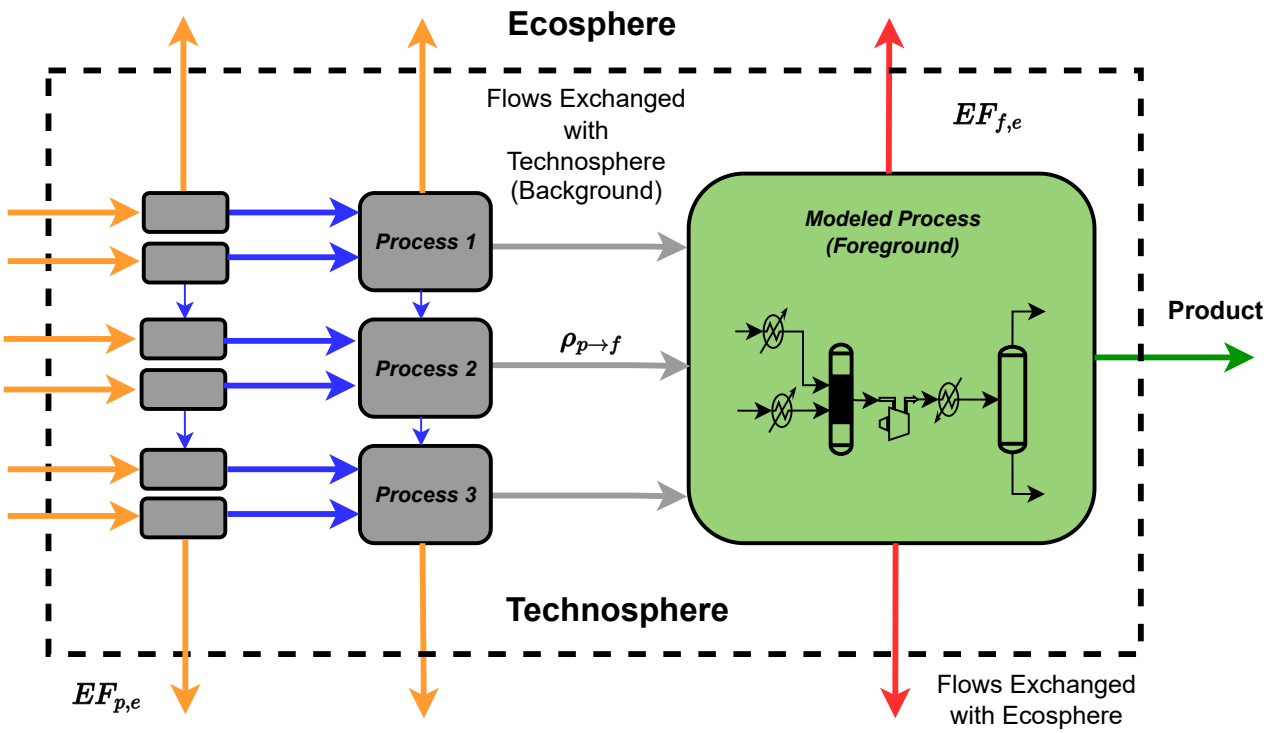

Figure 6.2: Conceptual diagram of a cradle-to-gate inventory illustrating the flows linking the foreground and background processes within the technosphere and with the ecosphere. The green arrow indicates the main product's flow out of the foreground process, assuming a single product. The red arrows show elementary flows $\mathrm{EF}_{\mathrm{f},e}$ exchanged between the foreground process and the ecosphere, while the orange arrows indicate elementary flows $\mathrm{EF}_{p,e}$ between the background process and the ecosphere. The intermediate flows shown with grey arrows are those exchanged between the foreground process and background processes located immediately upstream in the technosphere, and those with blue arrows are the intermediate flows between background processes in the technosphere. Similarly, a cradle-to-grave LCA can be depicted by including the background processes downstream of the foreground process.

6.2.1 Modelling of foreground and background life-cycle inventories

The overall environmental impact EI_z in a category $z \in Z$ is determined using Equation (R6.1), expressed in units of impact per functional unit. $\mathrm{LCI}_e^{\mathrm{tot}}$ denotes the total life-cycle inventory of an elementary flow $e \in E$ that is either consumed by a process within the technosphere or released by a process to the ecosphere, with units of elementary flow per functional unit. $\mathrm{CF}_{e,z}$ is the characterisation factor of the elementary flow e in impact category z, with units of impact per elementary flow.

$$\mathrm{EI}_z = \sum_{e \in E} \mathrm{LCI}_e^{\mathrm{tot}}\ \mathrm{CF}_{e,z} \tag{R6.1}$$

In particular, $\mathrm{LCI}_e^{\mathrm{tot}}$ encompasses all the elementary flows in a reference product's life

cycle, including those exchanged between the foreground processes and the ecosphere and between the background processes and the ecosphere. For illustration, the diagram in Figure 6.2 depicts a cradle-to-gate LCI, where the foreground process exchanges elementary flows both with the ecosphere and with several background processes in the technosphere. This distinction between foreground and background processes is reflected in Equation (R6.2). There, $\mathrm{EF}_{\mathrm{f},e}$ denotes the elementary flow e exchanged between the foreground processes (indexed with f) and the ecosphere, in the same units as $\mathrm{LCI}_e^{\mathrm{tot}}$. $\mathcal{U}_{\mathrm{f}}$ and $\mathcal{D}_{\mathrm{f}}$ are the sets of processes immediately upstream and downstream of the foreground process, respectively. $\mathrm{LCI}_{p,e}^{\mathrm{up}}$ denotes the total inventory of elementary flow e from an immediate upstream process $p \in \mathcal{U}_{\mathrm{f}}$ and all the processes upstream of p in the process tree, with units of elementary flow per reference flow of mass or energy in process p, while using the factor $\rho_{p\to\mathrm{f}}$ to rescale the elementary flow $\mathrm{LCI}_{p,e}^{\mathrm{up}}$ in terms of a functional unit. Likewise, $\mathrm{LCI}_{p,e}^{\mathrm{down}}$ denotes the total inventory of elementary flow e from an immediate downstream process $p' \in \mathcal{D}_{\mathrm{f}}$, with the factor $\rho_{\mathrm{f}\leftarrow p'}$ rescaling $\mathrm{LCI}_{p',e}^{\mathrm{down}}$ per functional unit.

$$\mathrm{LCI}_e^{\mathrm{tot}} = \mathrm{EF}_{\mathrm{f},e} + \sum_{p\in\mathcal{U}_{\mathrm{f}}} \rho_{p\to\mathrm{f}} \mathrm{LCI}_{p,e}^{\mathrm{up}} + \sum_{p'\in\mathcal{D}_{\mathrm{f}}} \rho_{\mathrm{f}\leftarrow p'} \mathrm{LCI}_{p',e}^{\mathrm{down}} \tag{R6.2}$$

In turn, the total upstream inventory $\mathrm{LCI}_{p,e}^{\mathrm{up}}$ depends on the elementary flows $\mathrm{EF}_{p,e}$ from process p and $\mathrm{EF}_{p',e}$ from all the processes p' upstream of p within the technosphere, as well as all intermediate flows between any two background processes upstream of p. The total downstream inventory $\mathrm{LCI}_{p',e}^{\mathrm{down}}$ has similar dependencies.

6.2.2 Foreground and background uncertainty quantification

For those background processes in which inventories are available in state-of-the-art LCI databases, such as ecoinvent, the uncertainty quantification follows the Pedigree matrix approach [113, 159], where the data sources are assessed according to the six characteristics of reliability, completeness, temporal correlation, geographic correlation, further technological correlation, and sample size, in addition to relying on expert judgements. For each uncertain elementary or intermediate flow (reference product flow excluded), a set of six indicator scores U^c is considered. These scores are combined with a basic uncertainty factor U^0 to determine the standard deviation

of a log-normal distribution for the corresponding flow. For instance, the case of an uncertain elementary flow $\mathrm{EF}_{p,e}$ is reported in Equations (R6.3)–(R6.4), where $\mathrm{EF}_{p,e}^{\mathrm{nom}}$ is the nominal value of the elementary flow (determined in Step I of the methodology, see Figure 6.1).

$$\ln(\mathrm{EF}_{p,e}) \sim \mathcal{N}(\mathrm{EF}_{p,e}^{\mathrm{nom}}, [\sigma_{p,e}^{\mathrm{EF}}]^2) \tag{R6.3}$$

$$\text{with:}\quad \sigma_{p,e}^{\mathrm{EF}} = \exp\left(\sqrt{\ln(U_{p,e}^{0})^2 + \sum_{c=1}^{6} \ln(U_{p,e}^{c})^2}\right) \tag{R6.4}$$

In contrast, for the foreground processes and those background processes that are unavailable in state-of-the-art LCI databases, the main sources of uncertainty need to be characterised on a case-by-case basis. Detailed process models are developed to bridge such inventory gaps, and henceforth, a key assumption is that the uncertainty can be described as uncertain parameter values in those models. These uncertain model parameters may either be linked to experimental errors in lab-scale procedures or inferred from expert opinions. This knowledge informs the choice of a probability distribution for each parameter, including their shape, mean value, variance, and support set. It is possible to further distinguish uncertain parameters corresponding to operating conditions that may be adjusted to mitigate impacts using process optimisation, such as temperatures and pressures in unit operations, from uncertain physical parameters whose variation ranges may be refined through dedicated experiments or predictive ab-initio simulations, including thermophysical properties, separation yields, reaction rates, and conversions.

The uncertain background flows are collectively denoted with the vector $\boldsymbol{\varphi}$ below, and the uncertain foreground parameters with the vector $\boldsymbol{\omega}$. In Equation (R6.2), all of the elementary flows $\mathrm{EF}_{\mathrm{f},e}$ exchanged between the foreground processes and the ecosphere, as well as the scaling factors $\rho_{p\to\mathrm{f}}$ and $\rho_{\mathrm{f}\leftarrow p'}$, directly depend on the foreground uncertainty realisation $\boldsymbol{\omega}$, whereas the total upstream and downstream inventories $\mathrm{LCI}_{p,e}^{\mathrm{up}}$ and $\mathrm{LCI}_{p',e}^{\mathrm{down}}$ depend on the background uncertainty realisation $\boldsymbol{\varphi}$.

The uncertainty propagation relies on a discretisation of the foreground and background uncertainty $(\boldsymbol{\omega}, \boldsymbol{\varphi})$ into a set of uncertainty scenarios by sampling their probability distributions. The proposed implementation proceeds by first simulating the foreground process flowsheets

using Aspen HYSYS for each realisation of $\boldsymbol{\omega}$, resulting in the foreground elementary flows $\mathrm{EF}_{\mathrm{f},e}(\boldsymbol{\omega})$ and the scaling factors $\rho_{p\to\mathrm{f}}(\boldsymbol{\omega})$ and $\rho_{\mathrm{f}\leftarrow p'}(\boldsymbol{\omega})$. Next, the elementary and intermediate flows in the background system are computed for the corresponding uncertainty realisations of $\boldsymbol{\varphi}$ using Matlab. This may also involve simulating other process flowsheets developed for bridging gaps in the background inventories. All these flows are then combined into the total upstream and downstream inventories $\mathrm{LCI}^{\mathrm{up}}_{p,e}(\boldsymbol{\varphi})$ and $\mathrm{LCI}^{\mathrm{down}}_{p,e}(\boldsymbol{\varphi})$. Finally, these background inventories are rescaled and combined with the corresponding elementary flows $\mathrm{EF}_{\mathrm{f},e}$ from the foreground processes (Equation R6.2), before applying a characterisation method to determine the predicted impacts EI_z in the midpoint or endpoint categories of interest for each uncertainty scenario (Equation R6.1). The uncertainty scenario generation and propagation are also coordinated using Matlab. The relative error ϵ of the sample mean $\hat{\mu}_{\mathrm{EI}_z}$ for a sample size N at a given confidence level $(1-\alpha)100\%$ is estimated using Equation (R6.5), where $\hat{\sigma}_{\mathrm{EI}_z}$ is the corresponding sample standard deviation [228]. This estimate could also be used as a termination condition inside a loop that can incrementally increase the number of uncertainty scenarios.

$$\epsilon = \frac{\hat{\sigma}_{\mathrm{EI}_z}\, t_{\frac{\alpha}{2},N-1}}{\hat{\mu}_{\mathrm{EI}_z}\sqrt{N}} \tag{R6.5}$$

6.2.3 Sensitivity analysis of foreground and background uncertainties

Analysing the sensitivity of each environmental impact EI_z with respect to both the uncertain foreground parameters $\boldsymbol{\omega}$ and background parameters $\boldsymbol{\varphi}$ entails quantifying the contribution of each of these parameters to the total variance of EI_z. A key challenge is the presence of interactions between multiple uncertain parameters, so the total variance of EI_z may not be explained by simply adding up separate contributions from each parameter. Such interactions are evident from Equation (R6.2), where $\mathrm{LCI}^{\mathrm{up}}_{p,e}(\boldsymbol{\varphi})$ and $\mathrm{LCI}^{\mathrm{down}}_{p',e}(\boldsymbol{\varphi})$ are respectively multiplied by $\rho_{p\to\mathrm{f}}(\boldsymbol{\omega})$ and $\rho_{\mathrm{f}\leftarrow p'}(\boldsymbol{\omega})$. Additional interactions may also occur between the uncertain foreground parameters. OTSA is inappropriate in this context because it ignores such interactions, so it is necessary to resort to global sensitivity analysis (GSA) instead. The focus herein is on

variance-based GSA techniques, which compute so-called Sobol indices that can be directly interpreted as measures of sensitivity. This class of GSA techniques is attractive because they measure sensitivity across the whole input space and compare favourably to other GSA approaches [229], yet they have not been widely applied in LCA applications thus far [206].

A second challenge with analysing the sensitivity of the environmental impacts EI_z is the high dimensionality of the uncertain parameters $\boldsymbol{\varphi}$ in the background system. Herein, this high dimensionality may be reduced by lumping multiple background parameters, as shown in Equation (R6.6). The new parameters $\mathrm{BEI}^{\mathrm{up}}_{p,z}$ (Equation R6.7) represent the background environmental impact in category z, generated by the immediate upstream process $p \in \mathcal{U}_\mathrm{f}$, either directly or via the processes upstream of p in the technosphere. The new parameters $\mathrm{BEI}^{\mathrm{down}}_{p',z}$ (Equation R6.8) have a similar interpretation for the immediate downstream process $p' \in \mathcal{D}_\mathrm{f}$. For each impact category z, the size of these two sets of lumped parameters corresponds to the number of processes immediately upstream or downstream of the foreground processes times, a much smaller number compared to all the elementary and intermediate flows in the background system. Naturally, a follow-up sensitivity analysis can be conducted for any lumped parameter $\mathrm{BEI}^{\mathrm{up}}_{p,z}$ or $\mathrm{BEI}^{\mathrm{down}}_{p',z}$ to identify its main contributing factors.

$$\mathrm{EI}_z = \sum_{e\in E} \mathrm{EF}_{\mathrm{f},e}(\boldsymbol{\omega})\,\mathrm{CF}_{e,z} + \sum_{p\in\mathcal{U}_\mathrm{f}} \rho_{p\to\mathrm{f}}(\boldsymbol{\omega})\,\mathrm{BEI}^{\mathrm{up}}_{p,z}(\boldsymbol{\varphi}) + \sum_{p'\in\mathcal{D}_\mathrm{f}} \rho_{\mathrm{f}\leftarrow p'}(\boldsymbol{\omega})\,\mathrm{BEI}^{\mathrm{down}}_{p',z}(\boldsymbol{\varphi}) \tag{R6.6}$$

$$\text{with:}\qquad \mathrm{BEI}^{\mathrm{up}}_{p,z}(\boldsymbol{\varphi}) = \sum_{e\in E} \mathrm{LCI}^{\mathrm{up}}_{p,e}(\boldsymbol{\varphi})\,\mathrm{CF}_{e,z} \tag{R6.7}$$

$$\mathrm{BEI}^{\mathrm{down}}_{p',z}(\boldsymbol{\varphi}) = \sum_{e\in E} \mathrm{LCI}^{\mathrm{down}}_{p',e}(\boldsymbol{\varphi})\,\mathrm{CF}_{e,z} \tag{R6.8}$$

The computation of the Sobol indices is conducted using the software SobolGSA [230, 231], where the following indirect approach is selected. In the first step, metamodels are regressed for each impact EI_z with respect to the foreground uncertainties $\boldsymbol{\omega}$ and the lumped background uncertainties $\mathrm{BEI}^{\mathrm{up}}_{p,z}, \mathrm{BEI}^{\mathrm{down}}_{p',z}$, by leveraging the available samples from the foreground-background uncertainty propagation (Step III). The metamodel representation of choice is the random-sampling high-dimensional model representation (RS-HDMR) [232, 233], where only low-order interactions (up to second-order interaction) between input parameters are accounted for to

reduce the computational time and tackle problems with several dozen input parameters. In the second step, the coefficients of the RS-HDMR metamodel are used to compute the Sobol sensitivity indices [234] at no additional cost. These sensitivity indices measure how much of the total variance of EI_z is attributable to the uncertain parameters, either separately (first-order effects) or in combination with other parameters (second- and total-order effects). Notably, SobolGSA implements other metamodelling techniques and GSA approaches, which is convenient for making comparisons.

6.3 Case study definition and implementation

The proposed case study compares the environmental impacts associated with the production at the industrial scale of two dialkylimidazolium ILs: 1-butyl-3-methylimidazolium tetrafluoroborate [BMIM][BF_4] and 1-butyl-3-methylimidazolium hexafluorophosphate [BMIM][PF_6]. Process flowsheeting in Aspen HYSYS (version 9.0) is used to scale-up experimental synthesis procedures for [BMIM][BF_4] and [BMIM][PF_6],[235] which comprise the foreground system. Process flowsheeting is also used to bridge inventory gaps for two of their precursors in ecoinvent as part of the background system, namely 1-butyl-3-methylimidazolium chloride [BMIM]Cl and 1-chlorobutane. The relevant process models and the methods and tools used to conduct the LCA are described in the following subsections, after which the main steps of the uncertainty quantification are summarised.

6.3.1 Modelling of ionic liquid production processes

[BMIM][BF_4] and [BMIM][PF_6] Production The syntheses of [BMIM][BF_4] and [BMIM][PF_6] follow the metathesis procedure proposed by Chen et al. [148] (Figure 6.3). For [BMIM][BF_4], the synthesis proceeds via anion exchange between [BMIM]Cl and sodium tetrafluoroborate $NaBF_4$, producing solid NaCl as a by-product—Reaction (R6.9) with X := BF_4 and Y := Na. For [BMIM][PF_6], the anion exchange occurs between [BMIM]Cl and lithium hexafluorophosphate

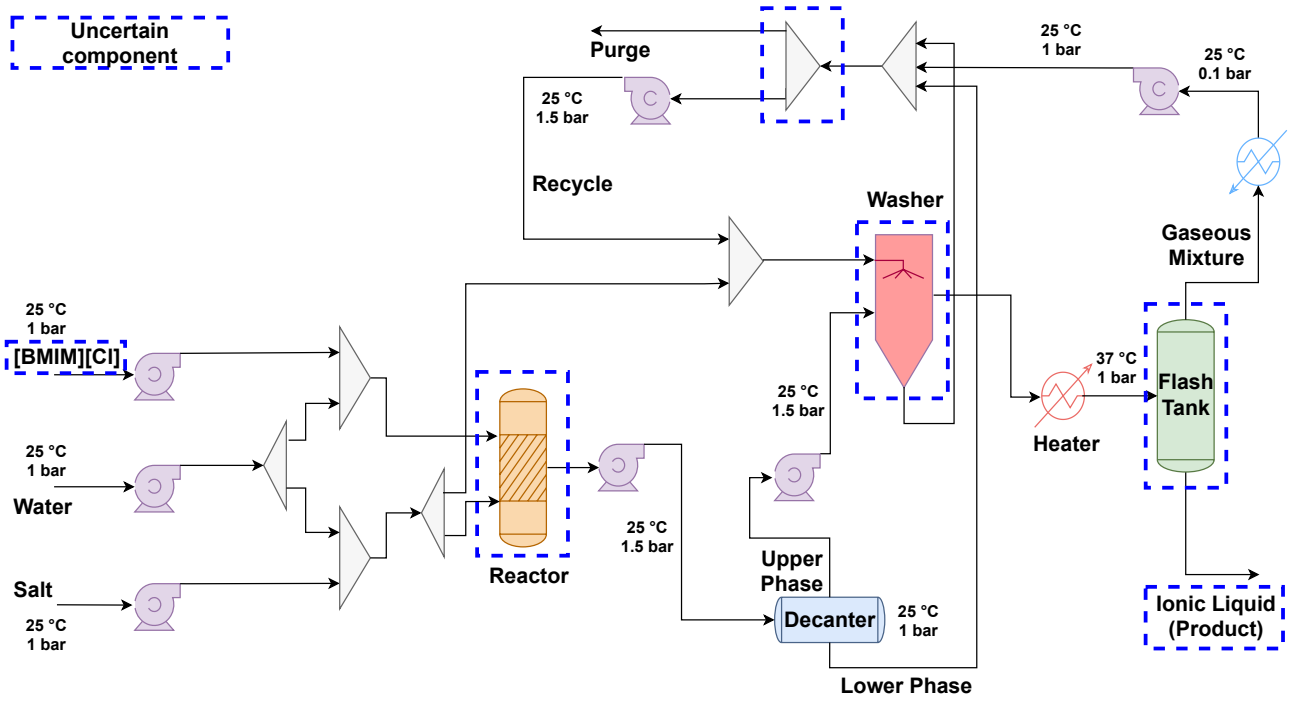

Figure 6.3: Process flow diagram of scale-up ionic liquid production. The dotted blue box indicates the unit operations with uncertain parameters.

$LiPF_6$—Reaction (R6.9) with X := PF_6 and Y := Li.

$$[\text{BMIM}]\text{Cl} + \text{YX} \longrightarrow [\text{BMIM}][\text{X}] + \text{YCl} \tag{R6.9}$$

[BMIM]Cl is mixed with an excess of YX under atmospheric conditions. The reaction mixture is separated into an upper phase, which contains the main aqueous product with impurities, and a lower phase containing solid YCl and undissolved YX. The upper phase is sent to a 3-stage washer using YX solution to remove impurities. In the final step, [BMIM][Y] is separated from water in a vacuum flash vessel, resulting in aqueous [BMIM][X] with 25 wt% water content.

[BMIM]Cl production The production process of the [BMIM]Cl precursor (Figure S1) is based on the experimental procedure reported by Baba et al. [150]. It starts by mixing 1-methylimidazole in toluene with excess 1-chlorobutane and running the reaction at 112 °C under atmospheric pressure. [BMIM]Cl is separated in a vacuum flash vessel from toluene and other unreacted materials, which are returned to the reactor.

1-Chlorobutane production The production process of 1-chlorobutane (Figure S2) starts by reacting 1-butanol with an excess of hydrochloric acid at 120 °C.[152] The product mixture is cooled down to 25 °C and sent to a flash vessel tank, where the vapour phase containing mainly hydrochloric acid is separated. The liquid phase is then reheated to 69 °C and sent to a second flash vessel, where 1-chlorobutane is isolated from the residual 1-butanol and excess water.

Physical property estimation UNIQUAQ is used as the thermodynamic package in Aspen HYSYS. Since [BMIM][BF_4], [BMIM][PF_6], [BMIM]Cl, $NaBF_4$, $LiPF_6$, LiCl, and 1-methylimidazole are currently unavailable in the Aspen HYSYS database, pseudo-components are created to estimate their properties. The methodology is described in Chapter 3, while the complete set of properties is reported in Tables A.1–A.2, A.5, A.9, C.1–C.3. Physical properties, such as densities, are retrieved from the literature [121]. Critical properties and normal boiling points of the ILs are estimated using the group contribution method reported by Valderrama and Rojas [122]. Properties of other pseudo-components are estimated from their molecular structure using the Aspen HYSYS built-in property constant estimation system. The heat of formations are determined using quantum calculations.

6.3.2 Environmental assessment

The LCA follows the ISO 14040 principles and is conducted using the software SimaPro (version 9.0) interfaced with ecoinvent 3.5 [109].

(i) Goal and scope The goal of the environmental assessment is to compare the production of the dialkylimidazolium ILs, [BMIM][BF_4] and [BMIM][PF_6]. A cradle-to-gate scope is adopted, which includes all processes from raw material extraction to IL production, but excludes any further processing, use or waste management after the production. Since ILs are commonly sold by weight, and the functional unit is defined as "1 kg of ionic liquid". Furthermore, it is assumed that [BMIM][BF_4] and [BMIM][PF_6] are the single products of each process alternative, so no allocation is needed, and the geographical location is chosen as Europe.

(ii) Life-cycle inventory (LCI) The mass and energy flows for the production processes of [BMIM][BF_4] and [BMIM][PF_6] and both precursors, [BMIM]Cl and 1-chlorobutane, are predicted using process flowsheeting in Aspen HYSYS. These inventories are combined with data gathered from ecoinvent for the rest of the background processes to quantify the LCIs of [BMIM][BF_4] and [BMIM][BF_6]. A complete list of the foreground inventory flows, expressed for the functional unit, can be found in Tables A.24, A.26—A.27, C.4. The methods used to quantify the air and water emissions are reported in Table 3.1. They follow the guidelines set by Hischier et al. [111], which are used for many processes in ecoinvent and ensure consistency.

(iii) Life-cycle impact assessment (LCIA) The LCI entries are converted into environmental impacts using the ReCiPe 2016 methodology [112]. These impacts are first categorised into 18 midpoint indicators, including global warming, toxicity, ozone depletion, and land use, and then further aggregated into three endpoint categories: the damage areas of resources, human health, and ecosystems quality. The assessment follows the hierarchist perspective, which is based on the cultural theory of scientific agreement and adopts a medium timeframe of 100 years for the environmental impacts. The complete ReCiPe midpoint and endpoint results are given in Tables C.5 & C.6, respectively, for the functional unit.

(iv) Interpretation and uncertainty analysis The quantification of both foreground and background uncertainties follows the proposed methodology (Steps II to IV in Figure 6.1). In the foreground system, nine uncertain parameters are considered in the process models of [BMIM][BF_4] and [BMIM][PF_6] production (cf. Table C.9 & C.7). Five of them correspond to uncertain operating conditions, namely the pressure drops in the reactor (ΔP_{R}) and in the washer (ΔP_{W}), the temperature (T_{VF}) and pressure (P_{VF}) in the vacuum flash vessel, and the purge split ratio (PUR); cf. Figure 6.3, where the corresponding units are identified. Most of these operating conditions ($\Delta P_{\mathrm{R}}, \Delta P_{\mathrm{W}}, P_{\mathrm{VF}}, \mathrm{PUR}$) are highly uncertain since the process models are scaled up from experimental synthesis procedures, and thus, described by a triangular distribution with a range of wide $\pm 50\%$ around their nominal values. A smaller uncertainty range of $\pm 20\%$ is considered for the operating temperature T_{VF} in the vacuum flash unit as the nominal temperature corresponds to the maximal product yield, and the

temperature can easily be controlled around this value in practice. The remaining four uncertain parameters correspond to thermophysical properties, namely the heats of formation and densities of [BMIM][BF_4], [BMIM][PF_6], and [BMIM]Cl. These uncertainties are also modelled using triangular distributions, with nominal values and uncertainty ranges based on experimental errors from the literature. Concerning the background system, parametric uncertainties are considered in the process model of [BMIM]Cl and 1-chlorobutane production in the same way. These uncertain parameters are reported in Tables C.8 & C.9 with their corresponding nominal values and uncertainty ranges. Sample generation for all these uncertain parameters is coordinated from Matlab using quasi-Monte Carlo sampling based on low-discrepancy Sobol sequences [236], and interfaced with Aspen HYSYS for simulating the process flowsheets in each uncertainty scenario. As explained in the methodology section, these are combined with uncertainty scenarios of the elementary and intermediate background flows to predict the distribution of each environmental impact EI_z. A total of 10,000 uncertainty scenarios are used for the various cases discussed in the following section. The relative error ϵ of the mean of each environmental impact, estimated using Equation (R6.5) at a 95% confidence level, is in the range between 0.04-0.05.

Table 6.1: Uncertain model parameters, uncertainty sources, and ranges in flowsheet simulation of [BMIM][BF_4] production. Each uncertain parameter is assumed to follow a triangular distribution.

Type	**Parameter**	**Range**	**Units**
Operating Condition	ΔP_R[1]	10±50%	kPa
	ΔP_W[1]	10±50%	kPa
	T_{VF}[2]	80±20%	°C
	P_{VF}[1]	10±50%	kPa
	PUR[1]	0.1±50%	–
Thermophysical Property	$\rho_{[BMIM][BF_4]}$[3]	1208±19%	kg m^{-3}
	$\rho_{[BMIM]Cl}$[3]	1080±19%	kg m^{-3}
	$\Delta H_{f\,[BMIM][BF_4]}$[4]	−6.50±1.59*e*5	kJ kmol^{-1}
	$\Delta H_{f\,[BMIM]Cl}$[4]	−2.37±1.59*e*5	kJ kmol^{-1}

[1] Estimate based on heuristics.
[2] Mean value based on an optimised base case.
[3] Estimate based on the group contribution methods developed by Valderrama and Rojas [122] with maximum standard deviation of 19 %.
[4] Estimate based on the lattice energy and computational chemistry methods proposed by Gao et al. [124] with a maximum deviation of −159 kJ mol^{-1}.

In the sensitivity analysis, following the uncertainty propagation (Step IV), the following seven lumped background impacts are considered alongside the nine uncertain foreground parameters: production of [BMIM]Cl ($BEI_z^{[BMIM]Cl}$), production of sodium tetrafluoroborate ($BEI_z^{NaBF_4}$) or lithium hexafluorophosphate ($BEI_z^{LiPF_6}$), production of construction materials (BEI_z^{mat}), production of thermal energy (BEI_z^{th}), production of electricity (BEI_z^{el}), production of water (BEI_z^{wat}), and wastewater treatment (BEI_z^{wwt}). Recall that the uncertainty realisations for all these lumped background impacts can be computed using the elementary and intermediate background flow samples that are already available from the uncertain propagation (Step III, Equations R6.7 & R6.8). But since the lumped background impacts are specific to a particular impact category, a separate GSA needs to be conducted for each impact category z. Of the 10,000 samples available from the uncertainty propagation, 9,000 are used to construct the RS-HDMR metamodels in SobolGSA, and the remaining 1,000 samples are used for testing. The coefficients of the RS-HDMR metamodels are estimated via regression. The statistical fitness measure for the metamodels of different endpoint impact categories for both ILs is $R^2 > 0.90$. Finally, the Sobol indices derived from the RS-HDMR model coefficients are normalised by the sample variance of the corresponding impact EI_z (rather than the sum of the first- and second-order indices) to detect the presence of higher-order interactions.

6.4 Case study results and discussions

6.4.1 Nominal environmental assessment

The bar charts in Figure 6.4 summarise the nominal LCA results for all three endpoint damage categories—human health, ecosystem quality, and resources—on a per-weight basis of ionic liquid. The complete set of midpoint and endpoint indicators can be found in Tables C.5 & C.6 of Appendix C. This nominal comparison suggests that the production of [BMIM][BF_4] presents lower environmental impacts than [BMIM][PF_6] in all damage areas. Damages to human health are reduced by 21%, ecosystems quality damage by 16%, and resources by 10%. Since both ILs are produced using the same process and share the same cation, these differences are attributed to the different anions and their respective production trees.

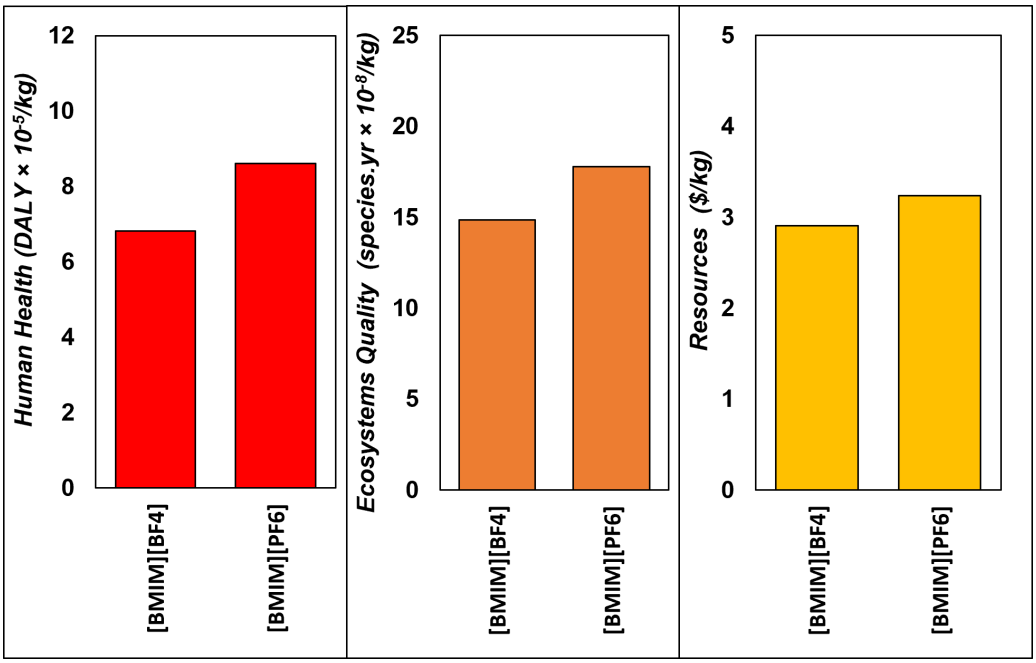

Figure 6.4: Nominal LCA comparison of endpoint indicators for the production of [BMIM][BF_4] and [BMIM][PF_6].

Regarding the damage area of human health, producing the precursor [BMIM]Cl contributes 32% and 20% of the life-cycle impacts of [BMIM][BF_4] and [BMIM][PF_6], respectively. This is significantly less than the production of their anionic counterparts, $NaBF_4$ and $LiPF_6$, which contribute 65% and 79%, respectively. The largest midpoint contributions to this endpoint damage area for both ILs are global warming, mostly due to carbon dioxide emissions, and fine particulate formation, mainly due to emissions of sulphur dioxide and $<2.5\,\mu m$ particulate matter.

Concerning the area of ecosystem quality, [BMIM]Cl production is responsible for 45% and 29% of the impacts of [BMIM][BF_4] and [BMIM][PF_6], respectively, while their anionic counterparts, $NaBF_4$ and $LiPF_6$, contribute a larger share of 51% and 69%, respectively. The main midpoint contributions to this endpoint damage area for both ionic liquids are global warming (>50%), acidification, terrestrial ozone formation, and water consumption. Acidification is mainly due to sulphur dioxide emissions, ozone formation to toluene emissions, and water consumption to hydropower electricity production.

For the resource area, the production of [BMIM]Cl is responsible for a majority (56%) of the impacts of [BMIM][BF_4], followed by the production of $NaBF_4$ (42%). These contributions

are flipped for [BMIM][PF_6], with the production of $LiPF_6$ causing a majority of the impacts (61%) compared to the production of [BMIM]Cl (38%). Part of this difference is explained by the fact that the anion [PF_6]$^-$ is heavier than [BF_4]$^-$, making up 51% of the molecular weight of [BMIM][PF_6], while [BF_4]$^-$ only accounts for 38% of the molecular weight of [BMIM][BF_4]. Nearly all of these endpoint damages are caused by fossil fuel scarcity (>99%) at the midpoint level, mainly due to natural gas (>45%) and crude oil (>45%) used in various processes and for the transportation of intermediates.

6.4.2 Effect of the foreground and background uncertainties

Comparing both ILs in terms of their nominal LCA performance may lead to the idea that the production of [BMIM][BF_4] presents lower environmental impacts than [BMIM][PF_6] in all damage areas, and therefore, it is reasonable to discard the latter. However, the box plots in Figure 6.5 depict a different reality, whereby the range of impacts of both ILs overlap significantly.

When all the foreground and background uncertainties are considered simultaneously (scenario A), the damage caused by [BMIM][BF_4] on human health (left plot), ecosystem quality (middle plot), and resources (right plot) are higher than those caused by [BMIM][PF_6] in 21%, 15%, and 29% of the uncertainty scenarios, respectively (cf. top plot of Figure C.2). This overlap is significantly larger than that for the traditional approach considering solely the background uncertainties (scenario C), where the damage caused by [BMIM][BF_4] on human health, ecosystem quality, and resources are higher than those of [BMIM][PF_6] in 8%, 5%, and 20% of the scenarios (cf. bottom plot of Figure C.2). Thus, adding the foreground uncertainty to the background uncertainty (scenario A) is necessary for a more reliable comparative assessment of these two ILs.

When considering the foreground uncertainties alone (scenario B), notice that [BMIM][BF_4] presents lower impacts on human health, ecosystem quality, and resources in nearly all of the uncertainty scenarios. But even though the effect of the foreground uncertainties appears to be modest in comparison to that of the background uncertainties, the combined effect of the foreground and background uncertainties is significantly larger, with interquartile ranges

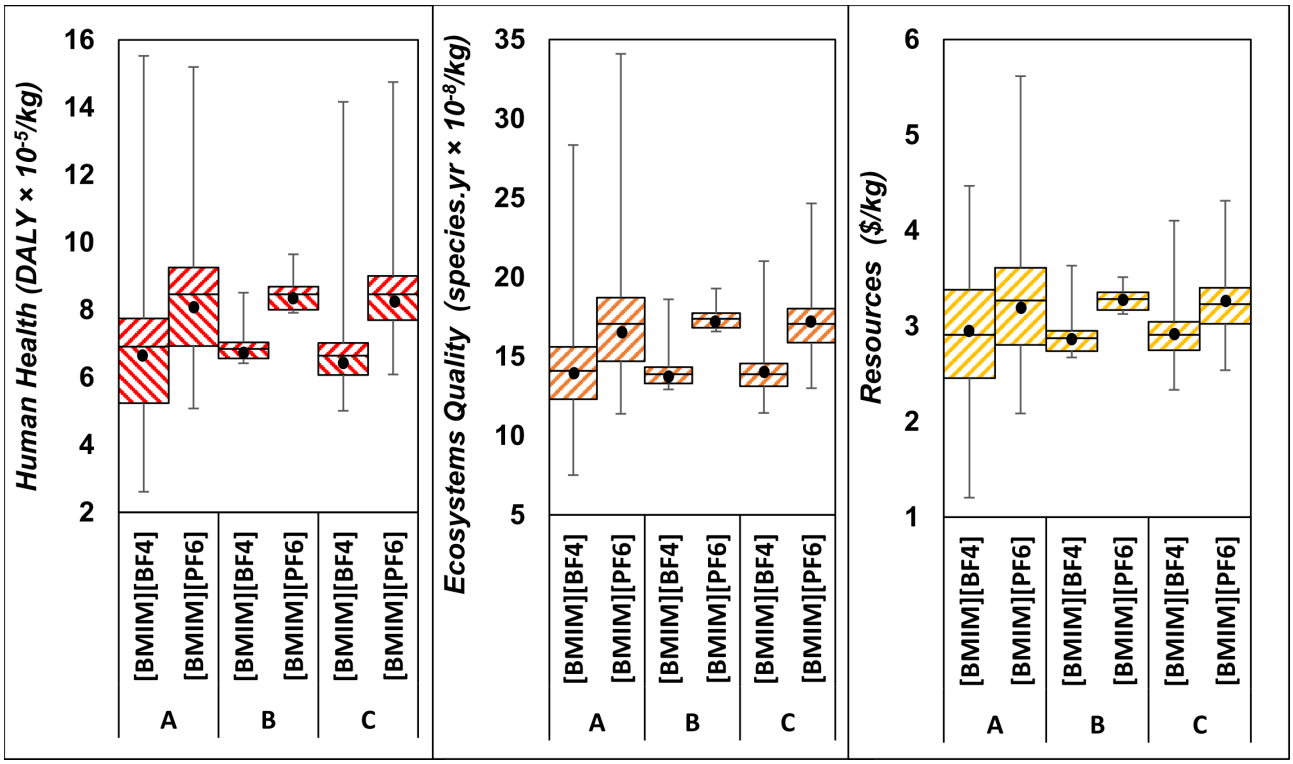

Figure 6.5: LCA comparison of endpoint indicators for the production of [BMIM][BF_4] and [BMIM][PF_6] under combined foreground/background uncertainty (A), foreground uncertainty only (B), and background uncertainty only (C). A total of 10,000 uncertainty scenarios are used in each case. The black points represent the mean. The central line inside each box represents the median. The lower and upper ends of the box represent the first and third quartiles, respectively. The lower and upper extended lines of the box represent the minimum and maximum values, respectively.

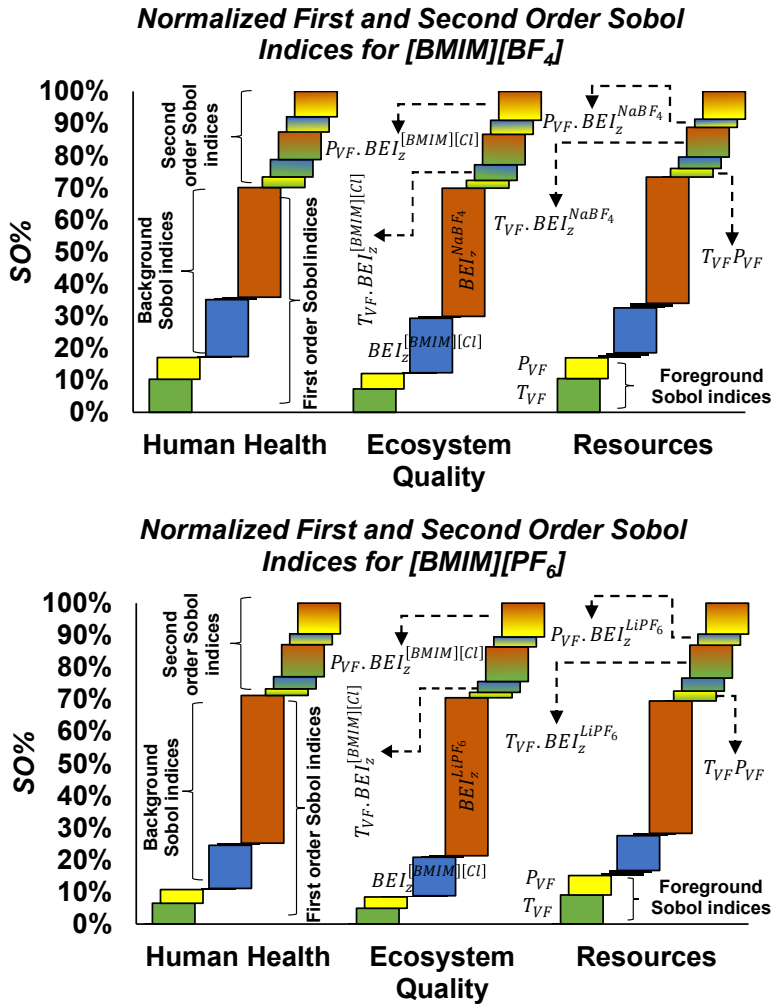

Figure 6.6: Breakdown of the sampled variance of each endpoint impact EI_z in terms of their first- and second-order Sobol indices for [BMIM][BF_4] (top) and [BMIM][PF_6] (bottom).

approximately two-fold greater for the environmental impacts in scenario A compared to scenario C. This is mainly due to the multiplicative effect between foreground and background uncertainties, as illustrated in Equation (R6.6).

6.4.3 Global sensitivity analysis of the impact assessment

The bar charts in Figure 6.6 show a breakdown of the sampled variance of each endpoint impact EI_z in terms of their first- and second-order Sobol indices, for both IL production processes and under combined foreground/background uncertainty. The complete set of Sobol indices can be found in Tables C.10 & C.11. It is found that a majority of the endpoint impact variance is attributable to the background uncertainties, which agrees with the comparison between

scenarios B and C in Figure 6.5. In the case of the ecosystem quality impact of [BMIM][PF_6] for instance, the first-order effects of the background uncertainty add up to 62%, while the combined first-order effects of the foreground uncertainty are only 9%. Specifically, the most sensitive background lumped parameters correspond to the production of the metal salt precursors $NaBF_4$ and $LiPF_6$ used, respectively, for synthesising [BMIM][BF_4] and [BMIM][PF_6], and to a lower extend the precursor ionic liquid [BMIM]Cl. This is not surprising because the production of these precursors involves several complex synthesis steps, some of which feature highly uncertain parameters, in comparison to other established background activities such as thermal energy and electricity production. Regarding the foreground uncertainty, the most sensitive process parameters correspond to the temperature T_{VF} and pressure P_{VF} in the vacuum flash vessel. The former impacts the evaporative (trace) losses of IL, whereas the latter modifies the phase equilibrium of the IL-water mixture, which are both impacting the final yields of IL. On top of these first-order effects, second-order interactions between the foreground and background parameters also contribute significantly (around 30%) to the variance of the environmental impacts, while higher-order interactions are negligible in this case. Such second-order effects were indeed expected given that the variance in scenario A of Figure 6.5 is much larger than those of scenarios B and C combined. The largest interactions are between the lumped background parameters $\mathrm{BEI}_z^{[\mathrm{BMIM}]\mathrm{Cl}}$, $\mathrm{BEI}_z^{\mathrm{NaBF_4}}$ or $\mathrm{BEI}_z^{\mathrm{LiPF_6}}$ and the vacuum flash temperature T_{VF} and pressure P_{VF} in the foreground processes. A small interaction is also observed between the two foreground parameters T_{VF} and P_{VF} due to their joint effect on the phase equilibrium of the IL-water mixture, whereas no interaction between the lumped background parameters is permitted here due to their additive structure in Equation (R6.6). Notably, since the foreground uncertainty parameters correspond to the same operational uncertainties in both production processes of [BMIM][BF_4] and [BMIM][PF_6], they would likely be set consistently in industrial processes. It may be overly conservative, therefore, to treat these uncertainties independently.

Given the prominent role of the IL precursors on the variance of the environmental impacts, a follow-up GSA may be conducted to further apportion the uncertainty in the lumped background parameters $\mathrm{BEI}_z^{[\mathrm{BMIM}]\mathrm{Cl}}$, $\mathrm{BEI}_z^{\mathrm{NaBF_4}}$ and $\mathrm{BEI}_z^{\mathrm{LiPF_6}}$, now acting as outputs, in terms of their upstream process activities. To demonstrate this process, the bar charts in Figure 6.7 show

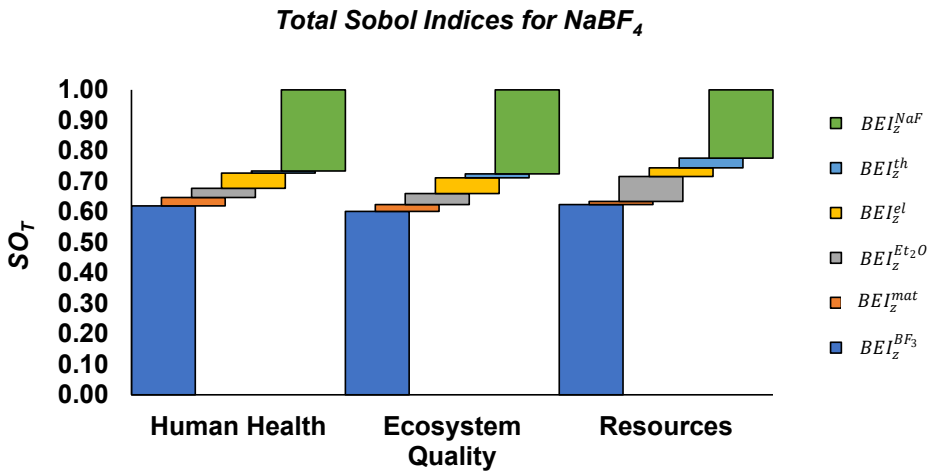

Figure 6.7: Breakdown of the sampled variance of the lumped background parameters $\mathrm{BEI}_z^{\mathrm{NaBF_4}}$ in all three endpoint impact categories in terms of Sobol indices, using combined foreground and background uncertainty.

a breakdown of the sampled variance of $\mathrm{BEI}_z^{\mathrm{NaBF_4}}$ in each endpoint impact category z, where the corresponding lumped background activities are: production of boron trifuoride ($\mathrm{BEI}_z^{\mathrm{BF_3}}$), production of sodium fluoride ($\mathrm{BEI}_z^{\mathrm{NaF}}$), production of diethyl ether ($\mathrm{BEI}_z^{\mathrm{Et_2O}}$), production of construction materials ($\mathrm{BEI}_z^{\mathrm{mat}}$), production of thermal energy ($\mathrm{BEI}_z^{\mathrm{th}}$), and production of electricity ($\mathrm{BEI}_z^{\mathrm{el}}$). The production of the main reagents BF_3 and NaF, both required in large quantities, accounts for most of the variance in this background parameter, namely $\mathrm{BEI}_z^{\mathrm{BF_3}}$ (58–60%) and $\mathrm{BEI}_z^{\mathrm{NaF}}$ (25–30%)—cf. Table C.12 for the complete sensitivity results. In the resources damage area, diethly ether also contributes a non-negligible share (8%) of the variance of $\mathrm{BEI}_z^{\mathrm{NaBF_4}}$ as this solvent is fossil-based and subject to large evaporative losses. By construction, the lumped background parameters $\mathrm{BEI}_z^{\mathrm{BF_3}}$, $\mathrm{BEI}_z^{\mathrm{NaF}}$, $\mathrm{BEI}_z^{\mathrm{Et_2O}}$, $\mathrm{BEI}_z^{\mathrm{mat}}$, $\mathrm{BEI}_z^{\mathrm{th}}$ and $\mathrm{BEI}_z^{\mathrm{el}}$ contribute additively to $\mathrm{BEI}_z^{\mathrm{NaBF_4}}$, so this apportionment only comprises first-order Sobol indices. Similar conclusions can be drawn on apportioning the variance of $\mathrm{BEI}_z^{\mathrm{[BMIM]Cl}}$ and $\mathrm{BEI}_z^{\mathrm{LiPF_6}}$ in terms of their upstream activities.

Instead of applying variance-based GSA, other approaches, such as OTSA, can be pursued to analyse the LCA results. Applied to the foreground system, OTSA allows the ranking of the uncertain foreground parameter in the order of importance. One caveat with OTSA, however, is that it keeps all the parameters but one constant at their nominal values, thereby neglecting cross-interactions amongst parameters as well as nonlinearity effects for the set parameters.

Using the same uncertainty ranges as in Table C.9, OTSA dramatically underestimates the sensitivity of the temperature T_{VF} and pressure P_{VF} in the vacuum flash vessel compared to the other foreground parameters (cf. Tables C.10 & C.11). This is because these two parameters present a strong mutual interaction and cause large variations when their values are low compared to the nominal temperature and pressure. Regarding the background system, it is possible to apply a similar parameter lumping as in Equation (R6.6) to reduce the dimensionality of the sensitivity analysis. Nevertheless, the main limitation is that OTSA cannot account for any of the interactions between the foreground and background parameters, which are known to contribute significantly to the variance of the environmental impacts (cf. Figures 6.5 & 6.6). This is in contrast to variance-based GSA methods that evaluate the effect of a parameter while also varying all the other parameters, thereby accounting for cross-interactions between parameters and being independent of choosing a nominal point. The interpretation of the Sobol indices is also unambiguous in terms of apportioning the variance of the environmental impacts to the foreground and background parameters. All for the results suggest that variance-based GSA is the method of choice in LCA of early-stage technologies.

6.5 Conclusions

This chapter presented a methodology for the reliable life-cycle assessment of emerging technologies. The methodology relies on detailed process simulation to bridge the gaps in the foreground and background inventory data. This methodology builds upon nominal LCA to quantify the environmental impacts in different damage areas and identify the activities contributing the most to these impacts. One main novelty involves quantifying the variance of the environmental impacts via joint uncertainty propagation in the foreground and background inventories, and for the first time, including uncertain physical parameters and uncertain design or operating parameters in the process models used to predict the performance of early-stage technology at scale. A second key contribution is a tailored GSA approach to apportioning the variance of each environmental impact in terms of the foreground and background uncertainties, where a reduced set of lumped background parameters corresponding to the immediate upstream

and downstream processes is considered rather than the complete set of uncertain background flows. This lumping facilitates the sensitivity results interpretation, while not impairing the generality of the analysis since a follow-up GSA may be conducted for the most sensitive lumped parameters if necessary. Additionally, unlike traditional approaches for ranking the uncertain parameters in order of importance, such as OTSA, variance-based GSA measures sensitivity across the whole parameter space, including cross-interactions between parameters and making it intuitive to interpret the resulting Sobol indices in terms of variance contributions. Another advantage of this methodology is that its implementation leverages state-of-the-art software, such as the process simulator Aspen HYSYS, along with the database ecoinvent, interfaced with Matlab and GSA toolkit SobolGSA, and may be conveniently orchestrated from a platform such as Matlab.

IL production, which remains at a low TRL, has provided an ideal case study for demonstrating the methodology. A nominal LCA comparison between the dialkylimidazolium ILs, [BMIM][BF_4] and [BMIM][PF_6], showed that the former has lower environmental impacts by 10–20% in all three endpoint damage areas and nearly all of these impacts are associated with the production of the precursors [BMIM]Cl, $NaBF_4$ and $LiPF_6$. However, a different reality emerged after quantifying the effects of both foreground and background uncertainties on the environmental impact predictions, due to significant overlaps between the impact ranges of [BMIM][BF_4] and [BMIM][PF_6]. This analysis also revealed that the consideration of foreground uncertainty alongside the background uncertainty can approximately double the impact ranges compared to the effect of background uncertainty alone. The results of the variance-based GSA can establish that a majority of the impact ranges are caused by only four uncertain parameters: the lumped background parameters representing the production impacts of the precursors [BMIM]Cl and either $NaBF_4$ or $LiPF_6$—the variations that attributed mainly to the production of solvents and reagents; and the vacuum flash temperature and pressure in the foreground processes. Significant interactions were also revealed between the foreground and background parameters, in agreement with the uncertainty quantification results. Overall, these findings illustrate how foreground uncertainties in early-stage technology assessment can exacerbate the variability of environmental impacts and therefore should not be ignored. For completeness,

a follow-up work would be needed for expanding this uncertainty-GSA framework to include LCC uncertainties embedded in raw materials and utilites market prices volatility throughout the whole supply chain. Finally, looking beyond ILs, the application of this methodology may provide useful insight into the assessment of early-stage CO_2 technology and other feedstock recycling technologies for certain types of plastic waste.

Chapter 7

Conclusions and Future Work

7.1 Conclusions and contributions made

The contributions of this dissertation have one common objective, which is to promote holistic sustainability assessment modelling approaches and effective decision-making tools to evaluate the economic and environmental performance of ILs through life-cycle reasoning. The novelties are based on the integration of process systems engineering methods with LCA and LCC along with decision-making and analysis approaches and tools to help researchers and decision-makers working with IL technologies to address the challenges of conducting such assessments for novel technologies while improving the sustainability of their processes and products. The case studies presented in this thesis have demonstrated the efficiency of these methods and tools. The following section will discuss these contributions in detail.

- A systematic framework for the sustainability assessment of ILs was developed. This not only establishes a basis for evaluating ILs and compares them with their counterparts but also ensures assessment completeness, addresses gaps and inconsistencies commonly found in the literature, and reduces evaluation uncertainty. The framework consists of integrated methods, approaches, and tools, with two main objectives. First, the framework aims to provide a clear structure and specific guidelines for conducting LCA and LCC of ILs, which have been successfully applied throughout this work. Second, the framework aims to address the gaps in data by implementing state-of-the-art LCA and process engineering

approaches and tools, e.g., LCA proxy data for inventory analysis and semi-empirical data for IL physiochemical properties. The framework was successfully applied to two novel case studies, stressing the importance of incorporating both economic and environmental indicators while ensuring these indicators fully cover environmental protection areas, e.g., ReCiPe endpoints, for complete and meaningful assessment. The LCA results of [BMIM][BF_4] obtained from the metathesis route show that using incomplete data and short-cut approaches, such as stoichiometric calculations, can have a severe impact on the evaluation, and in this particular case, it can underestimate the actual impacts of [BMIM][BF_4].

- Monetization was incorporated to improve the decision-making process using the base framework. This is especially critical when facing multi-criteria problems and comparing alternatives with trade-offs. The method was applied in the case study of [HSO_4]-based ILs and proved to be effective, especially when comparing the economic and environmental indicators for the production of the different biomass pretreatment solvents. The results showed that [HMIM][HSO_4] had the highest cost, glycerol had the highest human health and ecosystem impacts, and acetone had the highest damage on resources. Using monetization turned this multi-criteria problem into a single-criterion problem, which is the total cost, by converting environmental impacts into indirect costs (externalities). When adding up direct and indirect costs, glycerol had the highest total cost due to several activities involved in its production such as deforestation and land use. Therefore, it was revealed that renewable chemicals, such as glycerol, may reduce the amount of non-renewable sources drastically, but this can be at the cost of higher environmental impacts in other categories such as human health and ecosystem quality, i.e., shifting the burdens from one category to another. By using monetization, these hidden costs can be quantified, and sustainability assessment decision-making is improved by looking at all the conflicting economic and environmental indicators from a single criterion.

- The case study of the metathesis [BMIM][BF_4] and halide-free [BMIM][BF_4] proves that it is of paramount importance to consider the different alternative synthesis routes of

ILs. The results showed that the cost of halide-free [BMIM][BF_4] was nearly half of the metathesis [BMIM][BF_4]. Similarly, the environmental impacts were cut by over 65% in all categories: human health, ecosystem quality, and resources when halide-free [BMIM][BF_4] was used instead. This credit in cost and environmental impacts obtained by switching to an alternative synthesis route proved to be highly effective when the IL was compared against its counterparts in fuel desulfurization. In particular, the halide-free [BMIM][BF_4] had the lowest cost and environmental impacts in all categories among the desulfurization solvents while the metathesis [BMIM][BF_4] had higher human health and ecosystem quality impacts and its cost was relatively higher than acetonitrile. This shows that the choice of the IL synthesis route can have a significant impact on the assessment results and that in turn can affect decision-making when considering their use in different applications.

- The results obtained from the [BMIM][BF_4] in fuel desulfurization and HSO_4 ILs in biomass pretreatment case studies stress the importance of including the use phase in the assessment of ILs, especially when compared to other types of chemical like VOCs. For example, [BMIM][BF_4] production cost in both synthesis routes in the fuel desulfurization case study was much higher than that of acetonitrile and DMF. They also had higher environmental impacts, except for halide-free [BMIM][BF_4] in resource depletion, in all categories. However, when the use phase was included, both cost and environmental impacts were reduced significantly, and the cost and environmental impacts of the use of the halide-free [BMIM][BF_4] were lower than its counterparts. Similarly, the cost and environmental impacts for the combined production and use of both protic ILs in the biomass pretreatment case study were much lower than the conventional solvents acetone and glycerol compared to the case of accounting for the production phase only where ILs could be higher. In both cases, the significant reduction in the economic and environmental indicators of ILs is mainly due to their negligible losses pertaining to their superior recyclability which is a key advantage for their use over conventional chemicals to improve sustainability.

- A framework combining LCA, uncertainty analysis, and global sensitivity analysis with process design and simulation was developed. This is necessary to address the common approach followed when conducting an LCA uncertainty analysis and sensitivity analysis. Unlike the conventional uncertainty analysis, which omits uncertainties embedded in the simulation model and considers only background uncertainties obtained from databases, the developed framework considers both process model uncertainties (foreground uncertainties) and background uncertainties simultaneously. Additionally, the framework improves existing approaches of sensitivity analysis that follow the OTSA method, i.e., varying parameters one at a time, by applying a global approach that varies all parameters within the entire input space simultaneously. The framework was applied to the case study of the production of [BMIM][BF_4] and [BMIM][PF_6] and proves to be effective in presenting the full range of uncertainty and identifying the actual key uncertain parameters. The results showed that [BMIM][BF_4] is favourable under all categories when foreground uncertainties only were considered, and its effect was stressed when combined with background uncertainties causing a significant uncertainty overlap, which is over 30% higher compared to the case where only background uncertainties were considered. Therefore, not accounting for the foreground uncertainties can lead to erroneous results, especially when comparing processes and products with impacts of the same order. It was also shown that using GSA reduced the number of key uncertain parameters from seven down to only two which is over 70% due to the binary contributions accounted for in GSA. Thus, in this specific case study, GSA proves to be superior to OTSA in identifying key uncertain parameters and using it can make the experiment or simulation, especially those which require thousands of samples or run slow, to run more efficiently. Finally, this uncertainty-GSA framework further enhances and complements the base framework used throughout this thesis, and combined, they offer a more robust and complete framework that can be applied to ILs and similar novel chemicals.

7.2 Future work

The thesis focused on developing a methodological framework applied through case studies to improve the sustainability assessment of ILs. However, this work may provide guidance and a basis for future research. The following section will discuss some ideas and directions for potential research projects that can accelerate endeavours aimed towards sustainability-based evaluation and screening of ILs at an early stage, which helps speed up their adoption on a large scale.

- The scope of the assessment in this thesis included the production and use of ionic liquids. This is to assess the potential of ILs as sustainable alternatives knowing that their losses are negligible (assuming stability and non-aqueous losses) in most applications compared to conventional chemicals such as VOCs. However, it is still not considered complete without including the disposal phase. Unfortunately, data about the fate, exposure, and effect of ILs and their quantified impacts on the environment are limited, regardless of the large number of studies investigating their environmental characteristics, including toxicity and biodegradability. In addition, existing characterisation models, such as USEtox, are limited to certain chemicals and may not be suitable for predicting the toxicity of ILs. Therefore, ILs characterisation models need to be developed based on actual experiments to help LCA practitioners and experts quantify the environmental impacts of ILs when disposed of to improve the accuracy of the assessments.

- In this thesis, only a few ILs representing the two main classes of ILs have been studied. However, there are thousands of ILs with properties suitable for many applications that also need to be considered, for example, certain applications where the use of ILs is more advantageous but its losses are non-negligible and may require ILs that are less harmful to the environment. In this case, this may refer to the use of ILs, such as choline-based ILs, which were found to be harmless and readily biodegradable. However, this should also be combined with a careful study of the different available synthesis routes because the impacts from the production will be more stressed when non-negligible losses are present.

- The advantage of ILs over conventional chemicals in the presented case studies does not necessarily mean that their use is superior in all applications from a sustainability point of view, and hence, more applications where ILs are used need to be studied and evaluated. Every application involves certain factors and requirements that need to be accounted for when considering the use of ILs. For example, ILs tend to be less attractive in applications where they are consumed rather than re-used, e.g., energetic ILs, due to their complex synthesis as presented in this work. Additionally, the assessment of the use phase included in the case studies may not be accurate since they were based on a few parameters believed to be the determining factors of the overall performance. However, detailed modelling of the use phase, similar to what has been done on the production of ILs in this work, should be used to further improve the reliability of the assessment.

- The uncertainty-GSA framework presented in Chapter 6 focused mainly on uncertainties in the LCA part, which come from process parameters as well as background inventory. However, volatility of market prices of feedstocks and utilities may affect LCC results as well. Therefore, a revised uncertainty-GSA framework is needed to include LCC uncertainties for completeness in a similar fashion to LCA. Additionally, the monetization values presented in Chapter 5 carry a wide range of uncertainty, which also need be accounted for in LCA when implementing this framework.

- Finally, to accelerate the efforts mentioned above and improve the reliability of the assessment, it is necessary to develop fast prediction models based on actual experimental data for estimating the different pure and mixed IL properties. This is required to improve the underlying data and enable researchers to conduct further experiments or run process simulations that can utilise such data. For example, phase equilibrium properties and activity coefficients are needed to improve the accuracy of process simulations involving multi-phase mixture separations. Additionally, to address the extensive number of ILs available, the results of the detailed assessments can be fed into other models for predicting the economic and environmental indicators for fast and reliable screening of ILs in terms of their sustainability.

Bibliography

[1] IEA. Energy Technology Perspectives 2017 Excerpt Informing Energy Sector Transformations. *IEA: Paris, France*, 2017.

[2] Hannah Ritchie, Max Roser, and Pablo Rosado. CO and Greenhouse Gas Emissions. *Our World in Data*, May 2020.

[3] IEA. Key World Energy Statistics 2021. *IEA: Paris, France*, 2021.

[4] Will Steffen, Paul J. Crutzen, and John R. McNeill. The Anthropocene: Are Humans Now Overwhelming the Great Forces of Nature. *AMBIO: A Journal of the Human Environment*, 36:614–621, December 2007.

[5] Edward Broughton. The Bhopal disaster and its aftermath: a review. *Environmental Health*, 4, May 2005.

[6] J. Chander. Water contamination: a legacy of the union carbide disaster in Bhopal, India. *International Journal of Occupational and Environmental Health*, 7(1):72–73, March 2001.

[7] BP. Statistical Review of World Energy 2020. Technical report, 2020.

[8] Vaclav Smil. *Energy Transitions: Global and National Perspectives, 2nd Edition*. December 2016.

[9] The World Bank. World Development Indicators. Technical report, 2016.

[10] Irving M. Mintzer, editor. *Confronting Climate Change: Risks, Implications and Responses*. Cambridge, 1992.

[11] A. Haines. Global warming and health. *British Medical Journal*, 302:669–670, 1991.

[12] Pervez Alam and Kafeel Ahmade. Impact of Solid Waste on Health and the Environment. *International Journal of Sustainable Development and Green Economics*, 2(2315):4, 2013.

[13] Garrett Hardin. The Tragedy of the Commons. *Journal of Natural Resources Policy Research*, 1(3):243–253, July 2009.

[14] Gro Harlem Brundtland. Report of the World Commission on Environment and Development:'Our Common Future', United Nations. 1987.

[15] Ayça Tokuç. Rio Declaration on Environment and Development (UN). In Samuel O. Idowu, Nicholas Capaldi, Liangrong Zu, and Ananda Das Gupta, editors, *Encyclopedia of Corporate Social Responsibility*, pages 2087–2094. Springer, Berlin, Heidelberg, 2013.

[16] UN. Transforming our world : the 2030 Agenda for Sustainable Development, 2015.

[17] US EPA. Summary of the Pollution Prevention Act, 1990.

[18] Paul T Anastas and John C Warner. *Green Chemistry: Theory and Practice*. Oxford University Press, 1998.

[19] Mark A. Shannon, Paul W. Bohn, Menachem Elimelech, John G. Georgiadis, Benito J. Mariñas, and Anne M. Mayes. Science and technology for water purification in the coming decades. *Nature*, 452(7185):301–310, March 2008.

[20] Željko Knez, Milica Pantić, Darija Cör, Zoran Novak, and Maša Knez Hrnčič. Are supercritical fluids solvents for the future? *Chemical Engineering and Processing - Process Intensification*, 141:107532, July 2019.

[21] Peter Wasserscheid and Thomas Welton. *Ionic liquids in synthesis*. John Wiley & Sons, 2008.

[22] Hua Zhao and Sanjay V Malhotra. Applications of ionic liquids in organic synthesis. *Aldrichimica Acta*, 2002.

[23] A Bösmann, L Datsevich, A Jess, A Lauter, C Schmitz, and P Wasserscheid. Deep desulfurization of diesel fuel by extraction with ionic liquids. *Chemical Communications*, (23):2494–2495, 2001.

[24] Mehrdad Khamooshi, Kiyan Parham, and Ugur Atikol. Overview of ionic liquids used as working fluids in absorption cycles. *Advances in Mechanical Engineering*, 5:620592, 2013.

[25] J. Qu, J. J. Truhan, S. Dai, H. Luo, and P. J. Blau. Ionic liquids with ammonium cations as lubricants or additives. *Tribology Letters*, 22(3):207–214, June 2006.

[26] Maciej Galiński, Andrzej Lewandowski, and Izabela Stepniak. Ionic liquids as electrolytes. *Electrochimica acta*, 51(26):5567–5580, 2006.

[27] Lynnette A Blanchard, Dan Hancu, Eric J Beckman, and Joan F Brennecke. Green processing using ionic liquids and CO 2. *Nature*, 399(6731):28, 1999.

[28] John D Holbrey, W Matthew Reichert, RG Reddy, and RD Rogers. Ionic liquids as green solvents: progress and prospects. In *ACS symposium series*, volume 856, pages 121–133. American Chemical Society Washington, DC, 2003.

[29] Zhen Yang and Wubin Pan. Ionic liquids: Green solvents for nonaqueous biocatalysis. *Enzyme and Microbial Technology*, 37(1):19–28, 2005.

[30] Agnieszka Brandt, John Gräsvik, Jason P. Hallett, and Tom Welton. Deconstruction of lignocellulosic biomass with ionic liquids. *Green chemistry*, 15(3):550–583, 2013.

[31] Douglas R. MacFarlane, Kenneth R. Seddon, Douglas R. MacFarlane, and Kenneth R. Seddon. Ionic Liquids—Progress on the Fundamental Issues. *Australian Journal of Chemistry*, 60(1):3–5, February 2007.

[32] Vinícius Gonçalves Maciel, Dominic J. Wales, Marcus Seferin, Cássia Maria Lie Ugaya, and Victor Sans. State-of-the-art and limitations in the life cycle assessment of ionic liquids. *Journal of Cleaner Production*, 217:844–858, April 2019.

[33] Rebecca Renner. Ionic liquids: An industrial cleanup solution. *Environmental Science & Technology*, 35(19):410A–413A, October 2001.

[34] Yi Zhang, Bhavik R. Bakshi, and E. Sahle Demessie. Life Cycle Assessment of an Ionic Liquid versus Molecular Solvents and Their Applications. *Environmental Science & Technology*, 42(5):1724–1730, 2008.

[35] Miao Yu, Su-Mei Li, Xiao-Yu Li, Bang-Jun Zhang, and Jian-Ji Wang. Acute effects of 1-octyl-3-methylimidazolium bromide ionic liquid on the antioxidant enzyme system of mouse liver. *Ecotoxicology and Environmental Safety*, 71(3):903–908, November 2008.

[36] N. Gathergood and P. J. Scammells. Design and Preparation of Room-Temperature Ionic Liquids Containing Biodegradable Side Chains. *Australian Journal of Chemistry*, 55(9): 557–560, 2002.

[37] Alistair C. Leitch, Tarek M. Abdelghany, Philip M. Probert, Michael P. Dunn, Stephanie K. Meyer, Jeremy M. Palmer, Martin P. Cooke, Lynsay I. Blake, Katie Morse, Anna K. Rosenmai, Agneta Oskarsson, Lucy Bates, Rodrigo S. Figueiredo, Ibrahim Ibrahim, Colin Wilson, Noha F. Abdelkader, David E. Jones, Peter G. Blain, and Matthew C. Wright. The toxicity of the methylimidazolium ionic liquids, with a focus on M8OI and hepatic effects. *Food and Chemical Toxicology*, 136:111069, February 2020.

[38] Dana Kralisch, Annegret Stark, Swen Körsten, Günter Kreisel, and Bernd Ondruschka. Energetic, environmental and economic balances: Spice up your ionic liquid research efficiency. *Green Chemistry*, 7(5):301–309, May 2005.

[39] Hye Kyung Timken, Huping Luo, Bong-Kyu Chang, Elizabeth Carter, and Matthew Cole. ISOALKY™ Technology: Next-Generation Alkylate Gasoline Manufacturing Process Technology Using Ionic Liquid Catalyst. In Mark B. Shiflett, editor, *Commercial Applications of Ionic Liquids*, Green Chemistry and Sustainable Technology, pages 33–47. 2020.

[40] Matthias Maase and Klemens Massonne. Biphasic Acid Scavenging Utilizing Ionic Liquids: The First Commercial Process with Ionic Liquids. In *Ionic Liquids IIIB: Fundamentals, Progress, Challenges, and Opportunities*, volume 902 of *ACS Symposium Series*, pages 126–132. March 2005.

[41] Ursula Tischner, Sandra Masselter, Bernd Hirschl, Germany, and Umweltbundesamt. *How to do EcoDesign?: a guide for environmentally and economically sound design*. 2000.

[42] Johan Jacquemin and Magdalena Bendová. Introduction on Special Issue: Ionic Liquids. *Journal of Solution Chemistry*, 44(3):379–381, April 2015.

[43] Natalia V. Plechkova and Kenneth R. Seddon. Applications of ionic liquids in the chemical industry. *Chemical Society Reviews*, 37(1):123–150, December 2007.

[44] Ezinne C. Achinivu, Reagan M. Howard, Guoqing Li, Hanna Gracz, and Wesley A. Henderson. Lignin extraction from biomass with protic ionic liquids. *Green Chemistry*, 16(3): 1114–1119, 2014.

[45] Wu Lan, Chuan-Fu Liu, and Run-Cang Sun. Fractionation of Bagasse into Cellulose, Hemicelluloses, and Lignin with Ionic Liquid Treatment Followed by Alkaline Extraction. *Journal of Agricultural and Food Chemistry*, 59(16):8691–8701, August 2011.

[46] Carla Luzia Borges Reis, Lorena Mara Alexandre e Silva, Tigressa Helena Soares Rodrigues, Anne Kamilly Nogueira Félix, Rílvia Saraiva de Santiago-Aguiar, Kirley Marques Canuto, and Maria Valderez Ponte Rocha. Pretreatment of cashew apple bagasse using protic ionic liquids: Enhanced enzymatic hydrolysis. *Bioresource Technology*, 224:694–701, January 2017.

[47] Pedro Verdía, Agnieszka Brandt, Jason P. Hallett, Michael J. Ray, and Tom Welton. Fractionation of lignocellulosic biomass with the ionic liquid 1-butylimidazolium hydrogen sulfate. *Green Chemistry*, 16(3):1617–1627, 2014.

[48] Tamar L. Greaves and Calum J. Drummond. Protic ionic liquids: properties and applications. *Chemical Reviews*, 108(1):206–237, 2008.

[49] Seung-Yul Lee, Atsushi Ogawa, Michihiro Kanno, Hirofumi Nakamoto, Tomohiro Yasuda, and Masayoshi Watanabe. Nonhumidified Intermediate Temperature Fuel Cells Using Protic Ionic Liquids. *Journal of the American Chemical Society*, 132(28):9764–9773, July 2010.

[50] Tomohiro Yasuda and Masayoshi Watanabe. Protic ionic liquids: Fuel cell applications. *MRS Bulletin*, 38(7):560–566, July 2013.

[51] Usman Ali Rana, Maria Forsyth, Douglas R. MacFarlane, and Jennifer M. Pringle. Toward protic ionic liquid and organic ionic plastic crystal electrolytes for fuel cells. *Electrochimica Acta*, 84:213–222, December 2012.

[52] Hirofumi Kondo. Protic Ionic Liquids with Ammonium Salts as Lubricants for Magnetic Thin Film Media. *Tribology Letters*, 31(3):211–218, September 2008.

[53] Jiayin Hu, Jun Ma, Qinggong Zhu, Zhaofu Zhang, Congyi Wu, and Buxing Han. Transformation of Atmospheric CO2 Catalyzed by Protic Ionic Liquids: Efficient Synthesis of 2-Oxazolidinones. *Angewandte Chemie International Edition*, 54(18):5399–5403, 2015.

[54] Ching K. Lee, Hsin W. Huang, and Ivan J. B. Lin. Simple amphiphilic liquid crystalline N-alkylimidazolium salts. A new solvent system providing a partially ordered environment. *Chemical Communications*, 0(19):1911–1912, January 2000.

[55] M. M. Waichigo, T. L. Riechel, and N. D. Danielson. Ethylammonium Acetate as a Mobile Phase Modifier for Reversed Phase Liquid Chromatography. *Chromatographia*, 61(1): 17–23, January 2005.

[56] Juliusz Pernak, Izabela Goc, and Ilona Mirska. Anti-microbial activities of protic ionic liquids with lactate anion. *Green Chemistry*, 6(7):323–329, July 2004.

[57] Barbara Kirchner, editor. *Ionic Liquids*, volume 290 of *Topics in Current Chemistry*. Springer Berlin Heidelberg, Berlin, Heidelberg, 2010.

[58] Youxing Fang, Kazuki Yoshii, Xueguang Jiang, Xiao-Guang Sun, Tetsuya Tsuda, Nada Mehio, and Sheng Dai. An AlCl3 based ionic liquid with a neutral substituted pyridine ligand for electrochemical deposition of aluminum. *Electrochimica Acta*, 160:82–88, April 2015.

[59] Gang Cheng, Patanjali Varanasi, Rohit Arora, Vitalie Stavila, Blake A. Simmons, Michael S. Kent, and Seema Singh. Impact of Ionic Liquid Pretreatment Conditions on

Cellulose Crystalline Structure Using 1-Ethyl-3-methylimidazolium Acetate. *The Journal of Physical Chemistry B*, 116(33):10049–10054, August 2012.

[60] T. Fischer, A. Sethi, T. Welton, and J. Woolf. Diels-Alder reactions in room-temperature ionic liquids. *Tetrahedron Letters*, 40(4):793–796, January 1999.

[61] E. I. Cooper and C. A. Angell. Versatile organic iodide melts and glasses with high mole fractions of LiI: Glass transition temperatures and electrical conductivities. *Solid State Ionics*, 9-10:617–622, December 1983.

[62] G. Wytze Meindersma, Anita Podt, Marianne B. Klaren, and André B. de Haan. Separation of Aromatic and Aliphatic Hydrocarbons with Ionic Liquids. *Chemical Engineering Communications*, 193(11):1384–1396, November 2006.

[63] Xiaoyong Li, Minqiang Hou, Zhaofu Zhang, Buxing Han, Guanying Yang, Xiaoling Wang, and Lizhuang Zou. Absorption of CO2 by ionic liquid/polyethylene glycol mixture and the thermodynamic parameters. *Green Chemistry*, 10(8):879–884, August 2008.

[64] Paul J. Corbett, Alastair J. S. McIntosh, Michael Gee, and Jason P. Hallett. Use of ionic liquids to minimize sodium induced internal diesel injector deposits (IDIDs). *Molecular Systems Design & Engineering*, 3(2):397–407, 2018.

[65] Daniel Klein-Marcuschamer, Blake A. Simmons, and Harvey W. Blanch. Techno-economic analysis of a lignocellulosic ethanol biorefinery with ionic liquid pre-treatment. *Biofuels, Bioproducts and Biorefining*, 5(5):562–569, 2011.

[66] S. Murat Sen, Joseph B. Binder, Ronald T. Raines, and Christos T. Maravelias. Conversion of biomass to sugars via ionic liquid hydrolysis: process synthesis and economic evaluation. *Biofuels, Bioproducts and Biorefining*, 6(4):444–452, 2012.

[67] L. Andreani and J. D. Rocha. Use of ionic liquids in biodiesel production: a review. *Brazilian Journal of Chemical Engineering*, 29:1–13, March 2012. Publisher: Brazilian Society of Chemical Engineering.

[68] Niall MacDowell, Nick Florin, Antoine Buchard, Jason Hallett, Amparo Galindo, George Jackson, Claire S. Adjiman, Charlotte K. Williams, Nilay Shah, and Paul Fennell. An overview of CO2 capture technologies. *Energy & Environmental Science*, 3(11):1645–1669, October 2010. Publisher: The Royal Society of Chemistry.

[69] L. Chen, M. Sharifzadeh, N. Mac Dowell, T. Welton, N. Shah, and J. P. Hallett. Inexpensive ionic liquids: [HSO4]-based solvent production at bulk scale. *Green Chemistry*, 16(6): 3098–3106, 2014.

[70] Anthe George, Agnieszka Brandt, Kim Tran, Shahrul M. S. Nizan S. Zahari, Daniel Klein-Marcuschamer, Ning Sun, Noppadon Sathitsuksanoh, Jian Shi, Vitalie Stavila, Ramakrishnan Parthasarathi, Seema Singh, Bradley M. Holmes, Tom Welton, Blake A. Simmons, and Jason P. Hallett. Design of low-cost ionic liquids for lignocellulosic biomass pretreatment. *Green Chemistry*, 17(3):1728–1734, 2015.

[71] Cinzia Chiappe, Andrea Mezzetta, Christian Silvio Pomelli, Gaetano Iaquaniello, Alessio Gentile, and Barbara Masciocchi. Development of cost-effective biodiesel from microalgae using protic ionic liquids. *Green Chemistry*, 18(18):4982–4989, 2016.

[72] Thi Phuong Thuy Pham, Chul-Woong Cho, and Yeoung-Sang Yun. Environmental fate and toxicity of ionic liquids: A review. *Water Research*, 44(2):352–372, January 2010.

[73] Patricia Lucía Amado Alviz and Alejandro J. Alvarez. Comparative life cycle assessment of the use of an ionic liquid ([Bmim]Br) versus a volatile organic solvent in the production of acetylsalicylic acid. *Journal of Cleaner Production*, 168:1614–1624, 2017.

[74] Jennifer Neumann, Olav Grundmann, Jorg Thöming, Michael Schulte, and Stefan Stolte. Anaerobic biodegradability of ionic liquid cations under denitrifying conditions. *Green Chemistry*, 12(4):620–627, 2010.

[75] Robert J. Cornmell, Catherine L. Winder, Gordon J. T. Tiddy, Royston Goodacre, and Gill Stephens. Accumulation of ionic liquids in Escherichia coli cells. *Green Chemistry*, 10 (8):836–841, 2008.

[76] Dimitri Devuyst, Luc Hens, and Walter De Lannoy. *How Green Is the City?: Sustainability Assessment and the Management of Urban Environments*. Columbia University Press, 2001.

[77] Barry Ness, Evelin Urbel-Piirsalu, Stefan Anderberg, and Lennart Olsson. Categorising tools for sustainability assessment. *Ecological economics*, 60(3):498–508, 2007.

[78] Roger A. Sheldon. Metrics of green chemistry and sustainability: Past, present, and future. *ACS Sustainable Chemistry & Engineering*, 6(1):32–48, 2017.

[79] Jun-Jie Cao, Feng Zhou, and Jian Zhou. Improving the Atom Efficiency of the Wittig Reaction by a "Waste as Catalyst/Co-catalyst" Strategy. *Angewandte Chemie International Edition*, 49(29):4976–4980, 2010.

[80] Maggel Deetlefs and Kenneth R. Seddon. Assessing the greenness of some typical laboratory ionic liquid preparations. *Green Chemistry*, 12(1):17–30, January 2010.

[81] Matthew J. Eckelman, Julie B. Zimmerman, and Paul T. Anastas. Toward Green Nano. *Journal of Industrial Ecology*, 12(3):316–328, 2008.

[82] Bruce H. Lipshutz and Subir Ghorai. Transitioning organic synthesis from organic solvents to water. What's your E Factor? *Green Chemistry*, 16(8):3660–3679, 2014.

[83] Roger A. Sheldon. Atom efficiency and catalysis in organic synthesis. *Pure and Applied Chemistry*, 72(7):1233–1246, 2009.

[84] Roger A Sheldon. Organic synthesis-past, present and future. *Chemistry and Industry*, (23):903–6, 1992.

[85] Jiannan Xiang, Akihiro Orita, and Junzo Otera. Fluorous Biphasic Esterification Directed towards Ultimate Atom Efficiency. *Angewandte Chemie International Edition*, 41(21): 4117–4119, 2002.

[86] Rolf Frischknecht, Franziska Wyss, Sybille Büsser Knöpfel, Thomas Lützkendorf, and Maria Balouktsi. Cumulative energy demand in LCA: the energy harvested approach. *The International Journal of Life Cycle Assessment*, 20(7):957–969, July 2015.

[87] Annick Anctil, Callie W. Babbitt, Ryne P. Raffaelle, and Brian J. Landi. Cumulative energy demand for small molecule and polymer photovoltaics. *Progress in Photovoltaics: Research and Applications*, 21(7):1541–1554, 2013.

[88] Michael Greiter, Senad Novalin, Martin Wendland, Klaus-Dieter Kulbe, and Johann Fischer. Electrodialysis versus ion exchange: comparison of the cumulative energy demand by means of two applications. *Journal of Membrane Science*, 233(1):11–19, April 2004.

[89] Dirk Gürzenich, Jyotirmay Mathur, Narendra Kumar Bansal, and Hermann-Josef Wagner. Cumulative energy demand for selected renewable energy technologies. *The International Journal of Life Cycle Assessment*, 4(3):143–149, May 1999.

[90] Merten Morales. *Process Design and Sustainability Assessment for Biorefinery Technologies*. Doctoral Thesis, ETH Zurich, 2016. URL `https://www.research-collection.ethz.ch/handle/20.500.11850/156074`.

[91] Dana Kralisch, Denise Reinhardt, and Günter Kreisel. Implementing objectives of sustainability into ionic liquids research and development. *Green Chemistry*, 9(12):1308–1318, 2007.

[92] Ruth E. Baltus, Robert M. Counce, Benjamin H. Culbertson, Huimin Luo, David W. DePaoli, Sheng Dai, and Douglas C. Duckworth. Examination of the Potential of Ionic Liquids for Gas Separations. *Separation Science and Technology*, 40(1-3):525–541, January 2005.

[93] Jared Edgar Peterson. *Ionic Liquid / CO2 Co-Fluid Refrigeration: CO2 Solubility Modeling and Life Cycle Analysis*. PhD thesis, University Of Notre Dame, September 2013.

[94] Sabine Huebschmann, Dana Kralisch, Holger Loewe, Denis Breuch, Jan Hauke Petersen, Thomas Dietrich, and Ralf Scholz. Decision support towards agile eco-design of microreaction processes by accompanying (simplified) life cycle assessment. *Green Chemistry*, 13 (7):1694–1707, 2011.

[95] Reza Farahipour, Arunprakash T. %J ACS Sustainable Chemistry Karunanithi, and Engineering. Life cycle environmental implications of CO2 capture and sequestration with ionic liquid 1-butyl-3-methylimidazolium acetate. 2(11):2495–2500, 2014.

[96] Rosa M Cuéllar-Franca, Pelayo García-Gutiérrez, SF Rebecca Taylor, Christopher Hardacre, and Adisa Azapagic. A novel methodology for assessing the environmental sustainability of ionic liquids used for CO2 capture. *Faraday Discussions*, 192:283–301, 2016.

[97] Serena Righi, Andrea Morfino, Paola Galletti, Chiara Samorì, Alessandro Tugnoli, and Carlo Stramigioli. Comparative cradle-to-gate life cycle assessments of cellulose dissolution with 1-butyl-3-methylimidazolium chloride and N-methyl-morpholine-N-oxide. *Green Chemistry*, 13(2):367–375, 2011.

[98] Walter Kloepffer. Life cycle sustainability assessment of products. *The International Journal of Life Cycle Assessment*, 13(2):89, February 2008.

[99] United Nations Environment Programme. Guidelines for Social Life Cycle Assessment of Products and Organisations 2020. 2020.

[100] Annekatrin Lehmann, Eva Zschieschang, Marzia Traverso, Matthias Finkbeiner, and Liselotte Schebek. Social aspects for sustainability assessment of technologies—challenges for social life cycle assessment (SLCA). *The International Journal of Life Cycle Assessment*, 18(8):1581–1592, September 2013.

[101] Methodological Sheets for Subcategories in Social Life Cycle Assessment (S-LCA) 2021. Technical report, Life Cycle Initiative, December 2021.

[102] ISO. ISO 14040:2006, 2006.

[103] Poritosh Roy, Daisuke Nei, Takahiro Orikasa, Qingyi Xu, Hiroshi Okadome, Nobutaka Nakamura, and Takeo Shiina. A review of life cycle assessment (LCA) on some food products. *Journal of Food Engineering*, 90(1):1–10, January 2009.

[104] Oscar Ortiz, Francesc Castells, and Guido Sonnemann. Sustainability in the construction industry: A review of recent developments based on LCA. *Construction and Building Materials*, 23(1):28–39, January 2009.

[105] Laurence Stamford and Adisa Azapagic. Life cycle sustainability assessment of UK electricity scenarios to 2070. *Energy for Sustainable Development*, 23:194–211, December 2014.

[106] Laurence Stamford and Adisa Azapagic. Life cycle environmental impacts of UK shale gas. *Applied Energy*, 134:506–518, December 2014.

[107] Athanasios I. Papadopoulos, Gulnara Shavalieva, Stavros Papadokonstantakis, Panos Seferlis, Felipe A. Perdomo, Amparo Galindo, George Jackson, and Claire S. Adjiman. An approach for simultaneous computer-aided molecular design with holistic sustainability assessment: Application to phase-change CO2 capture solvents. *Computers & Chemical Engineering*, 135:106769, April 2020.

[108] Mark Goedkoop, Anne De Schryver, Michiel Oele, Sipke Durksz, and Douwe de Roest. Introduction to LCA with SimaPro 7. *PRé Consultants, The Netherlands*, 2008.

[109] Gregor Wernet, Christian Bauer, Bernhard Steubing, Jürgen Reinhard, Emilia Moreno-Ruiz, and Bo Weidema. The ecoinvent database version 3 (part I): overview and methodology. *The International Journal of Life Cycle Assessment*, 21(9):1218–1230, September 2016.

[110] Amirhossein Mehrkesh and Arunprakash T. Karunanithi. Energetic Ionic Materials: How Green Are They? A Comparative Life Cycle Assessment Study. *ACS Sustainable Chemistry & Engineering*, 1(4):448–455, April 2013.

[111] Roland Hischier, Stefanie Hellweg, Christian Capello, and Alex Primas. Establishing life cycle inventories of chemicals based on differing data availability. *The International Journal of Life Cycle Assessment*, 10(1):59–67, 2005.

[112] Mark A. J. Huijbregts, Zoran J. N. Steinmann, Pieter M. F. Elshout, Gea Stam, Francesca Verones, Marisa Vieira, Michiel Zijp, Anne Hollander, and Rosalie van Zelm. ReCiPe2016: a harmonised life cycle impact assessment method at midpoint and endpoint level. *The International Journal of Life Cycle Assessment*, 22(2):138–147, February 2017.

[113] Bo Pedersen Weidema and Marianne Suhr Wesnæs. Data quality management for life cycle inventories—an example of using data quality indicators. *Journal of Cleaner Production*, 4(3):167–174, 1996.

[114] Richard Turton, Richard Bailie, Wallace Whiting, and Joseph Shaeiwitz. *Analysis, Synthesis, and Design of Chemical Processes*. Prentice Hall, 1999.

[115] Gavin Towler and Ray Sinnott. *Chemical Engineering Design: Principles, Practice and Economics of Plant and Process Design*. Elsevier, 2012.

[116] World Energy Prices.

[117] Naonori Nishida, George Stephanopoulos, and A. W. Westerberg. A review of process synthesis. *AIChE Journal*, 27(3):321–351, 1981.

[118] Anjan Kumar Tula, Mario R. Eden, and Rafiqul Gani. Process synthesis, design and analysis using a process-group contribution method. *Computers & Chemical Engineering*, 81:245–259, October 2015.

[119] James Merrill Douglas. *Conceptual Design of Chemical Processes*. McGraw-Hill, 1988.

[120] Ian C. Kemp. *Pinch Analysis and Process Integration: A User Guide on Process Integration for the Efficient Use of Energy*. Elsevier, April 2011. ISBN 978-0-08-046826-6. Google-Books-ID: gQMxilJQmV4C.

[121] Ionic Liquids Database - ILThermo, .

[122] José O. Valderrama and Roberto E. Rojas. Critical properties of ionic liquids. Revisited. *Industrial & Engineering Chemistry Research*, 48(14):6890–6900, 2009.

[123] Ramesh L. Gardas and João A. P. Coutinho. A group contribution method for viscosity estimation of ionic liquids. *Fluid Phase Equilibria*, 266(1):195–201, April 2008.

[124] Haixiang Gao, Chengfeng Ye, Crystal M. Piekarski, and Jean'ne M. Shreeve. Computational characterization of energetic salts. *The Journal of Physical Chemistry C*, 111(28): 10718–10731, 2007.

[125] H Jenkins, David Tudela, and Leslie Glasser. Lattice potential energy estimation for complex ionic salts from density measurements. *Inorganic Chemistry*, 41(9):2364–2367, 2002.

[126] T. F. Yee, I. E. Grossmann, and Z. Kravanja. Simultaneous optimization models for heat integration—I. Area and energy targeting and modeling of multi-stream exchangers. *Computers & Chemical Engineering*, 14(10):1151–1164, October 1990.

[127] John D. Holbrey, Kenneth R. Seddon, and Roger Wareing. A simple colorimetric method for the quality control of 1-alkyl-3-methylimidazolium ionic liquid precursors. *Green Chemistry*, 3(1):33–36, 2001.

[128] Annegret Stark, Peter Behrend, Oliver Braun, Anja Müller, Johannes Ranke, Bernd Ondruschka, and Bernd Jastorff. Purity specification methods for ionic liquids. *Green Chemistry*, 10(11):1152–1161, 2008.

[129] Jason A. Widegren, Arno Laesecke, and Joseph W. Magee. The effect of dissolved water on the viscosities of hydrophobic room-temperature ionic liquids. *Chemical Communications*, 0(12):1610–1612, 2005.

[130] Kenneth R. Seddon, Annegret Stark, and María-José Torres. Influence of chloride, water, and organic solvents on the physical properties of ionic liquids. *Pure and Applied Chemistry*, 72(12), January 2000.

[131] J. A. Heldal and P. C. Mørk. Chlorine-Containing compounds as copper catalyst poisons. *Journal of the American Oil Chemists Society*, 59(9):396–398, September 1982.

[132] Bozena Mendyka, Anna Musialik-Piotrowska, and Krystyna Syczewska. Effect of chlorine compounds on the deactivation of platinum catalysts. *Catalysis Today*, 11(4):597–610, January 1992.

[133] Roberto Fernando Souza, Viviane Rech, and Jairton Dupont. Alternative Synthesis of a Dialkylimidazolium Tetrafluoroborate Ionic Liquid Mixture and its Use in Poly(acrylonitrile-butadiene) Hydrogenation. *Advanced Synthesis & Catalysis*, 344(2):153–155, 2002. _eprint: https://onlinelibrary.wiley.com/doi/pdf/10.1002/1615-4169%28200202%29344%3A2%3C153%3A%3AAID-ADSC153%3E3.0.CO%3B2-D.

[134] William M. Nelson. Are Ionic Liquids Green Solvents? In *Ionic Liquids*, volume 818 of *ACS Symposium Series*, pages 30–41. American Chemical Society, July 2002.

[135] T. Welton. Ionic liquids in Green Chemistry. *Green Chemistry*, 13(2):225–225, 2011.

[136] J. B. Guinée, HA Udo De Haes, and G. Huppes. Quantitative life cycle assessment of products: 1: Goal definition and inventory. *Journal of Cleaner Production*, 1(1):3–13, 1993.

[137] Deborah L. Sills, Vidia Paramita, Michael J. Franke, Michael C. Johnson, Tal M. Akabas, Charles H. Greene, and Jefferson W. Tester. Quantitative Uncertainty Analysis of Life Cycle Assessment for Algal Biofuel Production. *Environmental Science & Technology*, 47 (2):687–694, January 2013. Publisher: American Chemical Society.

[138] Almudena Hospido and Héctor Rodríguez. *Encyclopedia of Ionic Liquids*. Springer, 2019.

[139] Amirhossein Mehrkesh and Arunprakash T. Karunanithi. Life-Cycle Perspectives on Aquatic Ecotoxicity of Common Ionic Liquids. *Environmental Science & Technology*, 50 (13):6814–6821, July 2016.

[140] Rosa M. Cuéllar-Franca, Pelayo García-Gutiérrez, Jason P. Hallett, and Niall Mac Dowell. A life cycle approach to solvent design: challenges and opportunities for ionic liquids – application to CO 2 capture. *Reaction Chemistry & Engineering*, 6(2):258–278, 2021.

[141] Husain Baaqel, Ismael Díaz, Víctor Tulus, Benoît Chachuat, Gonzalo Guillén-Gosálbez, and Jason P. Hallett. Role of life-cycle externalities in the valuation of protic ionic liquids – a case study in biomass pretreatment solvents. *Green Chemistry*, 22(10):3132–3140, May 2020.

[142] Yoshikazu Izumi, Takashi Ohshiro, Hiroshi Ogino, Yoshimitsu Hine, and Masayuki Shimao. Selective Desulfurization of Dibenzothiophene by Rhodococcus erythropolis D-1. *Applied and Environmental Microbiology*, 60(1):223–226, January 1994.

[143] William S. Linn, Deborah A. Shamoo, Charles E. Spier, Lupe M. Valencia, Ute T. Anzar, Theodore G. Venet, and Jack D. Hackney. Respiratory effects of 0.75 ppm sulfur dioxide in exercising asthmatics: Influence of upper-respiratory defenses. *Environmental Research*, 30(2):340–348, April 1983.

[144] Matteo Monai, Tiziano Montini, Michele Melchionna, Tomáš Duchoň, Peter Kúš, Chen Chen, Nataliya Tsud, Lucia Nasi, Kevin C. Prince, Kateřina Veltruská, Vladimír Matolín, Mahmoud M. Khader, Raymond J. Gorte, and Paolo Fornasiero. The effect of sulfur dioxide on the activity of hierarchical Pd-based catalysts in methane combustion. *Applied Catalysis B: Environmental*, 202:72–83, March 2017.

[145] J. M. Campos-Martin, M. C. Capel-Sanchez, P. Perez-Presas, and J. L. G. Fierro. Oxidative processes of desulfurization of liquid fuels. *Journal of Chemical Technology & Biotechnology*, 85(7):879–890, 2010. _eprint: https://onlinelibrary.wiley.com/doi/pdf/10.1002/jctb.2371.

[146] Jaganathan Joshua Raj, Sivapragasam Magaret, Matheswaran Pranesh, Kallidanthiyil Chellappan Lethesh, Wilfred Cecilia Devi, and M. I. Abdul Mutalib. Dual functionalized imidazolium ionic liquids as a green solvent for extractive desulfurization of fuel oil: Toxicology and mechanistic studies. *Journal of Cleaner Production*, 213:989–998, March 2019.

[147] Swapnil A. Dharaskar, Kailas L. Wasewar, Mahesh N. Varma, Diwakar Z. Shende, and ChangKyoo Yoo. Synthesis, characterization and application of 1-butyl-3-

methylimidazolium tetrafluoroborate for extractive desulfurization of liquid fuel. *Arabian Journal of Chemistry*, 9(4):578–587, July 2016.

[148] Zhengjian Chen, Zuopeng Li, Xiaoyun Ma, Panfeng Long, Yun Zhou, Lin Xu, and Shiguo Zhang. A facile and efficient route to hydrophilic ionic liquids through metathesis reaction performed in saturated aqueous solution. *Green Chemistry*, 19(5):1303–1307, March 2017. Publisher: The Royal Society of Chemistry.

[149] Alexandra C. Hetherington, Aiduan Li Borrion, Owen Glyn Griffiths, and Marcelle C. McManus. Use of LCA as a development tool within early research: challenges and issues across different sectors. *The International Journal of Life Cycle Assessment*, 19(1): 130–143, January 2014.

[150] Keita Baba, Hajime Ono, Eri Itoh, Sumitaka Itoh, Kyoko Noda, Toshinori Usui, Koji Ishihara, Masahiko Inamo, Hideo D. Takagi, and Tsutomu Asano. Kinetic Study of Thermal Z to E Isomerization Reactions of Azobenzene and 4-Dimethylamino-4-nitroazobenzene in Ionic Liquids [1-R-3-Methylimidazolium Bis(trifluoromethylsulfonyl)imide with R=Butyl, Pentyl, and Hexyl]. *Chemistry – A European Journal*, 12(20):5328–5333, July 2006.

[151] Klaus Ebel, Hermann Koehler, Armin O. Gamer, and Rudolf Jäckh. Imidazole and Derivatives, 2012.

[152] Ernst Langer, Heinz Rassaerts, Peter Kleinschmidt, Theodore R. Torkelson, and Klaus K. Beutel. Chloropropanes, Chlorobutanes, and Chlorobutenes. In *Ullmann's Encyclopedia of Industrial Chemistry*. American Cancer Society, 2011.

[153] International Maritime Organization (IMO). Consistent Implementation of MARPOL ANNEX VI, 2020.

[154] Xiaoxing Lu, Lei Yue, Minjie Hu, Qi Cao, Li Xu, Yongsheng Guo, Shenlin Hu, and Wenjun Fang. Piperazinium-Based Ionic Liquids with Lactate Anion for Extractive Desulfurization of Fuels. *Energy & Fuels*, 28(3):1774–1780, March 2014.

[155] Zhen Song, Qian Zeng, Jinwei Zhang, Hongye Cheng, Lifang Chen, and Zhiwen Qi. Solubility of imidazolium-based ionic liquids in model fuel hydrocarbons: A COSMO-RS and experimental study. *Journal of Molecular Liquids*, 224:544–550, December 2016.

[156] Hong-Tao Shang, Jun-Sheng Wu, Qing Zhou, and Li-Sheng Wang. Solubilities of Benzene, Toluene, and Xylene Isomers in 1-Butyl-3-methylimidazolium Tetrafluoroborate. *Journal of Chemical & Engineering Data*, 51(4):1286–1288, July 2006.

[157] Wen-Hen Lo, Hsiao-Yen Yang, and Guor-Tzo Wei. One-pot desulfurization of light oils by chemical oxidation and solvent extraction with room temperature ionic liquids. *Green Chemistry*, 5(5):639–642, October 2003.

[158] Amir Aghaei, Shahrokh Shahhosseini, and Mohammad Amin Sobati. Regeneration of different extractive solvents for the oxidative desulfurization process: An experimental investigation. *Process Safety and Environmental Protection*, 139:191–200, July 2020.

[159] Rolf Frischknecht and Gerald Rebitzer. The ecoinvent database system: a comprehensive web-based LCA database. *Journal of Cleaner Production*, 13(13):1337–1343, November 2005.

[160] R. Kerry Turner, David Pearce, and Ian Bateman. *Environmental economics: an elementary introduction.* Harvester Wheatsheaf, 1994.

[161] Massimo Pizzol, Bo Weidema, Miguel Brandão, and Philippe Osset. Monetary valuation in life cycle assessment: a review. *Journal of Cleaner Production*, 86:170–179, 2015.

[162] Francesco Bosello, Roberto Roson, and Richard S. J. Tol. Economy-wide estimates of the implications of climate change: Human health. *Ecological Economics*, 58(3):579–591, 2006.

[163] Sandra Díaz, Joseph Fargione, F. Stuart Chapin Iii, and David Tilman. Biodiversity loss threatens human well-being. *PLOS Biology*, 4(8):e277, 2006.

[164] Sofia Ahlroth, Måns Nilsson, Göran Finnveden, Olof Hjelm, and Elisabeth Hochschorner. Weighting and valuation in selected environmental systems analysis tools – suggestions for further developments. *Journal of Cleaner Production*, 19(2):145–156, January 2011.

[165] Ibrahim M. Algunaibet, Carlos Pozo, Ángel Galán-Martín, and Gonzalo Guillén-Gosálbez. Quantifying the cost of leaving the Paris Agreement via the integration of life cycle assessment, energy systems modeling and monetization. *Applied Energy*, 242:588–601, 2019.

[166] Bernard V Berg and Ada Ferrer-i-Carbonell. Monetary valuation of informal care: the well-being valuation method. *Health Economics*, 16(11):1227–1244, 2007.

[167] W Wouter Botzen and Jeroen Van Den Bergh. Monetary valuation of insurance against flood risk under climate change. *International Economic Review*, 53(3):1005–1026, 2012.

[168] Valentin Fougerit, Patrice Auclair, and Solène Bonhoure. Monetary weighting of LCA results to integrate a two-stage management system in the decision process. In *Proceedings 2nd LCA Conference*, volume 6, page 7, 2012.

[169] Thu Lan Thi Nguyen, Bertrand Laratte, Bertrand Guillaume, and Anthony Hua. Quantifying environmental externalities with a view to internalizing them in the price of products, using different monetization models. *Resources, Conservation and Recycling*, 109:13–23, 2016.

[170] Seong-Rin Lim, Yoo Ri Kim, Seung H. Woo, Donghee Park, and Jong Moon Park. System optimization for eco-design by using monetization of environmental impacts: a strategy to convert bi-objective to single-objective problems. *Journal of Cleaner Production*, 39: 303–311, 2013.

[171] Göran Finnveden, Michael Z. Hauschild, Tomas Ekvall, Jeroen Guinée, Reinout Heijungs, Stefanie Hellweg, Annette Koehler, David Pennington, and Sangwon Suh. Recent developments in Life Cycle Assessment. *Journal of Environmental Management*, 91(1):1–21, October 2009.

[172] Sofia Ahlroth. The use of valuation and weighting sets in environmental impact assessment. *Resources, Conservation and Recycling*, 85:34–41, April 2014.

[173] Isao Hasegawa, Kazuhide Tabata, Osamu Okuma, and Kazuhiro Mae. New pretreatment methods combining a hot water treatment and water/acetone extraction for thermochemical conversion of biomass. *Energy & Fuels*, 18(3):755–760, 2004.

[174] Wouter J. J. Huijgen, Johannes H. Reith, and Herman den Uil. Pretreatment and fractionation of wheat straw by an acetone-based organosolv process. *Industrial & Engineering Chemistry Research*, 49(20):10132–10140, 2010.

[175] Jian Liu, Rie Takada, Shuichi Karita, Takahito Watanabe, Yoichi Honda, and Takashi Watanabe. Microwave-assisted pretreatment of recalcitrant softwood in aqueous glycerol. *Bioresource Technology*, 101(23):9355–9360, 2010.

[176] Hasan Sadeghifar, Tyrone Wells, Rosemary Khuu Le, Fatemeh Sadeghifar, Joshua S. Yuan, and Arthur Jonas Ragauskas. Fractionation of organosolv lignin using acetone:water and properties of the obtained fractions. *ACS Sustainable Chemistry & Engineering*, 5(1): 580–587, 2017.

[177] Fubao Sun and Hongzhang Chen. Organosolv pretreatment by crude glycerol from oleochemicals industry for enzymatic hydrolysis of wheat straw. *Bioresource Technology*, 99(13):5474–5479, 2008.

[178] Claudio Arato, E. Kendall Pye, and Gordon Gjennestad. The Lignol Approach to Biorefining of Woody Biomass to Produce Ethanol and Chemicals. In Brian H. Davison, Barbara R. Evans, Mark Finkelstein, and James D. McMillan, editors, *Twenty-Sixth Symposium on Biotechnology for Fuels and Chemicals*, ABAB Symposium, pages 871–882. Humana Press, Totowa, NJ, 2005.

[179] Agnieszka Brandt-Talbot, Florence J. V. Gschwend, Paul S. Fennell, Tijs M. Lammens, Bennett Tan, James Weale, and Jason P. Hallett. An economically viable ionic liquid for the fractionation of lignocellulosic biomass. *Green Chemistry*, 19(13):3078–3102, 2017.

[180] Joan G. Lynam and Charles J. Coronella. Glycerol as an ionic liquid co-solvent for pretreatment of rice hulls to enhance glucose and xylose yield. *Bioresource Technology*, 166:471–478, August 2014.

[181] Florence J. V. Gschwend, Francisco Malaret, Somnath Shinde, Agnieszka Brandt-Talbot, and Jason P. Hallett. Rapid pretreatment of Miscanthus using the low-cost ionic liquid triethylammonium hydrogen sulfate at elevated temperatures. *Green Chemistry*, 20(15): 3486–3498, 2018.

[182] F. Joos, R. Roth, J. S. Fuglestvedt, G. P. Peters, I. G. Enting, W. von Bloh, V. Brovkin, E. J. Burke, M. Eby, N. R. Edwards, T. Friedrich, T. L. Frölicher, P. R. Halloran, P. B. Holden, C. Jones, T. Kleinen, F. T. Mackenzie, K. Matsumoto, M. Meinshausen, G.-K. Plattner, A. Reisinger, J. Segschneider, G. Shaffer, M. Steinacher, K. Strassmann, K. Tanaka, A. Timmermann, and A. J. Weaver. Carbon dioxide and climate impulse response functions for the computation of greenhouse gas metrics: a multi-model analysis. *Atmospheric Chemistry and Physics*, 13(5):2793–2825, 2013.

[183] Kim Pingoud, Tommi Ekholm, and Ilkka Savolainen. Global warming potential factors and warming payback time as climate indicators of forest biomass use. *Mitigation and Adaptation Strategies for Global Change*, 17(4):369–386, 2012.

[184] B. Y. Wu, Y. C. Chan, A. Middendorf, X. Gu, and H. W. Zhong. Assessment of toxicity potential of metallic elements in discarded electronics: A case study of mobile phones in China. *Journal of Environmental Sciences*, 20(11):1403–1408, 2008.

[185] Thomas E. McKone and Edgar G. Hertwich. The human toxicity potential and a strategy for evaluating model performance in life cycle impact assessment. *The International Journal of Life Cycle Assessment*, 6(2):106–109, 2001.

[186] Bo Pedersen Weidema. Using the budget constraint to monetarise impact assessment results. *Ecological economics*, 68(6):1591–1598, 2009.

[187] Jane Hall, Rosalie Viney, Marion Haas, and Jordan Louviere. Using stated preference

discrete choice modeling to evaluate health care programs. *Journal of Business Research*, 57(9):1026–1032, 2004.

[188] Roger Gates, Carl McDaniel, and Karin Braunsberger. Modeling consumer health plan choice behavior to improve customer value and health plan market share. *Journal of Business Research*, 48(3):247–257, 2000.

[189] Bo P Weidema. Comparing Three Life Cycle Impact Assessment Methods from an Endpoint Perspective. *Journal of Industrial Ecology*, 19(1):20–26, 2015. _eprint: https://onlinelibrary.wiley.com/doi/pdf/10.1111/jiec.12162.

[190] César A. G. Quispe, Christian J. R. Coronado, and João A. Carvalho Jr. Glycerol: Production, consumption, prices, characterization and new trends in combustion. *Renewable and Sustainable Energy Reviews*, 27:475–493, 2013.

[191] Archie McCulloch, Pauline M Midgley, and Paul Ashford. Releases of refrigerant gases (CFC-12, HCFC-22 and HFC-134a) to the atmosphere. *Atmospheric Environment*, 37(7): 889–902, March 2003.

[192] Bernard L. Cohen. Impacts of the Nuclear Energy Industry on Human Health and Safety: Evaluation of the hazards of various stages of power production, coupled with analysis of existing data on radiation effects, permits experts to predict the magnitude of the risk involved in an all-nuclear energy economy. *American Scientist*, 64(5):550–559, 1976.

[193] Philip M. Fearnside. Amazonian deforestation and global warming: carbon stocks in vegetation replacing Brazil's Amazon forest. *Forest Ecology and Management*, 80(1):21–34, 1996.

[194] Michael H. Graham. Effects of local deforestation on the diversity and structure of southern california giant kelp forest food webs. *Ecosystems*, 7(4):341–357, 2004.

[195] Richard B Norgaard. Economic indicators of resource scarcity: A critical essay. *Journal of Environmental Economics and Management*, 19(1):19–25, 1990.

[196] Clementine L. Chambon, Vivi Fitriyanti, Pedro Verdía, Shirley Min Yang, Servann Hérou, Maria-Magdalena Titirici, Agnieszka Brandt-Talbot, Paul S. Fennell, and Jason P. Hallett. Fractionation by Sequential Antisolvent Precipitation of Grass, Softwood, and Hardwood Lignins Isolated Using Low-Cost Ionic Liquids and Water. *ACS Sustainable Chemistry & Engineering*, 8(9):3751–3761, March 2020.

[197] Everton Skoronski, Mylena Fernandes, Francisco J. Malaret, and Jason P. Hallett. Use of phosphonium ionic liquids for highly efficient extraction of phenolic compounds from water. *Separation and Purification Technology*, 248:117069, October 2020.

[198] Sheikh Moniruzzaman Moni, Roksana Mahmud, Karen High, and Michael Carbajales-Dale. Life cycle assessment of emerging technologies: A review. *Journal of Industrial Ecology*, 24(1):52–63, 2020.

[199] Raul Calvo-Serrano, María González-Miquel, Stavros Papadokonstantakis, and Gonzalo Guillén-Gosálbez. Predicting the cradle-to-gate environmental impact of chemicals from molecular descriptors and thermodynamic properties via mixed-integer programming. *Computers & Chemical Engineering*, 108:179–193, January 2018.

[200] Raul Calvo-Serrano, María González-Miquel, and Gonzalo Guillén-Gosálbez. Integrating COSMO-Based -Profiles with Molecular and Thermodynamic Attributes to Predict the Life Cycle Environmental Impact of Chemicals. *ACS Sustainable Chemistry & Engineering*, 7(3):3575–3583, February 2019.

[201] Volker H. Hoffmann, Gregory J. McRae, and Konrad Hungerbühler. Methodology for Early-Stage Technology Assessment and Decision Making under Uncertainty: Application to the Selection of Chemical Processes. *Industrial & Engineering Chemistry Research*, 43 (15):4337–4349, July 2004.

[202] Carina L. Gargalo, Peam Cheali, John A. Posada, Ana Carvalho, Krist V. Gernaey, and Gürkan Sin. Assessing the environmental sustainability of early stage design for bioprocesses under uncertainties: An analysis of glycerol bioconversion. *Journal of Cleaner Production*, 139:1245–1260, December 2016.

[203] Mijndert Van der Spek, Eva Sanchez Fernandez, Nils Henrik Eldrup, Ragnhild Skagestad, Andrea Ramirez, and André Faaij. Unravelling uncertainty and variability in early stage techno-economic assessments of carbon capture technologies. *International Journal of Greenhouse Gas Control*, 56:221–236, January 2017.

[204] Mark A. J. Huijbregts, Gregory Norris, Rolf Bretz, Andreas Ciroth, Benoit Maurice, Bo von Bahr, Bo Weidema, and Angeline S. H. de Beaufort. Framework for modelling data uncertainty in life cycle inventories. *The International Journal of Life Cycle Assessment*, 6(3):127, May 2001.

[205] Shannon M. Lloyd and Robert Ries. Characterizing, propagating, and analyzing uncertainty in life-cycle assessment: A survey of quantitative approaches. *Journal of Industrial Ecology*, 11(1):161–179, 2007.

[206] Evelyne A. Groen, Eddie A. M. Bokkers, Reinout Heijungs, and Imke J. M. de Boer. Methods for global sensitivity analysis in life cycle assessment. *The International Journal of Life Cycle Assessment*, 22(7):1125–1137, July 2017.

[207] Elorri Igos, Enrico Benetto, Rodolphe Meyer, Paul Baustert, and Benoit Othoniel. How to treat uncertainties in life cycle assessment studies? *The International Journal of Life Cycle Assessment*, 24(4):794–807, April 2019.

[208] Mark A. J. Huijbregts. Application of uncertainty and variability in LCA. *The International Journal of Life Cycle Assessment*, 3(5):273, September 1998.

[209] Stuart Ross, David Evans, and Michael Webber. How LCA studies deal with uncertainty. *The International Journal of Life Cycle Assessment*, 7(1):47, January 2002.

[210] Jani Valkama and Marika Keskinen. Comparison of simplified LCA variations for three LCA cases of electronic products from the ecodesign point of view. In *2008 IEEE International Symposium on Electronics and the Environment*, pages 1–6, May 2008. doi: 10.1109/ISEE.2008.4562923. ISSN: 2378-7260.

[211] Wei Wei, Pyrene Larrey-Lassalle, Thierry Faure, Nicolas Dumoulin, Philippe Roux, and Jean-Denis Mathias. How to conduct a proper sensitivity analysis in life cycle assessment: Taking into account correlations within LCI data and interactions within the LCA calculation model. *Environmental Science & Technology*, 49(1):377–385, 2015.

[212] Husain Baaqel, Jason P. Hallett, Gonzalo Guillén-Gosálbez, and Benoît Chachuat. Uncertainty analysis in life-cycle assessment of early-stage processes and products: a case study in dialkyl-imidazolium ionic liquids. In Metin Türkay and Rafiqul Gani, editors, *31st European Symposium on Computer Aided Process Engineering*, volume 50 of *Computer Aided Chemical Engineering*, pages 785–790. 2021.

[213] Andrea Saltelli, Ksenia Aleksankina, William Becker, Pamela Fennell, Federico Ferretti, Niels Holst, Sushan Li, and Qiongli Wu. Why so many published sensitivity analyses are false: A systematic review of sensitivity analysis practices. *Environmental Modelling & Software*, 114:29–39, April 2019.

[214] Tobias Welz, Roland Hischier, and Lorenz M. Hilty. Environmental impacts of lighting technologies — Life cycle assessment and sensitivity analysis. *Environmental Impact Assessment Review*, 31(3):334–343, April 2011.

[215] E. Martínez, E. Jiménez, J. Blanco, and F. Sanz. LCA sensitivity analysis of a multi-megawatt wind turbine. *Applied Energy*, 87(7):2293–2303, July 2010.

[216] High-value propylene glycol from low-value biodiesel glycerol: a techno-economic and environmental assessment under uncertainty. 5.

[217] Marco Ratto, Terry Andres, Francesca Campolongo, Jessica Cariboni, Debora Gatelli, Michaela Saisana, Stefano Tarantola, and Andrea Saltelli. *Global Sensitivity Analysis: The Primer*. John Wiley & Sons, New York, 2008.

[218] S. Cucurachi, E. Borgonovo, and R. Heijungs. A protocol for the global sensitivity analysis of impact assessment models in life cycle assessment. *Risk Analysis*, 36(2):357–377, 2016.

[219] Zhang-Chun Tang, Lu Zhenzhou, Liu Zhiwen, and Xiao Ningcong. Uncertainty analysis and global sensitivity analysis of techno-economic assessments for biodiesel production. *Bioresource Technology*, 175:502–508, January 2015.

[220] Marie-Lise Pannier, Patrick Schalbart, and Bruno Peuportier. Comprehensive assessment of sensitivity analysis methods for the identification of influential factors in building life cycle assessment. *Journal of Cleaner Production*, 199:466–480, October 2018.

[221] Marc Jaxa-Rozen, Astu Sam Pratiwi, and Evelina Trutnevyte. Variance-based global sensitivity analysis and beyond in life cycle assessment: an application to geothermal heating networks. *The International Journal of Life Cycle Assessment*, 26(5):1008–1026, May 2021.

[222] Carlos F. Blanco, Stefano Cucurachi, Jeroen B. Guinée, Martina G. Vijver, Willie J. G. M. Peijnenburg, Roman Trattnig, and Reinout Heijungs. Assessing the sustainability of emerging technologies: A probabilistic LCA method applied to advanced photovoltaics. *Journal of Cleaner Production*, 259:120968, June 2020.

[223] Yuwei Qin and Sangwon Suh. Method to decompose uncertainties in LCA results into contributing factors. *The International Journal of Life Cycle Assessment*, 26(5):977–988, May 2021.

[224] Stefano Cucurachi, Carlos Felipe Blanco, Bernhard Steubing, and Reinout Heijungs. Implementation of uncertainty analysis and moment-independent global sensitivity analysis for full-scale life cycle assessment models. *Journal of Industrial Ecology*, 26(2):374–391, 2022.

[225] Aleksandra Kim, Christopher L. Mutel, Andreas Froemelt, and Stefanie Hellweg. Global sensitivity analysis of background life cycle inventories. *Environmental Science & Technology*, 56(9):5874–5885, May 2022.

[226] Anders Riisagera, Rasmus Fehrmanna, Marco Haumannb, and Peter Wasserscheidb. Supported ionic liquids: versatile reaction and separation media. *Topics in Catalysis*, 40 (1):91–102, November 2006.

[227] Mark B. Shiflett and A. Yokozeki. Separation of CO2 and H2S using room-temperature ionic liquid [bmim][PF6]. *Fluid Phase Equilibria*, 294(1):105–113, July 2010.

[228] Mike J. Gilman. A brief survey of stopping rules in Monte Carlo simulations. In *Proceedings of the Second Conference on Applications of Simulations, Winter Simulation Conference, IEEE, Piscataway, NJ*, pages 16–20, 1968.

[229] X-Y Zhang, Mn Trame, Lj Lesko, and S Schmidt. Sobol Sensitivity Analysis: A Tool to Guide the Development and Evaluation of Systems Pharmacology Models. *CPT: Pharmacometrics & Systems Pharmacology*, pages 69–79, January 2015. Publisher: John Wiley & Sons, Ltd.

[230] Sergei Kucherenko. *SOBOLHDMR: A General-Purpose Modeling Software*, pages 191–224. Humana Press, Totowa, NJ, 2013.

[231] SobolGSA Software.

[232] Herschel Rabitz and Ömer F. Aliş. General foundations of high-dimensional model representations. *Journal of Mathematical Chemistry*, 25(2):197–233, June 1999.

[233] M. Munoz Zuniga, S. Kucherenko, and N. Shah. Metamodelling with independent and dependent inputs. *Computer Physics Communications*, 184(6):1570–1580, 2013.

[234] I. M Sobol. Global sensitivity indices for nonlinear mathematical models and their Monte Carlo estimates. *Mathematics and Computers in Simulation*, 55(1):271–280, February 2001.

[235] Husain Baaqel, Jason P. Hallett, Gonzalo Guillén-Gosálbez, and Benoît Chachuat. Sustainability Assessment of Alternative Synthesis Routes to Aprotic Ionic Liquids: The Case of 1-Butyl-3-methylimidazolium Tetrafluoroborate for Fuel Desulfurization. *ACS Sustainable Chemistry & Engineering*, 10(1):323–331, January 2022.

[236] I. M Sobol'. On the distribution of points in a cube and the approximate evaluation of integrals. *USSR Computational Mathematics and Mathematical Physics*, 7(4):86–112, January 1967.

[237] 1-Methylimidazole M8878, . URL `https://www.sigmaaldrich.com/catalog/product/sigma/m8878`.

[238] S. P. Verevkin, D. H. Zaitsau, V. N. Emel'yanenko, Y. U. Paulechka, A. V. Blokhin, A. B. Bazyleva, and G. J. Kabo. Thermodynamics of ionic liquids precursors: 1-Methylimidazole. *Journal of Physical Chemistry B*, 115(15):4404–4411, 2011.

[239] K. S. Gavritchev, G. A. Sharpataya, A. A. Smagin, E. N. Malyi, and V. A. Matyukha. Calorimetric study of thermal decomposition of lithium hexafluorophosphate. *Journal of Thermal Analysis and Calorimetry*, 73(1):71–83, July 2003.

[240] Genyuan Li, Carey Rosenthal, and Herschel Rabitz. High Dimensional Model Representations. *The Journal of Physical Chemistry A*, 105(33):7765–7777, August 2001. Publisher: American Chemical Society.

Appendix A

Holistic Assessment of the Combined Production and Use of the Ionic Liquid 1-Butyl-3-Methylimidazolium Tetrafluoroborate: Application to Fuel Desulfurization

A.1 Modelling and simulation

Table A.1: 1-methylimidazole properties

Property	**Value**	**Units**
MW	82.10	g mol^{-1}
BP	198 [237]	°C
Density	1030 [237]	kg m^{-3}
ΔH_f	125700 [238]	kJ $kmol^{-1}$
T_c	490.90	°C
P_c	6086	kPa
V_c	0.26	m^3 $kmol^{-1}$
Acentricity	0.35	–

Table A.2: [BMIM][BF_4] properties

Property	**Value**	**Units**
MW	226	g mol^{-1}
BP	222.05 [122]	°C
Density	1208 [122]	kg m^{-3}
ΔH_f	-650300	kJ $kmol^{-1}$
T_c	370.10 [122]	°C
P_c	2038 [122]	kPa
V_c	0.66 [122]	m^3 $kmol^{-1}$
Acentricity	0.89 [122]	–

Table A.3: [BBIM][BF_4] properties

Property	**Value**	**Units**
MW	268	g mol^{-1}
BP	290.75 [122]	°C
Density	971 [122]	kg m^{-3}
ΔH_f	-817866	kJ $kmol^{-1}$
T_c	440.25 [122]	°C
P_c	1427 [122]	kPa
V_c	0.83 [122]	m^3 $kmol^{-1}$
Acentricity	0.88 [122]	–

Table A.4: [MMIM][BF_4] properties

Property	**Value**	**Units**
MW	184	g mol^{-1}
BP	153.45 [122]	°C
Density	1582 [122]	kg m^{-3}
ΔH_f	-585306	kJ $kmol^{-1}$
T_c	299.45 [122]	°C
P_c	3145 [122]	kPa
V_c	0.48 [122]	m^3 $kmol^{-1}$
Acentricity	0.88 [122]	–

Table A.5: [BMIM]Cl properties

Property	**Value**	**Units**
MW	175	g mol^{-1}
BP	285 [122]	°C
Density	1080 [122]	kg/m^3
ΔH_f	-237000	kJ $kmol^{-1}$
T_c	516 [122]	°C
P_c	2790 [122]	kPa
V_c	0.57 [122]	m^3 $kmol^{-1}$
Acentricity	0.49 [122]	–

Table A.6: Fluoroboric acid properties

Property	**Value**	**Units**
MW	87.80	g mol^{-1}
BP	130	°C
Density	1370	kg/m^3
ΔH_f	-1530000	kJ $kmol^{-1}$
T_c	386	°C
P_c	5710	kPa
V_c	0.24	m^3 $kmol^{-1}$
Acentricity	0.17	–

Table A.7: Boric acid properties

Property	**Value**	**Units**
MW	61.80	g mol^{-1}
BP	300	°C
Density	1440	kg/m^3
ΔH_f	-1090000	kJ $kmol^{-1}$
T_c	588	°C
P_c	2970	kPa
V_c	0.44	m^3 $kmol^{-1}$
Acentricity	0.25	–

Table A.8: Sodium bicarbonate properties

Property	**Value**	**Units**
MW	84	g mol^{-1}
BP	873	°C
Density	2200	kg/m^3
ΔH_f	-951000	kJ $kmol^{-1}$
T_c	1100	°C
P_c	1640	kPa
V_c	1.82	m^3 $kmol^{-1}$
Acentricity	1.81	–

Table A.9: Sodium tetrafluoroborate properties

Property	Value	Units
MW	110	g mol^{-1}
BP	500	°C
Density	2470	kg/m^3
ΔH_f	-1850000	kJ $kmol^{-1}$
T_c	782	°C
P_c	2260	kPa
V_c	0.82	m^3 $kmol^{-1}$
Acentricity	0.59	–

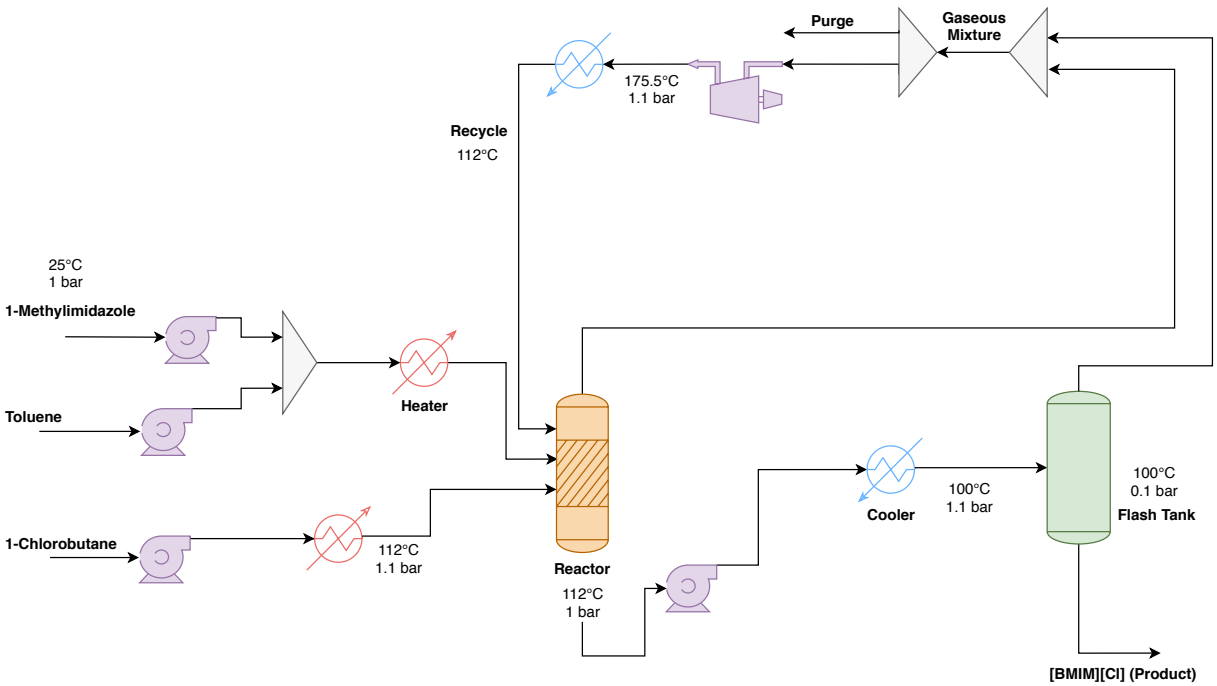

Figure A.1: [BMIM]Cl process flow diagram

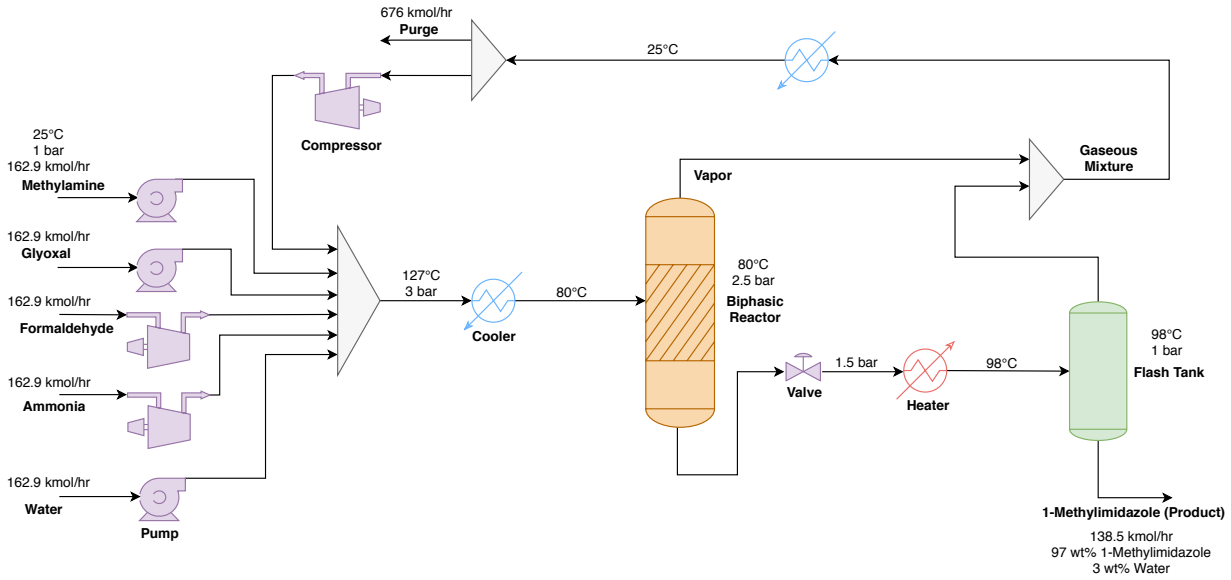

Figure A.2: 1-Methylimidazole process flow diagram

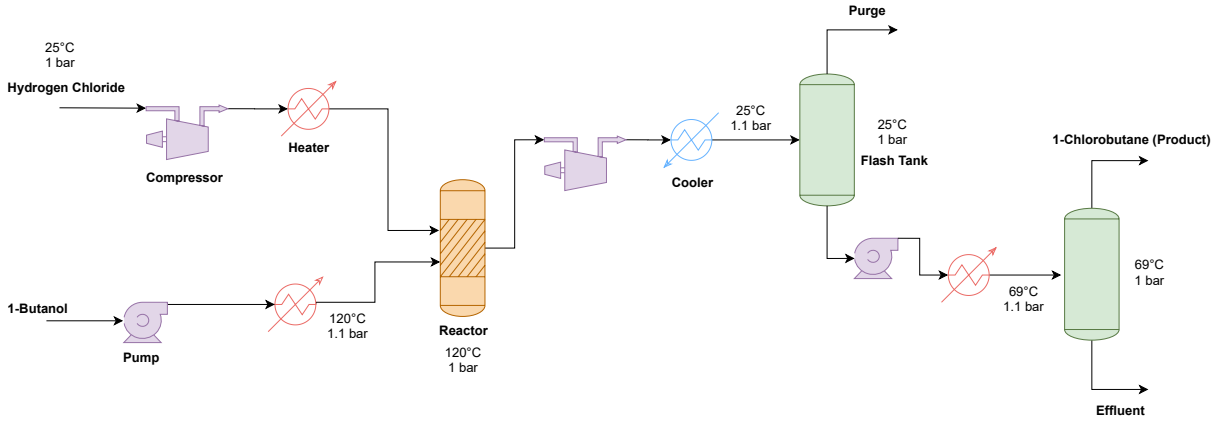

Figure A.3: 1-Chlorobutane process flow diagram

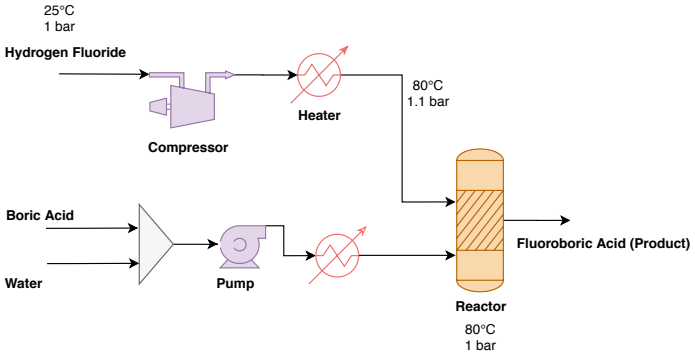

Figure A.4: Fluoroboric acid process flow diagram

A.2 Economic assessment

Table A.10: Commodity prices used in economic assessment

Commodity	**Price ($)**
Methylamine (kg)	1.16
Glyoxal (kg)	1.78
Formaldehyde (kg)	0.38
Ammonia (kg)	0.56
Sodium tetrafluoroborate (kg)	6.03
Diethylether (kg)	1.79
Sodium bicarbonate (kg)	0.38
Dichloromethane (kg)	1.57
Hydrogen chloride (kg)	0.20
1-Butanol (kg)	0.87
Hydrogen fluoride (kg)	3.2
Boric acid (kg)	1.89
Butylamine (kg)	1.71
Toluene (kg)	0.81
Ionized water (m^3)	0.87
Cooling water (kg)	0.50
Steam (1000 kg)	25.0
Electricity (kWh)	0.16

Table A.11: Detailed CAPEX costs for 1-methylimidazole

Unit	**Specifications**		**Eq. Cost ($ kg^{-1})**
Flash Tank	Diameter / Length (m)	6.35 / 22.22	1.48×10^{-4}
Reactor	Volume (m^3)	13.59	2.17×10^{-4}
Heater	Area (m^2)	2160.68	7.15×10^{-4}
Cooler 1	Area (m^2)	159.45	7.15×10^{-4}
Cooler 2	Area (m^2)	2265.48	7.15×10^{-4}
Cooling Tower	Vol Flow (L s^{-1})	4624.28	1.67×10^{-3}
Pump 1	Vol Flow (L s^{-1})	5.49	7.25×10^{-6}
Pump 2	Vol Flow (L s^{-1})	13.81	8.74×10^{-6}
Pump 3	Vol Flow (L s^{-1})	1.96	6.73×10^{-6}
Compressor 1	Power (kWh)	497.51	1.69×10^{-4}
Compressor 2	Power (kWh)	520.19	1.74×10^{-4}
Compressor 3	Power (kWh)	519.87	1.74×10^{-4}
Compressor 4	Power (kWh)	7621.36	8.28×10^{-4}
CAPEX Component			**Total Cost ($ kg^{-1})**
ISBL			4.1×10^{-3}
OSBL			1.6×10^{-3}
C_{Eng}			5.8×10^{-4}
C_{Con}			8.6×10^{-4}

Table A.12: Detailed OPEX costs for 1-methylimidazole

Feedstock/Utility	**Cost ($ kg^{-1})**
Methylamine	0.39
Glyoxal	1.34
Formaldehyde	0.15
Ammonia	0.12
Water	2×10^{-4}
Steam	0.03
Cooling Water	0.73
Electricity	0.05
OPEX Component	**Total Cost ($ kg^{-1})**
C_{CVP}	2.8235
C_{FCP}	0.0130

Table A.13: Detailed CAPEX costs for [BMIM][BF_4] from metathesis process

Unit	**Specifications**		**Eq. Cost ($ kg^{-1})**
Flash Tank	Diameter / Length (m)	8.60 / 34.50	4.25×10^{-4}
Reactor	Volume (m^3)	4.52	1.15×10^{-4}
Decanter	Volume (m^3)	4.52	1.15×10^{-4}
Washer	Volume (m^3)	10.20	2.56×10^{-4}
Heater	Area (m^2)	1150	4.46×10^{-4}
Cooler	Area (m^2)	1150	4.46×10^{-4}
Cooling Tower	Vol Flow (L s^{-1})	0.55	7.58×10^{-5}
Pump 1	Vol Flow (L s^{-1})	13.90	7.58×10^{-5}
Pump 2	Vol Flow (L s^{-1})	9.46	8.75×10^{-6}
Pump 3	Vol Flow (L s^{-1})	11.40	1.44×10^{-5}
Pump 4	Vol Flow (L s^{-1})	31.30	9.04×10^{-5}
Pump 5	Vol Flow (L s^{-1})	12.30	8.46×10^{-6}
Pump 6	Vol Flow (L s^{-1})	12.40	8.46×10^{-6}
Pump 7	Vol Flow (L s^{-1})	6.90	7.50×10^{-6}
CAPEX Component			**Total Cost ($ kg^{-1})**
ISBL			1.45×10^{-3}
OSBL			5.80×10^{-4}
C_{Eng}			2.03×10^{-4}
C_{Con}			3.05×10^{-4}

Table A.14: Detailed OPEX costs for [BMIM][BF_4] from metathesis process

Feedstock/Utility	**Cost ($ kg^{-1})**
1-Butyl-3-methylimidazolium chloride	3.36
Sodium Tetrafluoroborate	8.32
Water	3.41×10^{-5}
Steam	3.48×10^{-2}
Cooling Water	0.06
Electricity	0.03
OPEX Component	**Total Cost ($ kg^{-1})**
C_{VCP}	11.80
C_{FCP}	0.01

Table A.15: Detailed CAPEX costs for [BMIM][BF_4] from halide-free process

Unit	**Specifications**		**Eq. Cost ($ kg^{-1})**
Flash Tank	Diameter / Length (m)	4.60 / 34.50	1.53×10^{-4}
Reactor	Volume (m^3)	29.10	3.50×10^{-4}
Decanter	Volume (m^3)	32.60	3.92×10^{-4}
Extraction Column	Volume (m^3)	30.50	3.67×10^{-4}
Heater	Area (m^2)	464	1.86×10^{-4}
Cooler 1	Area (m^2)	397	1.86×10^{-4}
Cooler 2	Area (m^2)	246	1.86×10^{-4}
Cooling Tower	Vol Flow (L s^{-1})	0.36	7.58×10^{-5}
Pump 1	Vol Flow (L s^{-1})	1.99	6.75×10^{-6}
Pump 2	Vol Flow (L s^{-1})	3.83	7.00×10^{-6}
Pump 3	Vol Flow (L s^{-1})	3.01	6.87×10^{-6}
Pump 4	Vol Flow (L s^{-1})	2.51	6.79×10^{-6}
Pump 5	Vol Flow (L s^{-1})	1.42	6.67×10^{-6}
Pump 6	Vol Flow (L s^{-1})	1.41	6.67×10^{-6}
Pump 7	Vol Flow (L s^{-1})	83.40	2.57×10^{-5}
Pump 8	Vol Flow (L s^{-1})	97.60	2.97×10^{-5}
Pump 9	Vol Flow (L s^{-1})	17.70	9.50×10^{-6}
Pump 10	Vol Flow (L s^{-1})	17.90	9.54×10^{-6}
Pump 11	Vol Flow (L s^{-1})	7.49	7.58×10^{-4}
Compressor 1	Power (kWh)	102	7.17×10^{-6}
Compressor 2	Power (kWh)	105	7.29×10^{-6}
Compressor 3	Power (kWh)	929	2.42×10^{-4}

CAPEX Component	**Total Cost ($ kg^{-1})**
ISBL	1.51×10^{-3}
OSBL	6.03×10^{-4}
C_{Eng}	2.11×10^{-4}
C_{Con}	3.17×10^{-4}

Table A.16: Detailed OPEX costs for [BMIM][BF_4] from halide-free process

Feedstock/Utility	**Cost ($ kg^{-1})**
Methylamine	0.17
Glyoxal	0.48
Formaldehyde	0.06
Butylamine	0.59
Fluoroboric acid	1.79
Toluene	0.12
Water	1.06×10^{-4}
Diethylether	0.22
Sodium bicarbonate	5.23×10^{-3}
Dichloromethane	0.35
Steam	1.52×10^{-2}
Cooling water	9.98×10^{-3}
Electricity	2.56
OPEX Component	**Total Cost ($ kg^{-1})**
C_{VCP}	6.37
C_{FCP}	0.01

Table A.17: Detailed CAPEX costs for [BMIM]Cl

Unit	**Specifications**		**Eq. Cost ($ kg^{-1})**
Flash Tank	Diameter / Length (m)	3.68 / 12.89	1.39×10^{-4}
Reactor	Volume (m^3)	6.36	1.58×10^{-4}
Heater 1	Area (m^2)	84.70	1.58×10^{-4}
Heater 2	Area (m^2)	88.90	1.58×10^{-4}
Cooler 1	Area (m^2)	186	1.58×10^{-4}
Cooler 2	Area (m^2)	232	1.58×10^{-4}
Cooling Tower	Vol Flow (L s^{-1})	171	7.67×10^{-6}
Pump 1	Vol Flow (L s^{-1})	7.97	9.20×10^{-6}
Pump 2	Vol Flow (L s^{-1})	16.20	1.46×10^{-5}
Pump 3	Vol Flow (L s^{-1})	11.70	7.75×10^{-6}
Pump 4	Vol Flow (L s^{-1})	8.36	2.42×10^{-4}
Compressor	Power (kWh)	929	1.39×10^{-4}
CAPEX Component			**Total Cost ($ kg^{-1})**
ISBL			5.05×10^{-4}
OSBL			2.02×10^{-4}
C_{Eng}			7.08×10^{-4}
C_{Con}			1.06×10^{-4}

Table A.18: Detailed OPEX costs for [BMIM]Cl

Feedstock/Utility	**Cost ($ kg^{-1})**
1-Methylimidazole	1.34
1-Chlorobutane	1.35
Toluene	0.17
Steam	2.18×10^{-3}
Cooling Water	2.96×10^{-2}
Electricity	4.06×10^{-5}
OPEX Component	**Total Cost ($ kg^{-1})**
C_{VCP}	2.89
C_{FCP}	9.73×10^{-3}

Table A.19: Detailed CAPEX costs for 1-chlorobutane

Unit	**Specifications**		**Eq. Cost ($ kg^{-1})**
Flash Tank 1	Diameter / Length (m)	12.50 / 68.70	8.50×10^{-5}
Flash Tank 2	Diameter / Length (m)	12.50 / 43.70	6.79×10^{-5}
Reactor	Volume (m^3)	1.81	7.38×10^{-5}
Heater 1	Area (m^2)	69.66	2.84×10^{-4}
Heater 2	Area (m^2)	410	2.84×10^{-4}
Heater 3	Area (m^2)	47.78	2.84×10^{-4}
Cooler	Area (m^2)	1020	2.84×10^{-4}
Cooling Tower	Vol Flow (L s^{-1})	51.49	1.03×10^{-4}
Pump 1	Vol Flow (L s^{-1})	15.54	9.08×10^{-6}
Pump 2	Vol Flow (L s^{-1})	18.94	9.75×10^{-6}
Compressor 1	Power (kWh)	582	1.85×10^{-4}
Compressor 2	Power (kWh)	160	1.67×10^{-3}
CAPEX Component			**Total Cost ($ kg^{-1})**
ISBL			1.91×10^{-3}
OSBL			7.65×10^{-4}
C_{Eng}			2.68×10^{-4}
C_{Con}			4.02×10^{-4}

Table A.20: Detailed OPEX costs for 1-chlorobutane

Feedstock/Utility	**Cost ($ kg^{-1})**
Hydrogen chloride	0.19
1-Butanol	1.33
Cooling Water	0.02
Electricity	0.03
OPEX Component	**Total Cost ($ kg^{-1})**
C_{VCP}	1.57
C_{FCP}	0.01

Table A.21: Detailed CAPEX costs for fluoroboric acid

Unit	**Specifications**		**Eq. Cost ($ kg^{-1})**
Reactor	Volume (m^3)	4.70	1.18×10^{-4}
Heater 1	Area (m^2)	30.28	1.36×10^{-4}
Heater 2	Area (m^2)	12.98	1.36×10^{-4}
Pump	Vol Flow (L s^{-1})	15.11	8.99×10^{-6}
Compressor	Power (kWh)	962	2.46×10^{-4}
CAPEX Component			**Total Cost ($ kg^{-1})**
ISBL			3.68×10^{-4}
OSBL			1.47×10^{-4}
C_{Eng}			5.16×10^{-5}
C_{Con}			7.74×10^{-5}

Table A.22: Detailed OPEX costs for fluoroboric acid

Feedstock/Utility	**Cost ($ kg^{-1})**
Hydrogen fluoride	2.92
Boric acid	1.33
Water	1.37×10^{-4}
Steam	1.01×10^{-3}
Cooling water	5.67×10^{-2}
Electricity	2.39×10^{-2}
OPEX Component	**Total Cost ($ kg^{-1})**
C_{VCP}	4.33
C_{FCP}	9.85×10^{-3}

A.3 Environmental assessment

Table A.23: 1-methylimidazole inventory

Group	**Inventory**	**Flow** (per-kg product)	**STDEV**
Inputs from nature	Water, cooling, unspecified natural origin, RER	0.54639 m^3	1.0502
	Water, river, RER	0.27319 m^3	1.0502
	Water, well, in ground, RER	0.27319 m^3	1.0502
Inputs from technosphere (materials)	Methylamine {RER} | production | Cut-off	0.40601 kg	1.3269
	Chemical factory, organics {GLO} | market for | Cut-off	4.00×10^{-10} p	2.9905
	Heat, district or industrial, natural gas {RER} | market group for | Cut-off	6.03910 MJ	1.0502
	Electricity, medium voltage {RER} | market group for | Cut-off	0.29371 kWh	1.0502
	Heat, from steam, in chemical industry {RER} | market for heat, from steam, in chemical industry | Cut-off	0.67102 MJ	1.0502
	Glyoxal {RER} | production | Cut-off	0.7587 kg	1.3269
	Tap water {RER} | market group for | Cut-off	0.23551 kg	1.3269
	Formaldehyde {RER} | oxidation of methanol | Cut-off	0.39252 kg	1.3269
	Ammonia, liquid {RER} | ammonia production, steam reforming, liquid | Cut-off	0.22263 kg	1.3269
Emissions to air	Carbon dioxide, fossil	1.0246 kg	1.0502
	Methylamine	0.0008104 kg	1.0502
	Water/m^3	$2.232\,51 \times 10^{-5}$ m^3	1.0502
	Glyoxal	1.5144×10^{-3} kg	1.0502
	Ammonia	4.4437×10^{-4} kg	1.0502
	Formaldehyde	7.8347×10^{-4} kg	1.0502
Emissions to water	BOD5, Biological Oxygen Demand	8.2825×10^{-2} kg	1.4918
	COD, Chemical Oxygen Demand	8.2825×10^{-2} kg	1.4918
	DOC, Dissolved Organic Carbon	3.1021×10^{-2} kg	1.4918
	TOC, Total Organic Carbon	3.1021×10^{-2} kg	1.4918
	Water, RER	0.54662 m^3	1.0502
	Methylamine	9.7271×10^{-3} kg	1.0502
	Glyoxal	0.01118 kg	1.0502
	Formaldehyde	0.01373 kg	1.0502
	Ammonia	0.08065 kg	1.0502
	Imidazole	0.02934 kg	1.0502
Outputs to technosphere	Wastewater, average {Europe without Switzerland} | market for wastewater, average | Cut-off, U	0.00335 m^3	1.0502

Table A.24: Metathesis [BMIM][BF_4] inventory

Group	**Inventory**	**Flow** (per-kg product)	**STDEV**
Inputs from nature	Water, cooling, unspecified natural origin, RER	0.12 m^3	1.0502
	Water, river, RER	0.06 m^3	1.0502
	Water, well, in ground, RER	0.06 m^3	1.0502
Inputs from technosphere (materials)	1-Butyl-3-methylimidazolium chloride	1.16 kg	———
	Chemical factory, organics {GLO} | market for | Cut-off	4.00×10^{-10} p	2.9905
	Heat, district or industrial, natural gas {RER} | market group for | Cut-off	5.31 MJ	1.0502
	Electricity, medium voltage {RER} | market group for | Cut-off	2.11×10^{-4} kWh	1.0502
	Heat, from steam, in chemical industry {RER} | market for heat, from steam, in chemical industry | Cut-off	0.59 MJ	1.0502
	Sodium tetrafluoroborate {GLO} | market for | Cut-off	1.38 kg	1.3269
	Tap water {RER} | market group for | Cut-off	0.12 kg	1.3269
Emissions to air	Carbon dioxide, fossil	0.70 kg	1.0502
	Sodium tetrafluoroborate	5.02×10^{-3} kg	1.0502
	Water/m^3	4.78×10^{-3} m^3	1.0502
Emissions to water	BOD5, Biological Oxygen Demand	0.06 kg	1.4918
	COD, Chemical Oxygen Demand	0.06 kg	1.4918
	DOC, Dissolved Organic Carbon	0.02 kg	1.4918
	TOC, Total Organic Carbon	0.02 kg	1.4918
	Water, RER	0.12 m^3	1.0502
	Sodium chloride	0.27 kg	1.0502
	Imidazole	3.99×10^{-2} kg	1.0502
Outputs to technosphere	Wastewater, average {Europe without Switzerland} | market for wastewater, average | Cut-off, U	1.66×10^{-3} m^3	1.0502

Table A.25: Halide-free [BMIM][BF_4] inventory

Group	**Inventory**	**Flow** (per-kg product)	**STDEV**
Inputs from nature	Water, cooling, unspecified natural origin, RER	0.02 m^3	1.0502
	Water, river, RER	0.01 m^3	1.0502
	Water, well, in ground, RER	0.01 m^3	1.0502
Inputs from technosphere (materials)	Methylamine {RER} | production | Cut-off	0.15 kg	1.3269
	Chemical factory, organics {GLO} | market for | Cut-off	4.00×10^{-10} p	2.9905
	Heat, district or industrial, natural gas {RER} | market group for | Cut-off	2.32 MJ	1.0502
	Electricity, medium voltage {RER} | market group for | Cut-off	0.04 kWh	1.0502
	Heat, from steam, in chemical industry {RER} | market for heat, from steam, in chemical industry | Cut-off	0.26 MJ	1.0502
	Fluoroboric acid	0.41 kg	———
	Tap water {RER} | market group for | Cut-off	0.36 kg	1.3269
	Glyoxal {RER} | production | Cut-off, U	0.27 kg	1.3269
	Formaldehyde {GLO} | market for | Cut-off, U	0.14 kg	1.3269
	Butylamine {RER} | production | Cut-off, U	0.34 kg	1.3269
	Toluene, liquid {RER} | production | Cut-off, U	0.15 kg	1.3269
	Diethyl ether, without water, in 99.95% solution state {RER} | ethylene hydration | Cut-off, U	0.12 kg	1.3269
	Dichloromethane {RER} | production | Cut-off, U	0.23 kg	1.3269
Emissions to air	Carbon dioxide, fossil	0.81 kg	1.0502
	Methylamine	2.92×10^{-4} kg	1.0502
	Water/m^3	1.52×10^{-6} m^3	1.0502
	N-butylamine	6.88×10^{-4} kg	1.0502
	Glyoxal	5.46×10^{-4} kg	1.0502
	Formaldehyde	2.83×10^{-4} kg	1.0502
	Toluene	2.94×10^{-4} kg	1.0502
	Diethyl ether	2.42×10^{-4} kg	1.0502
	Methane, dichloro-, HCC-30	4.52×10^{-4} kg	1.0502
Emissions to water	BOD5, Biological Oxygen Demand	6.52×10^{-2} kg	1.4918
	COD, Chemical Oxygen Demand	6.52×10^{-2} kg	1.4918
	DOC, Dissolved Organic Carbon	2.44×10^{-2} kg	1.4918
	TOC, Total Organic Carbon	2.44×10^{-2} kg	1.4918
	Water, RER	0.02 m^3	1.0502
	Methylamine	7.15×10^{-4} kg	1.0502
	Glyoxal	1.34×10^{-3} kg	1.0502
	Formaldehyde	6.90×10^{-4} kg	1.0502
	N-butylamine	1.68×10^{-3} kg	1.0502
	Toluene	1.42×10^{-2} kg	1.0502
	Methane, dichloro-, HCC-30	0.02 kg	1.0502
	Diethyl ether	9.45×10^{-3} kg	1.0502
Outputs to technosphere	Wastewater, average {Europe without Switzerland} | market for wastewater, average | Cut-off, U	1.11×10^{-3} m^3	1.0502

Table A.26: [BMIM]Cl inventory

Group	**Inventory**	**Flow** (per-kg product)	**STDEV**
Inputs from nature	Water, cooling, unspecified natural origin, RER	5.92×10^{-3} m^3	1.0502
	Water, river, RER	2.96×10^{-3} m^3	0.03502
	Water, well, in ground, RER	2.96×10^{-3} m^3	0.03502
Inputs from technosphere (materials)	1-Methylimidazole	0.47 kg	1.3269
	Chemical factory, organics {GLO} | market for | Cut-off	4.00×10^{-10} p	2.9905
	Heat, district or industrial, natural gas {RER} | market group for | Cut-off	0.33 MJ	1.0502
	Electricity, medium voltage {RER} | market group for | Cut-off	1.79×10^{-4} kWh	1.0502
	Heat, from steam, in chemical industry {RER} | market for heat, from steam, in chemical industry | Cut-off	3.70×10^{-2} MJ	1.0502
	1-Chlorobutane	0.85 kg	1.3269
	Toluene, liquid {GLO} | market for | Cut-off, U	0.20 kg	1.3269
Emissions to air	Carbon dioxide, fossil	0.19 kg	1.0502
	Imidazole	0.03 kg	1.0502
	Chloride	7.70×10^{-3} kg	1.0502
	1,4-Dichloromethane	0.41 kg	1.0502
	Water/m^3	2.37×10^{-6} m^3	1.0502
	Toluene	0.39 kg	1.0502
Emissions to water	Water, RER	5.92×10^{-2} m^3	1.0502
	BOD5, Biological Oxygen Demand	1.57×10^{-2} kg	1.4918
	COD, Chemical Oxygen Demand	1.57×10^{-2} kg	1.4918
	DOC, Dissolved Organic Carbon	5.87×10^{-3} kg	1.4918
	TOC, Total Organic Carbon	5.87×10^{-3} kg	1.4918
	1,4-Dichloromethane	4.05×10^{-3} kg	1.0502
	Toluene	3.91×10^{-3} kg	1.0502
	Chloride	7.69×10^{-5} kg	1.0502
	Imidazole	3.02×10^{-4} kg	1.0502
Outputs to technosphere	Wastewater, average {Europe without Switzerland} | market for wastewater, average | Cut-off, U	8.34×10^{-5} m^3	1.0502

Table A.27: 1-Chlorobutane inventory

Group	**Inventory**	**Flow** (per-kg product)	**STDEV**
Inputs from nature	Water, cooling, unspecified natural origin, RER	4.68×10^{-2} m^3	1.0502
	Water, river, RER	2.34×10^{-2} m^3	0.03502
	Water, well, in ground, RER	2.34×10^{-2} m^3	0.03502
Inputs from technosphere (materials)	Hydrochloric acid, without water, in 30% solution state {RER} | hydrochloric acid production, from the reaction of hydrogen with chlorine | Cut-off, U	0.94 kg	1.3269
	Chemical factory, organics {GLO} | market for | Cut-off	4.00×10^{-10} p	2.9905
	Heat, district or industrial, natural gas {RER} | market group for | Cut-off	0.31 MJ	1.0502
	Electricity, medium voltage {RER} | market group for | Cut-off	2.48×10^{-2} kWh	1.0502
	Heat, from steam, in chemical industry {RER} | market for heat, from steam, in chemical industry | Cut-off	3.50×10^{-2} MJ	1.0502
	1-butanol {GLO} | market for | Cut-off, U	1.52 kg	1.3269
Emissions to air	Carbon dioxide, fossil	1.21 kg	1.0502
	Hydrogen chloride	0.31 kg	1.0502
	1-Butanol	5.23×10^{-3} kg	1.0502
	1,4-Dichlorbutane	0.11 kg	1.0502
	Water	7.51×10^{-5} m^3	1.0502
Emissions to water	Water, RER	0.05 m^3	1.0502
	BOD5, Biological Oxygen Demand	9.77×10^{-2} kg	1.4918
	COD, Chemical Oxygen Demand	9.77×10^{-2} kg	1.4918
	DOC, Dissolved Organic Carbon	3.66×10^{-2} kg	1.4918
	TOC, Total Organic Carbon	3.66×10^{-2} kg	1.4918
	1,4-Dichlorobutane	4.07×10^{-2} kg	1.0502
	1-Butanol	2.37×10^{-2} kg	1.0502
Outputs to technosphere	Wastewater, average {Europe without Switzerland} | market for wastewater, average | Cut-off, U	8.40×10^{-4} m^3	1.0502

Table A.28: Fluoroboric acid inventory

Group	**Inventory**	**Flow** (per-kg product)	**STDEV**
Inputs from nature	Water, cooling, unspecified natural origin, RER	0.11 m^3	1.0502
	Water, river, RER	5.67×10^{-2} m^3	0.03502
	Water, well, in ground, RER	5.67×10^{-2} m^3	0.03502
Inputs from technosphere (materials)	Hydrogen fluoride {GLO} | market for | Cut-off, U	0.91 kg	1.3269
	Chemical factory, organics {GLO} | market for | Cut-off	4.00×10^{-10} p	2.9905
	Heat, district or industrial, natural gas {RER} | market group for | Cut-off	0.15 MJ	1.0502
	Electricity, medium voltage {RER} | market group for | Cut-off	3.20×10^{-2} kWh	1.0502
	Heat, from steam, in chemical industry {RER} | market for heat, from steam, in chemical industry | Cut-off	1.72×10^{-2} MJ	1.0502
	Boric acid, anhydrous, powder {GLO} | market for | Cut-off, U	0.71 kg	1.3269
	Tap water {RER} | market group for | Cut-off	0.47 kg	1.3269
Emissions to air	Hydrogen fluoride	1.82×10^{-3} kg	1.0502
	Boric acid	1.41×10^{-3} kg	1.0502
	Water	5.47×10^{-5} m^3	1.0502
Emissions to water	Water, RER	0.11 m^3	1.0502

Table A.29: LCA ReCiPe midpoint results, for 1 kg of solvent

Impact indicator	**Unit**	**Metathesis [BMIM][BF_4]**	**Halide-free [BMIM][BF_4]**	**Acetonitrile**	**DMF**
Global warming	kg CO_2 eq	27.26	6.30	4.21	2.98
Stratospheric ozone depletion	kg CFC11 eq	1.04×10^{-5}	1.58×10^{-5}	6.08×10^{-7}	1.33×10^{-6}
Ionizing radiation	kBq Co-60 eq	2.18	2.91×10^{-1}	5.66×10^{-2}	1.87×10^{-1}
Ozone formation, Human health	kg NO_x eq	0.13	1.43×10^{-2}	5.87×10^{-3}	5.73×10^{-3}
Fine particulate matter formation	kg PM2.5 eq	0.05	1.02×10^{-2}	4.91×10^{-3}	4.76×10^{-3}
Ozone formation, Terrestrial ecosystems	kg NO_x eq	0.17	1.51×10^{-2}	6.24×10^{-3}	5.97×10^{-3}
Terrestrial acidification	kg SO_2 eq	0.11	2.74×10^{-2}	1.88×10^{-2}	1.12×10^{-2}
Freshwater eutrophication	kg P eq	1.05×10^{-2}	1.72×10^{-3}	4.22×10^{-4}	9.45×10^{-4}
Marine eutrophication	kg N eq	1.17×10^{-2}	2.77×10^{-4}	4.24×10^{-3}	3.06×10^{-3}
Terrestrial ecotoxicity	kg 1,4-DCB eq	73.49	17.60	8.82	10.20
Freshwater ecotoxicity	kg 1,4-DCB eq	0.79	0.16	4.40×10^{-2}	8.03×10^{-3}
Marine ecotoxicity	kg 1,4-DCB eq	1.12	0.23	6.64×10^{-2}	0.11
Human carcinogenic toxicity	kg 1,4-DCB eq	0.95	0.21	6.63×10^{-2}	8.88×10^{-2}
Human non-carcinogenic toxicity	kg 1,4-DCB eq	24.30	5.49	1.45	2.39
Land use	m^2a crop eq	4.39×10^{-1}	8.91×10^{-2}	2.61×10^{-2}	4.42×10^{-2}
Mineral resource scarcity	kg Cu eq	7.35×10^{-2}	1.81×10^{-2}	5.69×10^{-3}	8.35×10^{-3}
Fossil resource scarcity	kg oil eq	9.40	2.65	2.36	1.66
Water consumption	m^3	1.02	1.83×10^{-1}	6.35×10^{-2}	3.91×10^{-2}

Table A.30: LCA ReCiPe endpoint results, for 1 kg of solvent

Impact indicator	**Unit**	**Halide-free [BMIM][BF_4]**	**Metathesis [BMIM][BF_4]**	**Acetonitrile**	**DMF**
Human health	DALY	1.46×10^{-5}	6.81×10^{-5}	7.69×10^{-6}	6.69×10^{-6}
Ecosystem quality	species×yr	3.02×10^{-8}	1.49×10^{-7}	1.81×10^{-8}	1.32×10^{-8}
Resources	$US\$_{2020}$	0.96	2.91	0.95	0.58

Appendix B

Monetization for Multi-Criteria Decision-Making in Sustainability Assessment of Protic Ionic Liquids: Application to Biomass Pretreatment

B.1 Modelling and simulation

Table B.1: [HMIM][HSO_4] properties

Property	**Value**	**Units**
MW	180.20	g mol^{-1}
BP	401.800 [122]	°C
Density	1484 [122]	kg m^{-3}
ΔH_f	-938000	kJ $kmol^{-1}$
T_c	739.6 [122]	°C
P_c	9189 [122]	kPa
V_c	0.43 [122]	m^3 $kmol^{-1}$
Acentricity	0.67 [122]	–

Table B.2: [TEA][HSO_4] properties

Property	**Value**	**Units**
MW	199.30	g mol^{-1}
BP	377.10 [122]	°C
Density	1143 [122]	kg/m^3
ΔH_f	-884100	kJ $kmol^{-1}$
T_c	644.30 [122]	°C
P_c	4732 [122]	kPa
V_c	0.62 [122]	m^3 $kmol^{-1}$
Acentricity	0.74 [122]	–

B.2 Economic assessment

Table B.3: Commodity prices used in economic assessment

Commodity	**Price ($)**
Sulphuric acid (kg)	0.05
Triethylamine (kg)	1.36
1-Methylimidazole (kg)	2.84
Ionized water (m^3)	0.87
Cooling water (kg)	0.50
Steam (1000 kg)	25.0
Electricity (kWh)	0.16

Table B.4: Detailed CAPEX costs for [HMIM][HSO_4]

Unit	**Specifications**		**Eq. Cost ($ kg^{-1})**
Flash Tank	Diameter / Length (m)	3.55 / 12.80	1.48×10^{-4}
Reactor	Volume (m^3)	4.19	1.11×10^{-4}
Heater	Area (m^2)	227.21	8.74×10^{-4}
Cooler 1	Area (m^2)	299.69	8.74×10^{-4}
Cooler 2	Area (m^2)	136.58	8.74×10^{-4}
Cooler 3	Area (m^2)	4969.67	8.74×10^{-4}
Cooling Tower	Vol Flow (L s^{-1})	1211.98	5.54×10^{-4}
Pump 1	Vol Flow (L s^{-1})	2.45	6.80×10^{-6}
Pump 2	Vol Flow (L s^{-1})	12.16	8.42×10^{-6}
Pump 3	Vol Flow (L s^{-1})	2.30	6.78×10^{-6}
Pump 4	Vol Flow (L s^{-1})	10.07	8.04×10^{-6}
Pump 5	Vol Flow (L s^{-1})	2.08	6.75×10^{-6}
Pump 6	Vol Flow (L s^{-1})	3.69	6.98×10^{-6}
CAPEX Component			**Total Cost ($ kg^{-1})**
ISBL			1.68×10^{-3}
OSBL			6.72×10^{-4}
C_{Eng}			2.35×10^{-4}
C_{Con}			3.53×10^{-4}

Table B.5: Detailed OPEX costs for [HMIM][HSO_4]

Feedstock/Utility	**Cost ($ kg^{-1})**
Sulphuric Acid	0.03
1-Methylimidazole	1.30
Water	2×10^{-4}
Steam	4×10^{-3}
Cooling Water	0.12
Electricity	1.37×10^{-5}
OPEX Component	**Total Cost ($ kg^{-1})**
C_{CVP}	1.45
C_{FCP}	0.0108

Table B.6: Detailed CAPEX costs for [TEA][HSO_4]

Unit	**Specifications**		**Eq. Cost ($ kg^{-1})**
Flash Tank	Diameter / Length (m)	3.21 / 11.30	9.08×10^{-5}
Reactor	Volume (m^3)	3.79	1.05×10^{-4}
Heater	Area (m^2)	191.93	3.36×10^{-4}
Cooler 1	Area (m^2)	244.19	3.36×10^{-4}
Cooler 2	Area (m^2)	133.09	3.36×10^{-4}
Cooler 3	Area (m^2)	1527.61	3.36×10^{-4}
Cooling Tower	Vol Flow (L s^{-1})	575.07	3.20×10^{-4}
Pump 1	Vol Flow (L s^{-1})	2.22	6.77×10^{-6}
Pump 2	Vol Flow (L s^{-1})	5.77	7.30×10^{-6}
Pump 3	Vol Flow (L s^{-1})	11.76	8.35×10^{-6}
Pump 4	Vol Flow (L s^{-1})	2.26	6.77×10^{-6}
Pump 5	Vol Flow (L s^{-1})	10.07	8.04×10^{-6}
Pump 6	Vol Flow (L s^{-1})	1.68	6.70×10^{-6}
CAPEX Component			**Total Cost ($ kg^{-1})**
ISBL			8.96×10^{-4}
OSBL			3.58×10^{-4}
C_{Eng}			1.25×10^{-4}
C_{Con}			1.88×10^{-4}

Table B.7: Detailed OPEX costs for [TEA][HSO_4]

Feedstock/Utility	**Cost ($ kg^{-1})**
Sulphuric Acid	0.02
Triethylamine	0.69
Water	2×10^{-4}
Steam	3×10^{-3}
Cooling Water	5.27×10^{-2}
Electricity	1.23×10^{-5}
OPEX Component	**Total Cost ($ kg^{-1})**
C_{CVP}	0.7716
C_{FCP}	0.0101

B.3 Environmental assessment

For both human health and ecosystem quality expressed in biophysical units, monetization factors using the values in Table S18 were applied. Overall, the monetization proceeds as follows:

$$\text{Monetized Cost} = \sum_{i \in \text{Impacts}} \text{MF}_i \, \text{EP}_i \tag{B.1}$$

where MF_i denotes the monetization factor for endpoint impact i, and EP_i the corresponding damage. Next, a currency exchange factor and inflation factor are applied to express a monetary value in USD_{2019}. For resources already expressed in monetary value, only an inflation factor is used for the conversion into USD_{2019}.

Table B.8: [HMIM][HSO_4] inventory

Group	**Inventory**	**Flow** (per-kg product)	**STDEV**
Inputs from nature	Water, cooling, unspecified natural origin, RER	0.14759 m^3	1.0502
	Water, river, RER	0.0738 m^3	1.0502
	Water, well, in ground, RER	0.0738 m^3	1.0502
Inputs from technosphere (materials)	1-Methylimidazole	0.45657 kg	1.3269
	Chemical factory, organics {GLO} | market for | Cut-off	4.00×10^{-10} p	2.9905
	Heat, district or industrial, natural gas {RER} | market group for | Cut-off	0.84646 MJ	1.0502
	Electricity, medium voltage {RER} | market group for | Cut-off	0.00013 kWh	1.0502
	Heat, from steam, in chemical industry {RER} | market for heat, from steam, in chemical industry | Cut-off	0.09405 MJ	1.0502
	Tap water {RER} | market group for | Cut-off	0.27581 kg	1.3269
	Sulphuric acid {RER} | production | Cut-off, U	0.54543 kg	1.3269
Emissions to air	Imidazole	0.00091 kg	1.0502
	Water/m^3	$6.454\,11 \times 10^{-6}$ m^3	1.0502
	Sulphuric acid	0.00109 kg	1.0502
Emissions to water	Water, RER	0.14789 m^3	1.0502
Outputs to technosphere	Wastewater, average {Europe without Switzerland} | market for wastewater, average | Cut-off, U	2.50×10^{-5} m^3	1.0502

Table B.9: [TEA][HSO_4] inventory

Group	**Inventory**	**Flow** (per-kg product)	**STDEV**
Inputs from nature	Water, cooling, unspecified natural origin, RER	0.07003 m^3	1.0502
	Water, river, RER	0.0738 m^3	0.03502
	Water, well, in ground, RER	0.0738 m^3	0.03502
Inputs from technosphere (materials)	Triethylamine RER | production | Cut-off, U	0.50885 kg	1.3269
	Chemical factory, organics {GLO} | market for | Cut-off	4.00×10^{-10} p	2.9905
	Heat, district or industrial, natural gas {RER} | market group for | Cut-off	0.12841 MJ	1.0502
	Electricity, medium voltage {RER} | market group for | Cut-off	0.00012 kWh	1.0502
	Heat, from steam, in chemical industry {RER} | market for heat, from steam, in chemical industry | Cut-off	0.01427 MJ	1.0502
	Tap water {RER} | market group for | Cut-off	0.27104 kg	1.3269
	Sulphuric acid {RER} | production | Cut-off, U	0.49319 kg	1.3269
Emissions to air	Triethylamine	1.02×10^{-3} kg	1.0502
	Water/m^3	3.3422×10^{-6} m^3	1.0502
	Sulphuric acid	0.00098 kg	1.0502
Emissions to water	Water, RER	0.07032 m^3	1.0502
Outputs to technosphere	Wastewater, average {Europe without Switzerland} | market for wastewater, average | Cut-off, U	2.02×10^{-5} m^3	1.0502

Table B.10: LCA ReCiPe midpoint results, for 1 kg of solvent

Impact indicator	**Unit**	**[TEA][HSO_4]**	**[HMIM][HSO_4]**	**Acetone**	**Glycerol**
Global warming	kg CO_2 eq	1.69209	2.72340	2.44755	3.49701
Stratospheric ozone depletion	kg CFC11 eq	3.20×10^{-7}	7.32×10^{-7}	1.20×10^{-7}	1.94×10^{-5}
Ionizing radiation	kBq Co-60 eq	0.07024	0.20873	0.02407	0.11677
Ozone formation, Human health	kg NO_x eq	0.00366	0.00397	0.00560	0.00599
Fine particulate matter formation	kg PM2.5 eq	0.00281	0.00369	0.00293	0.00513
Ozone formation, Terrestrial ecosystems	kg NO_x eq	0.00414	0.00422	0.00615	0.00628
Terrestrial acidification	kg SO_2 eq	0.00897	0.01131	0.00840	0.01505
Freshwater eutrophication	kg P eq	0.00071	0.00078	0.00030	0.00075
Marine eutrophication	kg N eq	0.00052	0.00916	1.30E-05	0.00479
Terrestrial ecotoxicity	kg 1,4-DCB eq	7.85354	9.89144	1.71027	5.52801
Freshwater ecotoxicity	kg 1,4-DCB eq	0.05117	0.08063	0.01474	0.05628
Marine ecotoxicity	kg 1,4-DCB eq	0.07388	0.10394	0.02073	0.06780
Human carcinogenic toxicity	kg 1,4-DCB eq	0.05406	0.10076	0.04632	0.06241
Human non-carcinogenic toxicity	kg 1,4-DCB eq	1.71520	2.29409	0.42870	2.89151
Land use	m^2a crop eq	0.02964	0.03823	0.00876	4.96817
Mineral resource scarcity	kg Cu eq	0.00674	0.00847	0.00125	0.00640
Fossil resource scarcity	kg oil eq	0.99145	1.18605	1.40073	0.51561
Water consumption	m^3	0.10347	0.44592	0.03007	0.05052

Table B.11: LCA ReCiPe endpoint results, for 1 kg of solvent

Impact indicator	**Unit**	**[TEA][HSO_4]**	**[HMIM][HSO_4]**	**Acetone**	**Glycerol**
Human health	DALY	4.138×10^{-6}	6.700×10^{-6}	4.432×10^{-6}	7.467×10^{-6}
Ecosystem quality	species×yr	9.444×10^{-9}	1.765×10^{-8}	1.015×10^{-8}	5.920×10^{-8}
Resources	USD_{2013}	0.387	0.421	0.535	0.165

Table B.12: Monetization, currency exchange and inflation factors

Damage area	**Unit**	**Monetization** (EUR_{2003}/DALY)	**Currency factor** (USD_{2003}/EUR_{2003})	**Inflation factor** (USD_{2019}/USD_{2003})
Human health	DALY	74,000	1.16	1.46
Ecosystem quality	species×yr	9,500,000	1.16	1.46
Resourcs	USD_{2013}	–	–	1.08

B.4 Additional results

This section presents the direct cost and environmental impacts of the solvents using biomass loading as the functional unit. The data used to convert functional unit from kg of solvent to kg of biomass are reported in Table B.13.

Table B.13: Biomass pretreatment data used for converting the functional unit

Solvent	**Reference**	**Biomass**	**Ratio** (kg solvent/ kg biomass)	**Fraction** (wt%)	**Recycle** (%)	**Makeup** (kg solvent/ ton biomass)
[TEA][HSO_4]	ionoSolv[179, 181]	Miscanthus	5	80%	99.2%	32
[HMIM][HSO_4]	ionoSolv[179, 181]	Miscanthus	5	80%	99.2%	32
Acetone	Organosolv[178]	Wood	10	70%	98%	140
Glycerol	Lynam and Coronella [180]	Rice hull	10	100%	75%	2,500

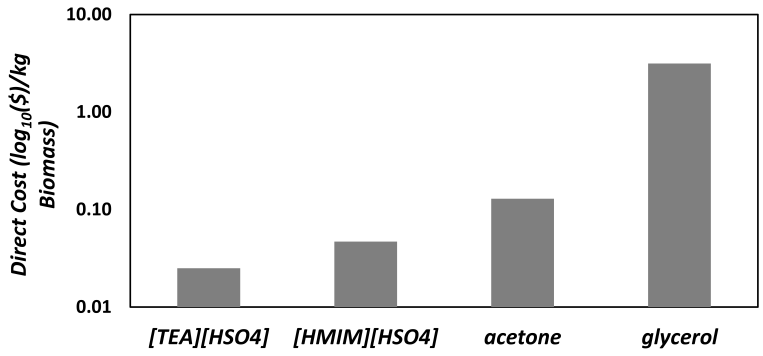

Figure B.1: Direct costs of solvents per kg of treated biomass

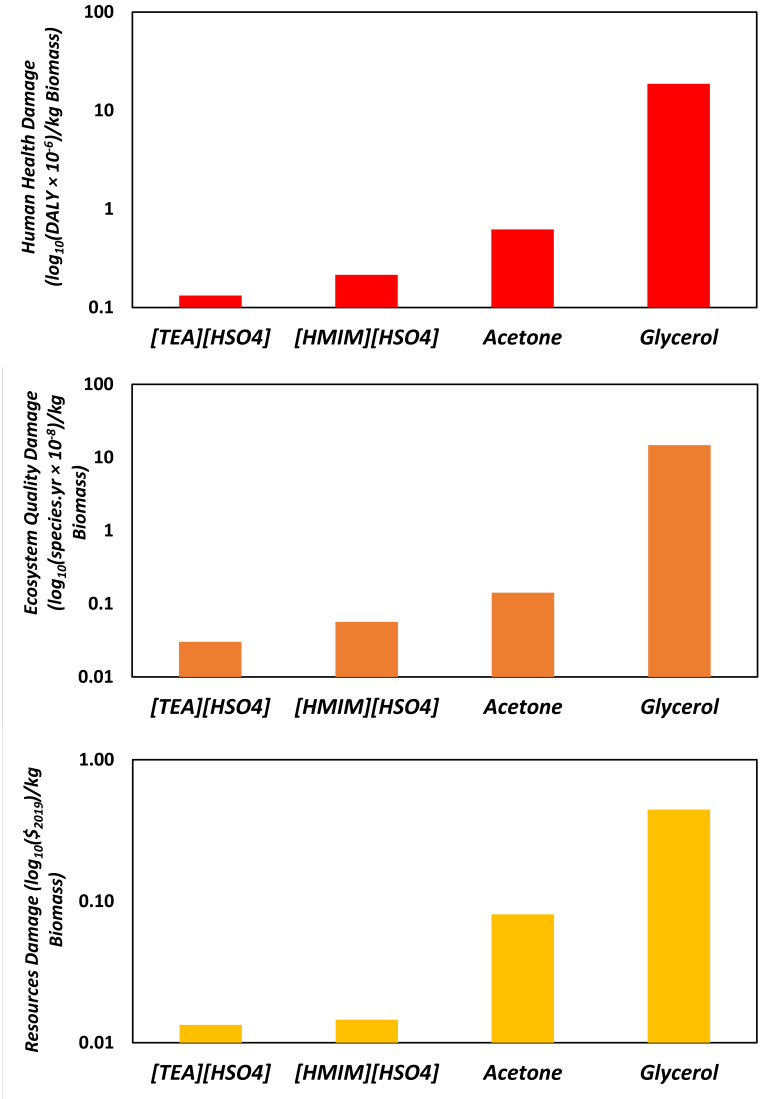

Figure B.2: Endpoint environmental impacts of solvents per kg of treated biomass

Appendix C

Global Sensitivity Analysis in Life-Cycle Assessment of Early-Stage Technology using Detailed Process Simulation: Application to Dialkylimidazolium Ionic Liquid Production

C.1 Modelling and simulation

Table C.1: [BMIM][PF_6] properties

Property	**Value**	**Units**
MW	284	g mol^{-1}
BP	281 [122]	°C
Density	1346 [122]	kg m^{-3}
ΔH_f	-1760000	kJ $kmol^{-1}$
T_c	446 [122]	°C
P_c	1728 [122]	kPa
V_c	0.76 [122]	m^3 $kmol^{-1}$
Acentricity	0.79 [122]	–

Table C.2: Lithium hexafluorophosphate properties

Property	**Value**	**Units**
MW	152	g mol^{-1}
BP	500	°C
Density	1500	kg/m^3
ΔH_f	-2300000 [239]	kJ $kmol^{-1}$
T_c	782	°C
P_c	2258	kPa
V_c	0.80	m^3 $kmol^{-1}$
Acentricity	0.59	–

Table C.3: Lithium chloride properties

Property	**Value**	**Units**
MW	42.4	g mol^{-1}
BP	1382	°C
Density	2070	kg/m^3
ΔH_f	-408300	kJ kmol^{-1}
T_c	1442	°C
P_c	1015	kPa
V_c	3.04	m^3 kmol^{-1}
Acentricity	2.52	–

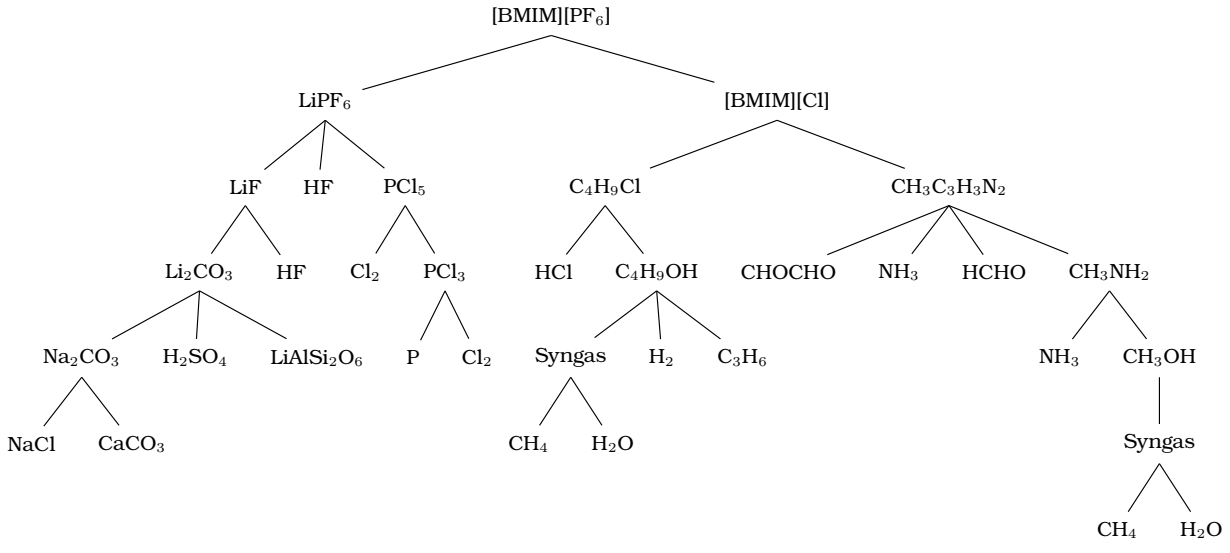

Figure C.1: Synthesis tree of [BMIM][PF_6]

C.2 Environmental assessment

Table C.4: [BMIM][PF_6] inventory

Group	**Inventory**	**Flow** (per-kg product)	**STDEV**
Inputs from nature	Water, cooling, unspecified natural origin, RER	0.07 m^3	1.0502
	Water, river, RER	0.03 m^3	1.0502
	Water, well, in ground, RER	0.03 m^3	1.0502
Inputs from technosphere (materials)	1-Butyl-3-methylimidazolium chloride	0.89 kg	———
	Chemical factory, organics {GLO} | market for | Cut-off	4.00×10^{-10} p	2.9905
	Heat, district or industrial, natural gas {RER} | market group for | Cut-off	2.17 MJ	1.0502
	Electricity, medium voltage {RER} | market group for | Cut-off	1.32×10^{-4} kWh	1.0502
	Heat, from steam, in chemical industry {RER} | market for heat, from steam, in chemical industry | Cut-off	0.24 MJ	1.0502
	Lithium hexafluorophosphate {GLO} | market for | Cut-off	1.06 kg	1.3269
	Tap water {RER} | market group for | Cut-off	0.09 kg	1.3269
Emissions to air	Carbon dioxide, fossil	0.49 kg	1.0502
	Lithium hexafluorophosphate	2.11×10^{-3} kg	1.0502
	Water/m^3	2.86×10^{-3} m^3	1.0502
Emissions to water	BOD5, Biological Oxygen Demand	0.04 kg	1.4918
	COD, Chemical Oxygen Demand	0.04 kg	1.4918
	DOC, Dissolved Organic Carbon	0.01 kg	1.4918
	TOC, Total Organic Carbon	0.01 kg	1.4918
	Water, RER	0.12 m^3	1.0502
	Lithium	0.03 m^3	1.0502
	Chloride	0.13 kg	1.0502
	Imidazole	3.00×10^{-2} kg	1.0502
Outputs to technosphere	Wastewater, average {Europe without Switzerland} | market for wastewater, average | Cut-off, U	1.01×10^{-3} m^3	1.0502

Table C.5: LCA ReCiPe midpoint results, for 1 kg of IL

Impact indicator	**Unit**	**[BMIM][BF_4]**	**[BMIM][PF_6]**
Global warming	kg CO_2 eq	27.3	32.5
Stratospheric ozone depletion	kg CFC11 eq	1.04×10^{-5}	1.17×10^{-5}
Ionizing radiation	kBq Co-60 eq	2.18	2.29
Ozone formation, Human health	kg NO_x eq	0.13	0.12
Fine particulate matter formation	kg PM2.5 eq	0.05	0.07
Ozone formation, Terrestrial ecosystems	kg NO_x eq	0.17	0.16
Terrestrial acidification	kg SO_2 eq	0.11	0.16
Freshwater eutrophication	kg P eq	1.05×10^{-2}	1.30×10^{-2}
Marine eutrophication	kg N eq	1.17×10^{-2}	1.14×10^{-2}
Terrestrial ecotoxicity	kg 1,4-DCB eq	74	131
Freshwater ecotoxicity	kg 1,4-DCB eq	0.79	1.16
Marine ecotoxicity	kg 1,4-DCB eq	1.12	1.66
Human carcinogenic toxicity	kg 1,4-DCB eq	0.95	1.21
Human non-carcinogenic toxicity	kg 1,4-DCB eq	24.3	38.7
Land use	m^2a crop eq	0.44	0.82
Mineral resource scarcity	kg Cu eq	0.07	0.64
Fossil resource scarcity	kg oil eq	9.40	9.76
Water consumption	m^3	1.02	0.98

Table C.6: LCA ReCiPe endpoint results, for 1 kg of IL

Impact indicator	**Unit**	**[BMIM][BF_4]**	**[BMIM][PF_6]**
Human health	DALY	6.81×10^{-5}	8.64×10^{-5}
Ecosystem quality	species×yr	1.49×10^{-7}	1.78×10^{-7}
Resources	$US\$_{2020}$	2.91	3.24

C.3 Uncertainty quantification and sensitivity analysis methodology and data

This section presents in detail the full methodology of the GSA using the RS-HDMR model and reports the uncertain parameters and their corresponding errors for simulating the production of ionic liquids and their precursors. Additionally, it presents a comparison of GSA and OTSA in terms of relative contributions calculated as well as a comparison of the probability [BMIM][BF_4] has higher impacts than [BMIM][PF_6] under all uncertainty scenarios.

All the background uncertainties were obtained from ecoinvent through an XML file. The file was converted, processed, and imported to Matlab. All sampling and uncertainty analysis was conducted in Matlab. GSA was conducted in SobolGSA. Simulating the background samples was conducted in MATLAB while the foreground samples were simulated using Matlab interfaced with Aspen HYSYS.

The following details the GSA methodology and equations used in SobolGSA to allocate the output variances to the different uncertain parameters. Assuming that the relationship between the output of concern, i.e., the environmental impact in a given category EI_z, and the uncertain parameters of concern affecting it can be expressed as shown in Equation S4:

$$EI_z(\boldsymbol{\gamma}) = EI_{z_0} + \sum_{i=1}^{n} EI_{z_i}(\boldsymbol{\gamma_i}) + \sum_{1\le i<j\le n} EI_{z_{ij}}(\boldsymbol{\gamma_i}, \boldsymbol{\gamma_j}) + ... + EI_{z_{1,2,...,n}}(\boldsymbol{\gamma_1}, \boldsymbol{\gamma_2}, ..., \boldsymbol{\gamma_n}) \qquad (C.1)$$

Where $\boldsymbol{\gamma}$ is a vector variable that includes the set of n uncertain parameters ($\boldsymbol{\omega}$,$\boldsymbol{\omega}$), EI_{z_0} is the zero-order term (mean effect), $EI_{z_i}(\boldsymbol{\gamma_i})$ is the first-order term that represents the effect of parameter $\boldsymbol{\gamma_i}$ and $EI_{z_{ij}}(\boldsymbol{\gamma_i}, \boldsymbol{\gamma_j})$ is the second-order term that models the cooperative effect between the parameters $\boldsymbol{\gamma}_i$ and $\boldsymbol{\gamma_j}$, and so on so forth until the term $EI_{z_{12\ldots n}}(\boldsymbol{\gamma_1}, \boldsymbol{\gamma_2}, \ldots, \boldsymbol{\gamma_v})$, which represents nth order term. Moreover, n is the number of uncertain variables. In this work, the truncated form, including terms up to the second-order, is used as it has been shown that higher-order terms can be neglected [240].

Furthermore, the following approximations are used to derive the RS-HDMR model:

$$EI_{z_0} \approx \frac{1}{N_z} \sum_{n_z}^{|N_z|} \mathrm{EI}_z(\boldsymbol{\gamma_1^{(n_z)}}, \boldsymbol{\gamma_2^{(n_z)}}, ..., \boldsymbol{\gamma_n^{(n_z)}}) \tag{C.2}$$

$$\mathrm{EI}_{z_i}(\boldsymbol{\gamma_i}) \approx \sum_{r=1}^{k} \alpha_r^i \varphi_r(\boldsymbol{\gamma_i}) \tag{C.3}$$

$$\mathrm{EI}_{z_{ij}}(\boldsymbol{\gamma_i}, \boldsymbol{\gamma_j}) \approx \sum_{p=1}^{l} \sum_{q=1}^{l'} \beta_{pq}^{ij} \varphi_p(\boldsymbol{\gamma_i}) \varphi_q(\boldsymbol{\gamma_j}) \tag{C.4}$$

Equation S5 is the approximation used for the zero-order term, defined as the average of $\mathrm{EI}_z(\boldsymbol{\gamma})$ for all $\boldsymbol{\gamma^{(n_z)}} = (\boldsymbol{\gamma_1^{(n_z)}}, \boldsymbol{\gamma_2^{(n_z)}}, \ldots, \boldsymbol{\gamma_n^{(n_z)}}), n_z = 1, 2, ..., N_z$, where N_z is the number of samples for a specific category z. The right-hand sides of Equations S6 and S7 are orthonormal polynomials used to approximate the first and second-order terms. Herein, k, l and l' are the order of the orthonormal polynomials, while α_r^i and β_{pq}^{ij} are the constant coefficients determined from fitting the data to the model. Finally, $\varphi_r(\boldsymbol{\gamma_i})$, $\varphi_p(\boldsymbol{\gamma_i})$, $\varphi_q(\boldsymbol{\gamma_j})$ are orthonormal basis functions.

Once the constant coefficients are obtained from the expansions above, the Sobol method is used to calculate the partial variances and effect indices. First, the partial variances of the first-order effects and second-order interactions are calculated as shown in Equations S8 and S9, respectively.

$$D_{z_i} \approx \sum_{r=1}^{k} (\alpha_r^i)^2 \quad \forall z \in Z \tag{C.5}$$

$$D_{z_{ij}} \approx \sum_{p=1}^{l} \sum_{q=1}^{l'} (\beta_{pq}^{ij})^2 \quad \forall z \in Z \tag{C.6}$$

Where D_{z_i} and $D_{z_{ij}}$ are the partial variances of the first-order effects and second-order interactions, respectively, for a given environmental indicator. We use next these partial variances and divide them by the total variance D_z to obtain the Sobol indices, as shown in Equations S10 and S11.

$$SO_{z_i} = \frac{D_{z_i}}{D_z} \quad \forall z \in Z \tag{C.7}$$

$$SO_{z_{ij}} = \frac{D_{z_{ij}}}{D_z} \quad \forall z \in Z \tag{C.8}$$

SO_{z_i} and $SO_{z_{ij}}$ are the Sobol indices of the first-order effects and second-order interactions for a specific environmental indicator. They measure the individual and cooperative contributions, respectively, to the output variance.

Finally, the sum of the first-order and second-order indices are used to calculate the total Sobol index as shown in Equation S12.

$$SO_{z_{T_i}} = SO_{z_i} + SO_{z_{ij}} + ... + SO_{z_{in}} \quad \forall z \in Z \tag{C.9}$$

Where $SO_{z_{T_i}}$ is the total Sobol index of an uncertain parameter for a specific environmental indicator.

The interpretation of these metrics is as follows. $SO_{z_{T_i}}$ is an indicator of how much contribution the variation of uncertain parameter $\boldsymbol{\gamma_i}$ has on the overall variance of the environmental impact of a specific category $\mathrm{EI}_z(\boldsymbol{\gamma_i})$ and it includes contributions from first-order effects and second-order interactions.

Table C.7: Uncertain model parameters, uncertainty sources and ranges in flowsheet simulation of [BMIM][PF_6] production.

Source	Parameter	Range	Units
Process	ΔP_R [1]	10±50%	kPa
	ΔP_W [1]	10±50%	kPa
	T_{VF} [2]	95±20%	°C
	P_{VF} [1]	10±50%	kPa
	PUR [1]	0.1±50%	–
Molecular	$\rho_{[BMIM][PF_6]}$ [3]	1346±19%	kg m^{-3}
	$\rho_{[BMIM]Cl}$ [3]	1080±19%	kg m^{-3}
	$\Delta H_{f[BMIM][PF_6]}$ [4]	$-1.76\pm0.16e6$	kJ kmol^{-1}
	$\Delta H_{f[BMIM]Cl}$ [3]	$-2.37\pm1.59e5$	kJ kmol^{-1}

[1] Estimate based on heuristics.
[2] Mean value based on an optimized base case.
[3] Estimate based on the group contribution methods developed by Valderrama and Rojas [122] with maximum standard deviation of 19 %.
[4] Estimate based on the lattice energy and computational chemistry methods proposed by Gao et al. [124] with maximum deviation of -159 kJ mol^{-1}.

Table C.8: Uncertain model parameters, uncertainty sources and ranges in flowsheet simulation of [BMIM]Cl production.

Source	Parameter	Range	Units
Process	ΔP_R [1]	10±50%	kPa
	T_{VF} [2]	100±20%	°C
	P_{VF} [1]	10±50%	kPa
Molecular	$\rho_{[BMIM]Cl}$ [3]	1080±19%	kg m^{-3}
	$\Delta H_{f[BMIM]Cl}$ [4]	$-2.37\pm1.59e5$	kJ kmol^{-1}

[1] Estimate based on heuristics.
[2] Mean value based on an optimized base case.
[3] Estimate based on the group contribution methods developed by Valderrama and Rojas [122] with maximum standard deviation of 19 %.
[4] Estimate based on the lattice energy and computational chemistry methods proposed by Gao et al. [124] with maximum deviation of -159 kJ mol^{-1}.

Table C.9: Uncertain model parameters, uncertainty sources and ranges in flowsheet simulation of 1-chlorobutane production.

Source	Parameter	Range	Units
Process	ΔP_{R}[1]	10±50%	kPa
	ΔP_{F1}[1]	10±50%	kPa
	ΔP_{F2}[1]	10±50%	kPa
	F_{HCl}[2]	37.5±10%	$\mathrm{kmol\,h^{-1}}$
	$F_{\text{1-butanol}}$[2]	30±50%	$\mathrm{kmol\,h^{-1}}$
	X_{R}[3]	0.8±10%	–

[1] Estimate based on heuristics.
[2] Mean value based on an optimized base case.
[3] Estimate based on yield values reported in the literature.

Table C.10: First-order and total Sobol indices for each end-point impact in the production of [BMIM][BF_4].

Parameter	Human Health		Ecosystem Quality		Resources	
	OTSA	GSA	OTSA	GSA	OTSA	GSA
ΔP_R	0.03	0.06	0.03	0.06	0.03	0.06
ΔP_W	0.03	0.05	0.03	0.06	0.03	0.05
T_{VF}	0.19	0.82	0.18	0.71	0.18	0.75
P_{VF}	0.08	0.61	0.11	0.59	0.10	0.61
$PUR\%$	0.10	0.20	0.11	0.20	0.11	0.20
$\rho_{[BMIM][BF_4]}$	0.00	0.00	0.00	0.00	0.00	0.00
$\rho_{[BMIM]Cl}$	0.00	0.00	0.00	0.00	0.00	0.00
$\Delta H_{f_{[BMIM][BF_4]}}$	0.04	0.08	0.05	0.08	0.04	0.08
$\Delta H_{f_{[BMIM]Cl}}$	0.05	0.09	0.05	0.08	0.05	0.08

Table C.11: First and total-order Sobol indices for each end-point impact in the production of [BMIM][PF_6].

Parameter	Human Health		Ecosystem Quality		Resources	
	OTSA	GSA	OTSA	GSA	OTSA	GSA
ΔP_R	0.03	0.05	0.03	0.05	0.03	0.05
ΔP_W	0.03	0.05	0.03	0.05	0.03	0.05
T_{VF}	0.20	0.75	0.19	0.69	0.19	0.70
P_{VF}	0.09	0.57	0.11	0.55	0.11	0.56
$PUR\%$	0.11	0.19	0.12	0.20	0.12	0.20
$\rho_{[BMIM][PF_6]}$	0.00	0.00	0.00	0.00	0.00	0.00
$\rho_{[BMIM]Cl}$	0.00	0.00	0.00	0.00	0.00	0.00
$\Delta H_{f_{[BMIM][PF_6]}}$	0.05	0.09	0.05	0.09	0.05	0.09
$\Delta H_{f_{[BMIM]Cl}}$	0.05	0.09	0.05	0.08	0.05	0.09

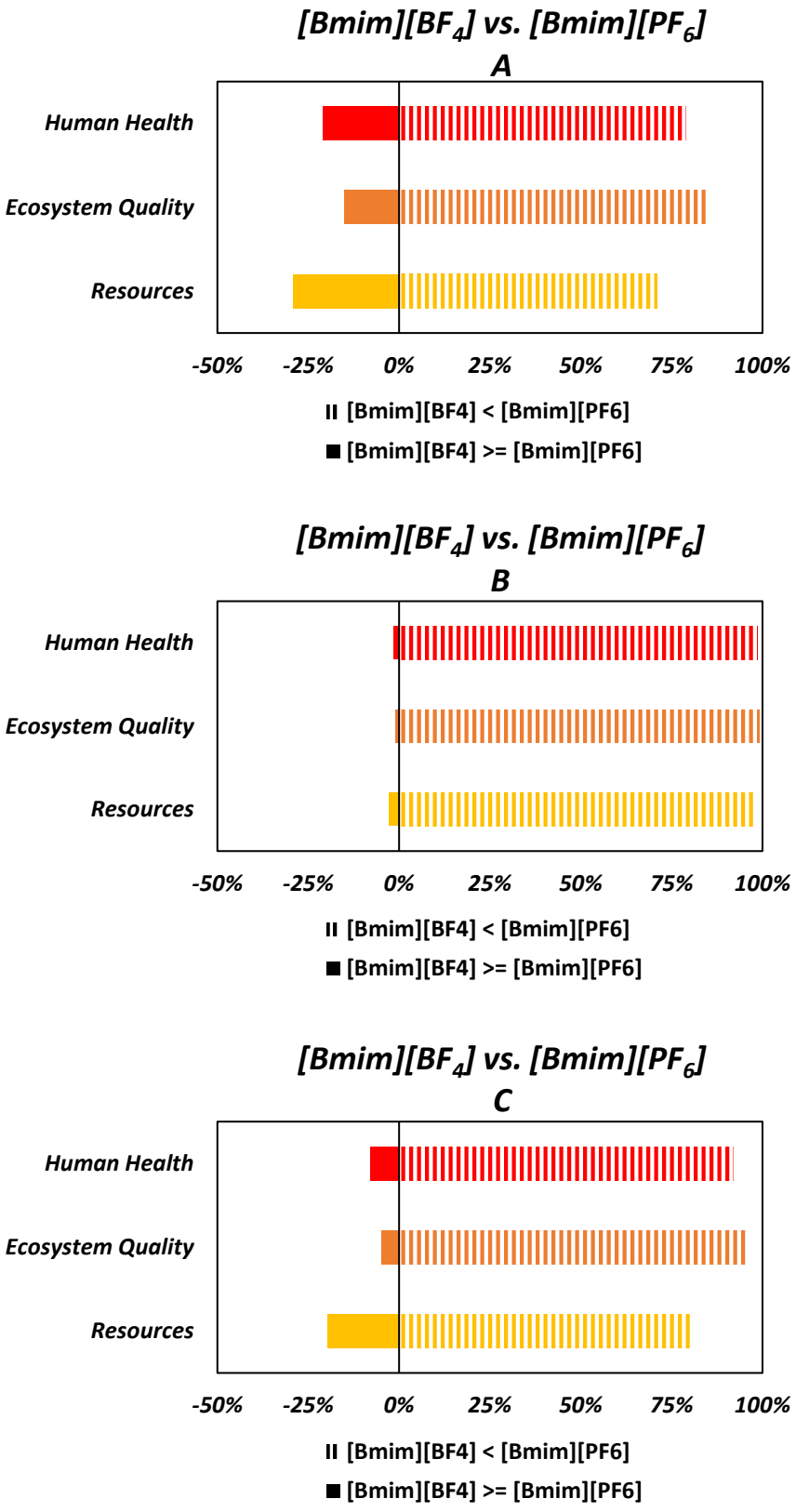

Figure C.2: Overall scenario-based comparison between the end-point impacts of [BMIM][BF_4] and [BMIM][PF_6], for 1 kg of ionic liquid.

Table C.12: First-order Sobol indices for each end-point impact in the production of $NaBF_4$.

Uncertain Parameter	**Human Health**	**Ecosystem Quality**	**Resources**
$BEI_z^{BF_3}$	0.60	0.58	0.60
BEI_z^{mat}	0.03	0.02	0.01
$BEI_z^{Et_2O}$	0.03	0.04	0.08
BEI_z^{el}	0.05	0.05	0.03
BEI_z^{th}	0.00	0.01	0.03
BEI_z^{NaF}	0.29	0.30	0.25

Table C.13: First-order Sobol indices for each end-point impact in the production of $LiPF_6$.

Uncertain Parameter	**Human Health**	**Ecosystem Quality**	**Resources**
BEI_z^{HF}	0.45	0.43	0.44
BEI_z^{mat}	0.03	0.02	0.01
$BEI_z^{Cl_5P}$	0.24	0.28	0.29
BEI_z^{el}	0.05	0.06	0.03
BEI_z^{th}	0.01	0.01	0.04
BEI_z^{LiF}	0.22	0.20	0.19